MCR-82-QD
MA58-33156

Final
Report

September 1982

Structural Dynamics Payload Loads Estimates

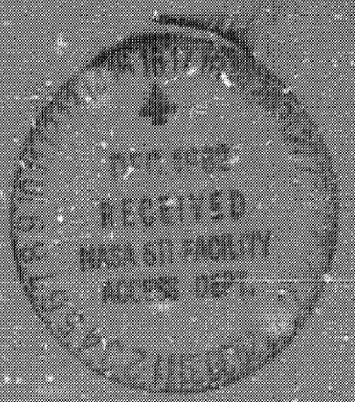

MARTIN MARIETTA

MCR-82-601
NAS8-33556

Final Report

September 1982

STRUCTURAL DYNAMICS PAYLOAD LOADS ESTIMATES

Author:
R. C. Engels

Approved:
Harry Hargrow
Program Manager

MARTIN MARIETTA CORPORATION
DENVER AEROSPACE
P.O. Box 179
Denver, CO 80201

PREFACE

This Final Report is submitted to the National Aeronautics and Space Administration's George C. Marshall Space Flight Center, Huntsville, Alabama, in response to the contract provisions of deliverable items associated with Structural Dynamics Payload Loads Estimates, Contract Number NAS8-33556.

The study took place during the period from August 1979 to October 1982 under the direction of Mr. W. Holland of MSFC, Huntsville, Alabama.

During this three year period the following documents were produced:

1. Methodology Assessment Report
   August 1980, MCR-80-553

2. Methodology Development Report
   August 1981, MCR-81-602

3. Final Report
   September 1982, MCR-82- 601

4. User Guide
   September 1982, MCR-82- 602

5. Monthly Progress Reports

The present Final Report together with the User Guide are intended to be largely self-contained. Chapter I deals with an overview of existing approaches to the problem of loads calculation. Chapter II introduces a full-scale version of an alternate numerical integration technique to solve the response part of a load cycle. A set of short-cut versions of this algorithm is developed in Chapter III. The implementation of these techniques is described in Chapter IV which deals with the software package. It should be noted that a complete documentation of the software can be found in the User Guide MCR-82-602 . Finally, in Chapter V the reader can find some tentative conclusions and a few suggestions of a more general nature. This report concludes with a rather extensive list of references.

The author wishes to thank D. Devers, H. Harcrow and G. Morosow for their constructive comments and for reviewing parts of the manuscript.

TABLE OF CONTENTS

TABLE OF CONTENTS (Continued)

INTRODUCTION

The design and subsequent development of today's aerospace structures require extensive analytical and experimental studies. These investigations are necessary to ensure complete confidence in the ability of the total system to perform its required functions. Over the years a sufficient body of technical know-how has been accumulated to allow for an adequate system analysis prior to launch. However, with the appearance of larger and more sophisticated space structures, many of the analysis techniques are now being stretched to the limit of their capabilities. Indeed, the problem at hand sometimes has to be adapted in order to fit the analysis technique. This is particularly evident when dealing with large space structures and their corresponding finite element models.

An important part of a design effort is the prediction of loads in the members of the structural system. A complete load cycle includes such items as modeling, modal reduction, modal analysis, load calculations, response analysis, etc. As mentioned above a load cycle for a relatively small structure is fairly well standardized. The first step consists of constructing a discrete model for the structure. The analyst has to worry about the phenomena he wants to represent, how he will model certain structural elements, what methods he should use, etc. If the structure is small, it is safe to say that an accurate structural model can be derived at reasonable cost. The next step in a load cycle is the calculation of the response of the structure to a given external force environment. Usually, a modal analysis technique is used, yielding a set of decoupled modal equations which are easily solved. Modes and frequencies essentially represent the physics of the structure and as such reveal much useful information besides the response. The last step in the load cycle is the actual calculation of the loads using the fact that the load vector is the product of the stiffness matrix ar the displacement vector. When the structure is small, all modes can be used to obtain the displacement vector and no acccuracy problems occur. The analyst finally sends the maximum loads to the stress engineer who calculates stresses and strains and finds out if certain structural members are correctly designed so they can survive the external force environment. When corrections in the design are necessary they will affect the overall response and therefore another load cycle is necessary.

The techniques used on small structures are well established and tested on numerous real life structures. Large space structures pose a new set of problems primarily related to size and cost. Booster vehicles with payloads, such as the space transportation system aside from being large, have their own peculiar set of difficulties. The United States utilizes a rather small family of launch vehicles (boosters) to support a varied spectrum of satellite and spacecraft (payloads) programs. These launch vehicles have been carefully designed to accomodate a wide range of payload configurations. In general, the payload interfaces with the launch vehicle at a limited subset of candidate structural "hard" points at the payload launch vehicle separation plane. The Shuttle Orbiter is the latest example and is unique in the sense that it is reusable. The shuttle orbiter/payload(s) system therefore is not only a large space structure but part of it, namely the orbiter, is the same structure in every flight configuration. This makes the shuttle a unique challenge from the structural analyst's point of view.

It is important that any candidate payload be designed to withstand the load environment transmitted to the payload from within the shielded payload compartment. Such environments commonly originate from a static (steady state) vehicle acceleration, a transient or dynamic event such as rocket motor ignition, or an acoustical environment. Very often, it is the transient dynamic response behavior of the payload that constitutes payload design load profiles; hence, it is important that proper attention be given to the payload transient response characteristics as influencing major design decisions. As an example let us consider the launching of the Shuttle Orbiter carrying a payload such as the Space Telescope. Obviously, when the rocket engines are ignited the Shuttle Orbiter will experience reaction forces. These forces will be transmitted to the Space Telescope in the cargo bay through the interface (i.e., through the connection points between the Orbiter and the Space Telescope). The space telescope then, will undergo elastic displacements. The question is, will the space telescope be able to withstand those vibrations without being critically damaged. The owner of this expensive telescope does not want to find out the answer to this question by trial and error. Therefore, an analysis is necessary. This analysis constitutes the load cycle as previously described. In the following we wish to point out some of the particular problems that arise during a load cycle conducted on a space structure such as the Shuttle Orbiter/Payload(s)/System.

The first step in the load cycle, i.e., the modeling of the structure already poses a few unique problems. Even though research and development in the area of modeling techniques should continue, the engineer has available to him an excellent choice of approaches. When the structure is large, the engineer has to take into consideration the size of the model. The question then becomes not so much do we have the necessary tools to model the structure? but: can we develop an adequate model of reasonable size and cost? To answer this question the engineer has to look at the particular phenomena he wants to describe and model accordingly. That is why the model developed by the structural engineer is often radically different from the model developed by the thermo dynamicist or the control engineer. Furthermore, if the booster model is reusable, the analyst must find ways to incorporate this established knowledge. Coordination between payload and booster organizations becomes critical. Reduction techniques must be considered. Is finite element modeling always recommended? Often, modeling cannot be done indiscriminately as not to result in oversized models, necessitating reductions of one kind or another. The analyst has to make sure he does not loose sight of the essential physical characteristics of the system in view of the large model. For example, is it necessary to model certain elements with two hundred degrees of freedom when the essential structural parameters only count five? Is there any benefit in hybrid models, partially discreet, partially continuous?

The next issue is the calculation of the response. Solving an eigenvalue problem for the full-up discreet model becomes virtually impossible because of the enormous size of the model. The important question of model reduction becomes inevitable. Reducing a model can be done in several ways. A widely used technique is static reduction or Guyan reduction. This technique has to be administered with great care. Error analyses are scarce and much engineering judgement is necessary. Another popular technique is modal synthesis. Many different approaches and improvements of these approaches are available and will be discussed in more detail in subsequent sections. Again, no real error analysis is available and care must be taken not to loose vital information about the system.

Once the modes and frequencies of the structure are known, the response can be calculated for several flight events. Many accurate and cost effective numerical integration techniques for the solution of a decoupled set of modal equations exist and have been used successfully. Large space structures should not present any special problem when the models can be reduced to acceptable sizes. The Space Shuttle however, poses a different kind of challenge. Indeed, the reusability of the shuttle makes it necessary to be able to deliver many load profiles at relatively short time intervals. The multitude of events, flights and payloads together with the reusability of certain models, flight data and other shuttle related knowledge, seems to require another breed of response techniques, indeed another approach to the entire load cycle. Short-cut methods in the load cycle which take complete advantage of the special nature of the shuttle problem should be developed. Much has been done but many possibilities still need to be looked at. Reduction techniques, response techniques, load calculation techniques, etc. should be investigated in the light of the particular needs of the shuttle. The relationship and interfacing between payload designer and payload integrator and booster organization and many other agencies and organizations is an integral part of this effort. Possibly, cookbook type approaches are necessary in order to facilitate the task of potential payload contractors or payload integration organizations. It seems appropriate to have short-cut techniques available in the preliminary design phase of a payload which are developed for specific circumstances and leave the payload designer with as much independence as possible. Only during the final verification cycle should expensive analysis tools be used.

One of the major objectives of this report is to provide the reader with some insight into the multitude of problems and corresponding attempts at solving them which are available in the literature. The other objective is to develop a short-cut method in order to numerically integrate the equations of motion of the booster/payload system. Finally, we wish to indicate also a few other possibilities for research in this quickly expanding field of payload integration techniques.

Finally, the actual calculation of the loads is also affected by the reduction of the model. In particular, when modal synthesis is employed, it is generally not possible anymore to use the straight forward approach where the loads are given by the product of stiffness and displacement. It was found that significant error can result from such a displacement technique. Therefore, the so called acceleration approach is introduced. It makes the numerical problem more complicated but it yields accurate results.

CHAPTER I. OVERVIEW OF EXISTING TECHNIQUES

A. FULL-SCALE TECHNIQUES

1. Introduction

The objective of this chapter is to identify and discuss some of the most prominent techniques used in the course of a typical structural load cycle. This will acquaint the reader with state-of-the-art methodologies and the necessary background information in terms of a unified nomenclature. Also, many of the features of these methods can be incorporated into possible short-cut approaches. In addition, this chapter will give us the opportunity to more clearly identify the requirements of an acceptable short-cut methodology in connection with the STS (Space Transportation System).

Any structural analysis starts with the derivation of the equations of motion for the system at hand. In the next section we shall derive a set of coupled differential equations describing the motion of a booster/payload system.

2. The Equations of Motion in the Discrete Time Domain

The objective of this section is the derivation of the equations of motion of the booster/payload system. This set of equations subsequently must be solved in order to generate displacement histories which are needed for load calculations.

Figure 1 shows the free body diagrams of the booster B and the payload P. The booster and the payload are connected to each other through the interface. Physically, the interface is the collection of structural "hard" points which the booster and the payload have in common. Mathematically, this means that the generalized interface displacement vector $\left\{ x_I^B \right\}$ on the booster side of the interface must be equal to its equivalent $\left\{ x_I^P \right\}$ on the payload side. Hence:

$$\left\{ x_I^B \right\} = \left\{ x_I^P \right\} , \qquad \text{for } \underline{\text{all}} \text{ times } t \tag{1}$$

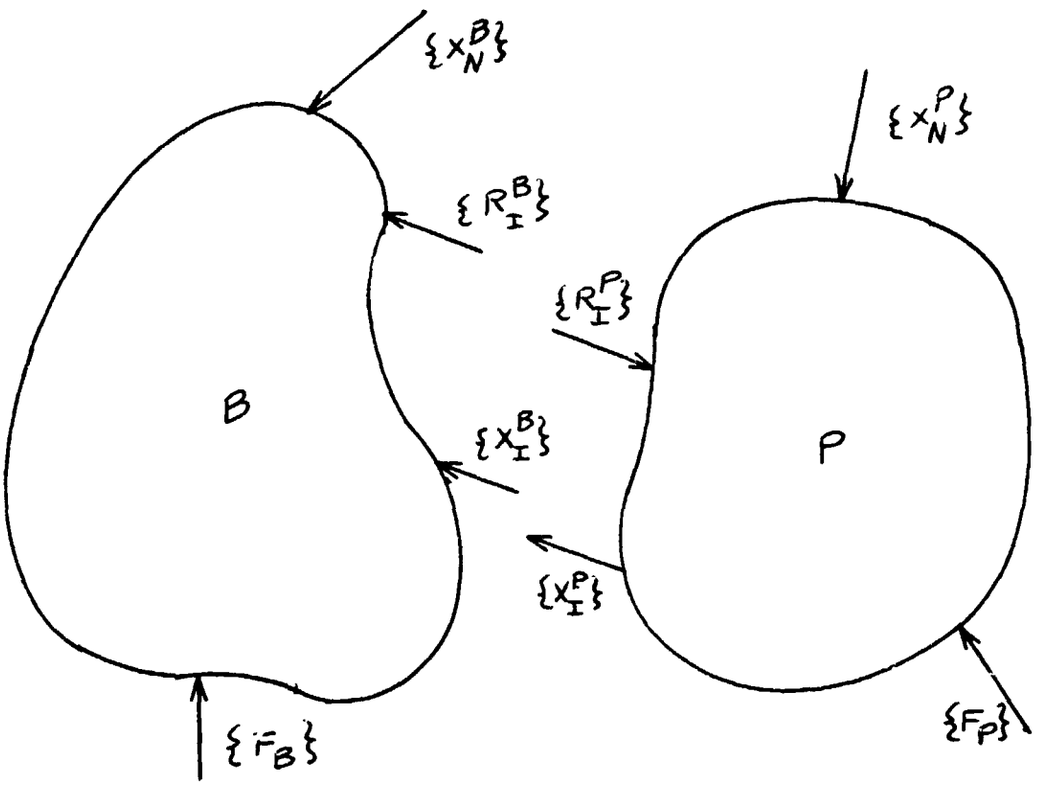

Figure 1. Free Body Diagrams of
Booster B and Payload P

Similarly, the generalized reaction vectors $\{R_I^B\}$ and $\{R_I^P\}$ at the interface satisfy,

$$\{R_I^B\} = -\{R_I^P\} \quad , \qquad \text{for } \underline{\text{all}} \text{ times } t \tag{2}$$

From the free body diagrams in Figure 1 we can easily write the equations of motion for the booster B and the payload P as,

$$\begin{bmatrix} M_B & \\ \hline & M_P \end{bmatrix} \begin{Bmatrix} \ddot{x}_B \\ \hline \ddot{x}_P \end{Bmatrix} + \begin{bmatrix} K_B & \\ \hline & K_P \end{bmatrix} \begin{Bmatrix} x_B \\ \hline x_P \end{Bmatrix} = \begin{Bmatrix} F_B \\ \hline F_P \end{Bmatrix} + \begin{Bmatrix} R_B \\ \hline R_P \end{Bmatrix} \tag{3}$$

where $\{x_B\}$ represents the generalized displacement vector of the booster B. Furthermore, the matrices $[M_B]$ and $[K_B]$ are the mass and stiffness matrices of the booster B, respectively. Finally, the vector $\{F_B\}$ represents the externally applied forces on the booster B and the vector $\{R_B\}$ denotes the reaction of payload P on the booster B. Similar quantities for the payload are defined.

Note that the top partition in equation (3) corresponding to the booster B, is still completely uncoupled from the bottom partition corresponding to the payload. In order to derive the equations of motion for the <u>coupled</u> booster/payload system, we need to eliminate the a priori unknown reaction vectors $\{R_B\}$ and $\{R_P\}$. We shall now establish a convenient and physically meaningful way to accomplish this elimination. To this end, let us first introduce the interface/non-interface partitioning. Indeed, $\{x_B\}$, $[M_B]$, $[K_B]$, $\{F_B\}$ and $\{R_B\}$ can be partitioned according to interface and non-interface degrees of freedom, as follows:

$$\{x_B\} = \begin{Bmatrix} x_N^B \\ \hline x_I^B \end{Bmatrix} \quad , \qquad \{F_B\} = \begin{Bmatrix} F_N^B \\ \hline F_I^B \end{Bmatrix} \quad , \qquad \begin{Bmatrix} R_N^B \\ \hline R_I^B \end{Bmatrix} \tag{4}$$

$$\left[M_B\right] = \left[\begin{array}{c|c} M^B_{NN} & M^B_{NI} \\ \hline M^B_{IN} & M^B_{II} \end{array}\right], \qquad \left[K_B\right] = \left[\begin{array}{c|c} K^B_{NN} & K^B_{NI} \\ \hline K^B_{IN} & K^B_{II} \end{array}\right] \tag{5}$$

Again, similar quantities can be written for P. Note that the subscript N stands for Non-interface and I for Interface. Because there are no non-interface reactions we can write:

$$\left\{R^B_N\right\} = \left\{0\right\} \quad , \qquad \left\{R^P_N\right\} = \left\{0\right\} \tag{6}$$

substituting equations (4), (5) and (6) into equation (3) yields

$$\left[\begin{array}{cc|cc} M^B_{NN} & M^B_{NI} & 0 & 0 \\ M^B_{IN} & M^B_{II} & 0 & 0 \\ \hline 0 & 0 & M^P_{NN} & M^P_{NI} \\ 0 & 0 & M^P_{IN} & M^P_{II} \end{array}\right] \left\{\begin{array}{c} \ddot{x}^B_N \\ \ddot{x}^B_I \\ \hline \ddot{x}^P_N \\ \ddot{x}^P_I \end{array}\right\} + \left[\begin{array}{cc|cc} K^B_{NN} & K^B_{NI} & 0 & 0 \\ K^B_{IN} & K^B_{II} & 0 & 0 \\ \hline 0 & 0 & K^P_{NN} & K^P_{NI} \\ 0 & 0 & K^P_{IN} & K^P_{II} \end{array}\right] \left\{\begin{array}{c} x^B_N \\ x^B_I \\ \hline x^P_N \\ x^P_I \end{array}\right\} = \left\{\begin{array}{c} F^B_N \\ \hline F^B_I + R^B_I \\ \hline F^P_N \\ \hline F^P_I + R^P_I \end{array}\right\} \tag{7}$$

Both equations (3) and (7) represent the uncoupled equations of motion of the undamped booster B and the undamped payload P.

Next, let us solve the third partition of equation (7) for the non-interface displacement vector $\left\{x^P_N\right\}$ of the payload P.

$$\left\{x^P_N\right\} = -\left[K^P_{NN}\right]^{-1}\left[K^P_{NI}\right]\left\{x^P_I\right\} + \left[K^P_{NN}\right]^{-1}\left(\left\{F^P_N\right\} - \left[M^P_{NN}\right]\left\{\ddot{x}^P_N\right\} - \left[M^P_{NI}\right]\left\{\ddot{x}^P_I\right\}\right) \tag{8}$$

It is now noted that the non-interface displacement vector $\{x_N^P\}$ consists of two parts. To understand the physical meaning of these two terms let us assume that the interface displacements are zero i.e. $\{x_I^P\} = \{0\}$. In that case it follows from Eq. (8) that the second term on the right-hand side can be interpreted as the non-interface displacement of the payload with respect to the interface. Let us denote this term by $\{\bar{x}_N^P\}$. It is then clear that the first term on the right-hand side of Eq. (8) represents the non-interface displacement of the payload due to the displacement $\{x_I^P\}$ of the interface only. Therefore, Eq. (8) can be written as :

$$\left\{x_N^P\right\} = \left[S_P\right]\left\{x_I^P\right\} + \left\{\bar{x}_N^P\right\} \tag{9}$$

with

$$\left[S_P\right] = -\left[K_{NN}^P\right]^{-1}\left[K_{NI}^P\right] \tag{10}$$

It should be clearly understood that $\left\{\bar{x}_N^P\right\}$ is not the non-interface displacement vector of the payload with respect to a fixed interface but with respect to the interface (i.e., as seen by an observer moving with the interface).

Equations (1), (9) and (10) can now be used to construct the following transformation:

$$\begin{matrix} \\ NB \\ IB \\ NP \\ IP \end{matrix} \begin{matrix} \\ \left(\begin{array}{c} x_N^B \\ \hline x_I^B \\ \hline x_N^P \\ \hline x_I^P \end{array}\right) \end{matrix} = \begin{matrix} \begin{matrix} NB & IB & NP \end{matrix} \\ \left[\begin{array}{c|c|c} I & 0 & 0 \\ \hline 0 & I & 0 \\ \hline 0 & S_P & I \\ \hline 0 & I & 0 \end{array}\right] \end{matrix} \left(\begin{array}{c} x_N^B \\ \hline x_I^B \\ \hline \bar{x}_N^P \end{array}\right) \tag{11}$$

Note that we indicated the row and column sizes of the matrix partitions in the above equation. NB = number of booster non-interface dofs. NP = the number of payload non-interface dofs. IP = IB = number of interface dofs.

Transformation (11) will eliminate the redundant set of interface displacements $\{x_I^P\}$ in Equation (7) and in the process will also eliminate the unknown reactions $\{R_I^B\}$ and $\{R_I^P\}$. First, let us introduce a more convenient notation:

$$\begin{array}{c} NB \\ IB \\ NP \\ IP \end{array}\left[\begin{array}{c|c|c} I & 0 & 0 \\ \hline 0 & I & 0 \\ \hline 0 & S_P & I \\ \hline 0 & I & 0 \end{array}\right] = \left[\begin{array}{c|c} I & 0 \\ \hline 0 & I \\ \hline T_P & I_P \end{array}\right]\begin{array}{l} B \\ \\ P \end{array} \triangleq A \qquad (12)$$

$NB\ IB\ NP \qquad B \qquad NP$

with B = NB + IB, P = NP + IP and,

$$\underset{P\times B}{[T_P]} = \left[\begin{array}{c|c} 0 & S_P \\ \hline 0 & I \end{array}\right], \quad \underset{P\times NP}{[I_P]} = \begin{array}{c} NP \\ \left[\begin{array}{c} I \\ \hline 0 \end{array}\right] \\ IP \end{array} \qquad (13)$$

With this notation we now substitute the transformation (11) into equation (7) and premultiply by A^T (T = transpose). This yields the following result:

$$\begin{array}{c} B \\ P \end{array}\left[\begin{array}{c|c} M_B + T_P^T M_P T_P & T_P^T M_P I_P \\ \hline I_P^T M_P T_P & I_P^T M_P I_P \end{array}\right]\left\{\begin{array}{c} \ddot{x}_B \\ \hline \ddot{x}_N^P \end{array}\right\} + \left[\begin{array}{c|c} K_B + T_P^T K_P T_P & T_P^T K_P I_P \\ \hline I_P^T K_P T_P & I_P^T K_P I_P \end{array}\right]\left\{\begin{array}{c} x_B \\ \hline x_N^P \end{array}\right\} =$$

$B \qquad NP$

$$= \left\{\begin{array}{c} G_B \\ \hline G_P \end{array}\right\} \qquad (14)$$

where

$$\underset{B\times 1}{\{G_B\}} = \begin{matrix} NB \\ IB \end{matrix}\left\{\begin{matrix} F_N^B \\ \hline F_I^B + S_P^T F_N^P + F_I^P \end{matrix}\right\}, \quad \underset{NP\times 1}{\{G_P\}} = \{F_N^P\} \tag{15}$$

We also used equations (2) and (4).

At this point a few remarks are in order. First we shall show that matrix product $[T_P]^T \cdot [K_P] \cdot [I_P]$ is always zero. From equations (5) and (13) we have:

$$[T_P]^T [K_P] [I_P] = \left[\begin{array}{c|c} 0 & 0 \\ \hline S_P^T & I \end{array}\right]\left[\begin{array}{c|c} K_{NN}^P & K_{NI}^P \\ \hline K_{IN}^P & K_{II}^P \end{array}\right]\left[\begin{array}{c} I \\ \hline 0 \end{array}\right] = \left[\begin{array}{c} 0 \\ \hline S_P^T K_{NN}^P + K_{IN}^P \end{array}\right] \tag{16}$$

Substituting the expression (10) for $[S_P]$ into the lower half of the right hand side of equation (16) yields:

$$[S_P]^T [K_{NN}^P] + [K_{IN}^P] = -[K_{NI}^P]^T [K_{NN}^P]^{-1} [K_{NN}^P] + [K_{IN}^P] = [0]$$

because

$$[K_{IN}^P] = [K_{NI}^P]^T \qquad \left([K_P] \text{ is symmetric}\right)$$

Secondly, the triple matrix product

$$[T_P]^T [K_P] [T_P] = \left[\begin{array}{c|c} 0 & 0 \\ \hline S_P^T & I \end{array}\right]\left[\begin{array}{c|c} K_{NN}^P & K_{NI}^P \\ \hline K_{IN}^P & K_{II}^P \end{array}\right]\left[\begin{array}{c|c} 0 & S_P \\ \hline 0 & I \end{array}\right] = \left[\begin{array}{c|c} 0 & 0 \\ \hline 0 & K_{IN}^P S_P + K_{II}^P \end{array}\right] \tag{17}$$

will be zero for a statically determinate interface. The interface is called statically determinate when the number of interface degrees of freedom is equal to the number of rigid body degrees of freedom of the structure at hand. Otherwise, the interface is called statically indeterminate. To show that $[K_{IN}]\,[S_P] + [K_{II}]$ in Equation (17) is zero for a statically determinate interface, let us first state that the numerical values of the elements of this matrix are independent of the dynamical state of the structure. More specifically, we could constrain the booster and consider a case of static equilibrium for the system under the action of a force $\{F_N^B\}$ and all other applied forces equal to zero. As far as the stiffness matrix $[K_P]$ is concerned, there will be no change. Therefore without loss of generality we consider the equilibrium equation of P under the action of $\{R_I^P\}$.

$$\left[K_P\right] \left\{x_P\right\} = \left\{\begin{array}{c} 0 \\ \hline R_I^P \end{array}\right\} \tag{18}$$

or using the partitioned form of $[K_p]$, we can write

$$\left[K_{NN}^P\right] \left\{x_N^P\right\} + \left[K_{NI}^P\right] \left\{x_I^P\right\} = \left\{0\right\} \tag{19}$$

$$\left[K_{IN}^P\right] \left\{x_N^P\right\} + \left[K_{II}^P\right] \left\{x_I^P\right\} = \left\{R_I^P\right\} \tag{20}$$

From equation (19) we can solve for $\left\{x_N^P\right\}$:

$$\left\{x_N^P\right\} = -\left[K_{NN}^P\right]^{-1} \left[K_{NI}^P\right] \left\{x_I^P\right\} = \left[S_P\right] \left\{x_I^P\right\} \tag{21}$$

where we used equation (10). Substituting equation (21) into equation (20) yields:

$$\left(\left[K_{IN}^P\right] \left[S_P\right] + \left[K_{II}^P\right]\right)\left\{x_I^P\right\} = \left\{R_I^P\right\} \tag{22}$$

At this point we should note that when the interface is statically determinate no stresses can be set up in P by the interface displacements $\left\{x_I^P\right\}$. Indeed, for a statically determinate interface the matrix $[S_P]$ becomes a rigid body transformation, transforming the interface displacements into equivalent rigid body displacements of the non-interface degrees of freedom of P. Because, in addition we assumed that no other forces are acting on P, it is clear that $\left\{R_I^P\right\}$ is zero in Equation (25), from which it follows that

$$\left[K_{IN}^P\right] \left[S_P\right] + \left[K_{II}^P\right] = 0 \tag{23}$$

This completes the proof.

Finally, we note that in most applications of interest to this contract, the externally applied forces $\left\{F_N^P\right\}$, $\left\{F_I^P\right\}$, and $\left\{F_I^B\right\}$ are nonexistent. For example, STS payloads will be enclosed in the cargo bay and will not be exposed to external forces. Therefore we write

$$\left\{F_N^P\right\} = \left\{F_I^B\right\} = \left\{F_I^P\right\} = \left\{0\right\} \tag{24}$$

Introducing Equation (24) into equations (15) and taking into account that $\left[T_P^T K_P I_P\right] = [0]$ we can write the final form of Equation (14):

$$\left[\begin{array}{c|c} M_B + T_P^T M_P T_P & T_P^T M_P I_P \\ \hline I_P^T M_P T_P & I_P^T M_P I_P \end{array}\right] \left\{\begin{array}{c} \ddot{x}_B \\ \hline \ddot{x}_N^P \end{array}\right\} + \left[\begin{array}{c|c} K_B + T_P^T K_P T_P & 0 \\ \hline 0 & I_P^T K_P I_P \end{array}\right] \left\{\begin{array}{c} x_B \\ \hline x_N^P \end{array}\right\} = \left\{\begin{array}{c} G_B \\ \hline 0 \end{array}\right\} \tag{25}$$

$$\left\{G_B\right\} = \left\{\begin{array}{c} F_N^B \\ \hline 0 \end{array}\right\} \tag{26}$$

also,

$$\{x_B\} = \begin{Bmatrix} x_N^B \\ - - \\ x_I^B \end{Bmatrix} \tag{27}$$

represents the generalized displacement vector of the free booster B. The vector $\{x_N^B\}$ contains all non-interface displacements of the booster and $\{x_I^B\}$ represents the interface degrees of freedom. Furthermore, the vector $\{\bar{x}_N^P\}$ represents the non-interface displacements of the payload P with respect to the interface. The matrices $[M_B]$ and $[M_P]$ represent the mass matrices of the booster and the payload respectively and $[K_B]$ and $[K_P]$ represent the stiffness matrices. The matrix $[T_P]$ is a constraint modal matrix, characteristic for the payload P. In case of a statically determinate interface $[T_P]$ represents a rigid body transformation. Finally, $\{F_N^B\}$ is the externally applied force vector acting on the booster B. The matrices $[T_P]^T [M_P] [T_P]$ and $[T_P]^T [K_P] [T_P]$ contribute only to the interface degrees of freedom as can be seen from Equation (17) and from

$$\begin{bmatrix} T_P \end{bmatrix}^T \begin{bmatrix} M_P \end{bmatrix} \begin{bmatrix} T_P \end{bmatrix} = \begin{bmatrix} 0 & 0 \\ S_P^T & I \end{bmatrix} \begin{bmatrix} M_{NN}^P & M_{NI}^P \\ M_{IN}^P & M_{II}^P \end{bmatrix} \begin{bmatrix} 0 & S_P \\ 0 & I \end{bmatrix} - \begin{bmatrix} 0 & 0 \\ 0 & M_2^P \end{bmatrix} \tag{28}$$

with

$$\begin{bmatrix} M_2^P \end{bmatrix} = \begin{bmatrix} S_P \end{bmatrix}^T \left(\begin{bmatrix} M_{NN}^P \end{bmatrix} \begin{bmatrix} S_P \end{bmatrix} + \begin{bmatrix} M_{NI}^P \end{bmatrix} \right) + \begin{bmatrix} M_{IN}^P \end{bmatrix} \begin{bmatrix} S_P \end{bmatrix} + \begin{bmatrix} M_{II}^P \end{bmatrix}$$

The matrix $[T_P]^T [M_P] [T_P]$ essentially represents the payload mass reduced down to the interface. Similarly $[T_P]^T [K_P] [T_P]$

represents the payload stiffness reduced down to the interface. Note that when the interface is statically determinate no stiffness is transferred (Equation (23)). When the interface is statically indeterminate there are what is commonly called "constraint modes" , i.e., the interface displacements $\{x_I^B\}$ not only induce rigid body displacements in the payload but also elastic deformations. This causes the triple product $[T_p]^T [K_p] [T_p]$ to be different from zero.

It should also be noted that damping is not included in Equation (25). However, modal damping can always be taken into account later. Finally, the matrices $[M_B]$, $[K_B]$, $[M_p]$ and $[K_p]$ must be constructed by the appropriate organizations. The booster and payload organization will usually be different contractors. If in addition the integrator is another organization it is clear that there is an interfacing problem. A fair amount of coordination is necessary to make the transfer of information between those three organizations optimal. Unfortunately, this coordination is very difficult to establish resulting in considerable time delays. Moreover, these costs and delays repeat themselves for every load cycle (i.e., every time a change is made in the booster or payload). A typical example is the development of the Viking Orbiter System . Upward of nine organizations were responsible for hardware or integration functions which directly affected the evaluation of dynamic transient loads. The number of interfaces between those organizations resulted in difficulties in arranging for the necessary analyses at each organization, in obtaining the necessary data, in establishing priorities, in establishing output requirements and in correctly transferring data between organizations. The time duration for one load cycle ranged from three to twelve months which depended on the number of events, forcing functions per event, and complexities of the analysis. Of course, if the booster already has its final design, many of these problems can be avoided. Theoretically, only one transfer of booster data to the payload organization would be necessary. This concludes this section on the equations of motion of the booster/payload system in the discrete time domain. This is a necessary first step in any load cycle.

3. The Solution of the Equations of Motion

a. The discrete time domain

As stated in the Introduction, the objective of this study is to determine design loads for the payload structure. These design loads are then used to calculate stresses and strains that would exist in the structural elements that make up the payload. The stresses and strains allow the designer to determine the correct physical and geometric properties of the elements (mass, stiffness, lengths, cross sections, etc.) so that the structure does not fail when subjected to the external forces $\{ F_N^B \}$. An element loads equation is written as

$$\left\{ L_e^P \right\} = \left[k_e \right] \left[T_e \right] \left\{ x_P \right\} \tag{29}$$

in which $\{L_e^P\}$ is the load vector of an individual element e of the payload P, $[k_e]$ is the stiffness matrix of the element, and $[T_e]$ is the geometric compatibility transformation. The vector $\{x_P\}$ is the time dependent displacement vector of the payload satisfying Equation (25). Consequently, in order to determine $\{L_e^P\}$ in Equation (29) we need to solve Equation (25).

The most straightforward approach to determine $\{x_P\}$ is to solve Equation (25) as a set of simultaneous second order differential equations. There are several well established response routines that handle such problems (Runge-Kutta, Newmark-Chan-Beta Numerical Integration, etc.). This direct approach has the advantage of simplicity and accuracy. However, the main drawback is the high computational cost due to the large number of degrees of freedom used to describe today's aerospace models. In this connection, as a counter argument, one could ask the question if such large models are really necessary. In any case, unless a drastic reduction of the model is possible, this direct integration approach is not favored. In addition, this approach does not yield much qualitative information about the system. As will be explained below a modal approach reveals more qualitative information.

b. Modal Analysis

In this section we shall discuss a technique commonly known as modal analysis. This approach will lead us to an alternate solution method for Equation (25) and we shall show that it has some definite advantages over the direct solution of the set of differential equations (25) as discussed in Section 3a.

We start the process with the homogeneous set of equations extracted from the top row of Equation (3).

$$\left[M_B \right] \left\{ \ddot{x}_B \right\} + \left[K_B \right] \left\{ x_B \right\} = \left\{ 0 \right\} \tag{30}$$

Associated with this equation is an eigenvalue problem,

$$\left(-\omega_B^2\left[M_B\right] + \left[K_B\right]\right)\left\{\phi_B\right\} = \left\{0\right\} \tag{31}$$

where the vector $\left\{\phi_B\right\}$ represents an eigenvector (mode shape) and ω_B an eigenvalue (natural frequency). The solution of this eigenvalue problem essentially produces a linear transformation matrix $[\phi_B]$ (modal transformation matrix) in which each column represents a mode shape of the booster B. The main property of this modal transformation is that in the new normal coordinate system $\{q_B\}$, the equations of motion (30) become uncoupled, i.e., if we apply the transformation,

$$\left\{x_B\right\} = \left[\phi_B\right]\left\{q_B\right\} \tag{32}$$

to Equation (30), and premultiply by $[\phi_B]^T$ we obtain

$$\left[\phi_B\right]^T\left[M_B\right]\left[\phi_B\right]\left\{\ddot{q}_B\right\} + \left[\phi_B\right]^T\left[K_B\right]\left[\phi_B\right]\left\{q_B\right\} = \left\{0\right\} \tag{33}$$

where the coefficient matrices of $\{\ddot{q}_B\}$ and $\{q_B\}$ are now diagonal,

$$\left[\phi_B\right]^T\left[M_B\right]\left[\phi_B\right] = \left[I\right], \quad \left[\phi_B\right]^T\left[K_B\right]\left[\phi_B\right] = \left[\omega_B^2\right] \tag{34}$$

where $[\phi_B]$ was normalized with respect to $[M_B]$. Equation (33) can then be written as

$$\left\{\ddot{q}_B\right\} + \left[\omega_B^2\right]\left\{q_B\right\} = \left\{0\right\} \tag{35}$$

The obvious advantage of applying the modal transformation Equation (32) is that Equation (35) now represents a set of decoupled independent second order differential equations that are easily solved. The price to pay however, is the cost of the solution of eigenvalue problem (31). There are many well established eigenvalue problem "solvers" available (Jacobi, Rayleigh-Ritz, etc.) .

The next step is to consider the homogenous equation,

$$\left[I_P\right]^T\left[M_P\right]\left[I_P\right]\left\{\ddot{\bar{x}}_N^P\right\} + \left[I_P\right]^T\left[K_P\right]\left[I_P\right]\left\{\bar{x}_N^P\right\} = \left\{0\right\} \tag{36}$$

Note that,

$$\left[I_P\right]^T \left[M_P\right] \left[I_P\right] = \left[M_{NN}^P\right], \left[I_P\right]^T \left[K_P\right] \left[I_P\right] = \left[K_{NN}\right] \tag{37}$$

So that Equation (36) becomes

$$\left[M_{NN}^P\right] \left\{ \ddot{\bar{x}}_N^P \right\} + \left[K_{NN}^P\right] \left\{ \bar{x}_N^P \right\} = \left\{ 0 \right\} \tag{38}$$

In the same way as we did for Equation (30) we can introduce a modal transformation,

$$\left\{ \bar{x}_N^P \right\} = \left[\phi_N^P \right] \left\{ \bar{q}_N^P \right\} \tag{39}$$

with

$$\left[\bar{\phi}_N^P \right]^T \left[M_{NN}^P \right] \left[\bar{\phi}_N^P \right] = \left[I \right], \left[\bar{\phi}_N^P \right]^T \left[K^P \right] \left[\bar{\phi}_N^P \right] = \left[\bar{\omega}_P^2 \right] \tag{40}$$

where we wrote $\left[\bar{\omega}_P^2 \right]$ instead of $\left[\bar{\omega}_N^{P^2} \right]$ to simplify the notation. The modal matrix $\left[\bar{\phi}_N^P \right]$ has as columns the "cantilevered" mode shapes of the payload P and $\left[\bar{\omega}_P^2 \right]$ has the natural frequencies squared of the cantilevered payload (i.e., fixed interface) on its diagonal. Using Equations (39-40), we can write Equation (38) as

$$\left\{ \ddot{\bar{q}}_N^P \right\} + \left[\bar{\omega}_P^2 \right] \left\{ \bar{q}_N^P \right\} = \left\{ 0 \right\} \tag{41}$$

Let us now apply the following transformation to Equation (25),

$$\left\{ \begin{array}{c} x_B \\ \hline \bar{x}_N^P \end{array} \right\} = \left[\begin{array}{c|c} \phi_B & \\ \hline & \bar{\phi}_N^P \end{array} \right] \left[\begin{array}{c} q_B \\ \hline \bar{q}_N^P \end{array} \right] \tag{42}$$

and premultiply by $\left[\begin{array}{c|c} \phi_B & \\ \hline & \bar{\phi}_N^P \end{array}\right]^T$. Taking into account Equations (34) & (41) we obtain,

$$\left[\begin{array}{c|c} I + \phi_B^T T_P^T M_P T_P \phi_B & \phi_B^T T_P^T M_P T_P \bar{\phi}_N^P \\ \hline \bar{\phi}_N^{PT} T_P^T M_P T_P \phi_B & I \end{array}\right] \left\{\begin{array}{c} \ddot{q}_B \\ \hline \ddot{\bar{q}}_N^P \end{array}\right\} + \left[\begin{array}{c|c} \left[\omega_B^2\right] + \phi_B^T T_P^T K_P T_P \phi_B & 0 \\ \hline 0 & \left[\bar{\omega}_P^2\right] \end{array}\right] \left\{\begin{array}{c} q_B \\ \hline \bar{q}_N^P \end{array}\right\} = \left\{\begin{array}{c} \phi_B^T G_B \\ \hline 0 \end{array}\right\} \quad (43)$$

At this point another eigenvalue problem could be solved for the coupled system represented by Equation (43). This would finally lead to a set of decoupled equations for the system. In fact, one could solve just one system eigenvalue problem for the homogeneous equation given by the homogeneous part of Equation (25). Numerically this approach does not yield much advantage over a direct solution. For one, the solution of a large eigenvalue problem is very expensive and essentially increases with the cube of the dimension. The modal approach has the advantage of uncoupling the system equations, which allows us to investigate several load cases with little added cost (if the structure and its constraints do not change). It also has the advantage of revealing physical characteristics. After all, modes and frequencies essentially embody all physical information. But their is potentially a much greater advantage present in the use of modes and frequencies. It can reduce the number of modal equations to be solved. This is why equation (43) was derived in a stepwise fashion.

c. Modal Synthesis Techniques

From what we have seen so far we can conclude that for small systems we have the necessary techniques to model the structure and subsequently find the response. The response can be found by direct integration of the discrete equations of motion or by first solving an eigenvalue problem. However, when the structure becomes large and the model has a very large number of degrees of freedom there is a problem. Direct numerical integration or solving a large system eigenvalue problem becomes prohibitive. Therefore, remedies have to be found. In section 3b we already layed the groundwork for a reduction technique called "modal synthesis". Indeed we introduced the free modes of the booster and the cantilevered modes of the payload(s). These mode groups are then "synthesized" so as to yield the final coupled set of equations (43). As pointed out, this procedure by itself does not reduce the size of the problem and actually requires the costly solution of several eigenvalue problems. However, in most practical applications there is a possibility of defining a so-called "cut-off frequency". In these cases a Fourier series expansion of the force vector $\{F_N^B\}$ shows that the energy content of the high frequency components is small compared to the energy contained in the low frequency components. Practically, this means that the response of the structure due to the high frequency content of $\{F_N^B\}$ can often be neglected. In this connection it should be noted that it is

relatively difficult to excite the higher modes of the structure to any large extent, especially when $\{F_N^B\}$ only contains a few elements (i.e., only a few application points). The idea then is to first truncate the booster modes and payload modes in Equations (32) and (39) according to that "cut-off frequency". No thorough investigation has been published concerning the approximation involved in such a mode truncation. It is largely a "practical" matter supported by some theoretical considerations and the fact that it works. Truncation of the modes on the substructure level reduces the size of the eigenvalue problem related to Equation (43). Once this reduced eigenvalue problem is solved another truncation is possible, this time on the system level. To make this clear let us write equation (43) as follows:

$$[M]\{\ddot{q}\} + [K]\{q\} = \{Q\} \tag{44}$$

with

$$[M] = \left[\begin{array}{c|c} I + \phi_B^T T_P^T M_P T_P \phi_B & \phi_B^T T_P^T M_P I_P \bar{\phi}_N^P \\ \hline \bar{\phi}_N^{P^T} I_P^T M_P T_P \phi_B & I \end{array}\right]$$

$$[K] = \left[\begin{array}{c|c} \left[\omega_B^2\right] + \phi_B^T T_P^T K_P T_P \phi_B & 0 \\ \hline 0 & \left[\omega_P^2\right] \end{array}\right] \tag{45}$$

$$\{q\} = \left\{\begin{array}{c} q_B \\ \hline \bar{q}_N^P \end{array}\right\} \quad , \quad \{Q\} = \left\{\begin{array}{c} \Phi_B^T G_B \\ \hline 0 \end{array}\right\}$$

where we should stress that $[\Phi_B]$ and $[\bar{\Phi}_N^P]$ are already truncated so that the size of [M] and [K] is significantly reduced. Now, we solve the eigenvalue problem associated with the following homogeneous equation:

$$[M]\{\ddot{q}\} + [K]\{q\} = \{0\} \tag{46}$$

leading to

$$\{q\} = [\Psi]\{\xi\} \tag{47}$$

$$[\Psi]^T[M][\Psi] = [I] \quad , \quad [\Psi]^T[K][\Psi] = [\Omega^2] \tag{48}$$

and

$$\{\ddot{\xi}\} + [2\zeta\Omega]\{\dot{\xi}\} + [\Omega^2]\{\xi\} = [\Psi]^T \{Q\} \tag{49}$$

where we introduced the customary modal damping. We also truncated the modes $[\Psi]$ again according to the present cut-off frequency. The final set of uncoupled Equations (49) is now solved with a numerical integrator such as a Runge-Kutta method.

Note that there are several synthesis techniques available, the purpose always being the reduction of the system size. When working with large structural systems and their corresponding large mathematical models, reduction methods become very important. Ways to reduce systems are: modal analysis, Guyan reduction, component mode synthesis, etc.

The component mode synthesis approach as described in Section 3c is approximate in nature. Several techniques are available to improve on the accuracy, two of which we shall now discuss.

d. The Residual Mass and Stiffness Method

As explained in Section 3c in many cases it is possible to define a cut-off frequency which enables us to truncate the higher modes in Equations (32), (39) and (49) thereby reducing the size of this equation. Obviously, some accuracy in the response of the structure is lost due to the truncation of these higher modes. This loss of accuracy is especially apparent at the interface. The residual mass and stiffness method, instead of omitting these high modes will replace them with a set of "residual modes". The computation of these residual modes does not require any knowledge of the payload so that they represent a one-time computation effort not to be repeated as long as the booster stays the same. In order to determine the residual modes let us consider Equation (32):

$$\left\{ x_B \right\} = \left[\phi_B \right] \left\{ q_B \right\} \tag{50}$$

which represents the modal transformation for the booster B. Assuming a cut-off frequency was determined we can partition Equation (50) as follows:

$$\left\{ x_B \right\} = \left[\phi_B^L \vdots \phi_B^H \right] \left\{ \begin{array}{c} q_B^L \\ \hline q_B^H \end{array} \right\} \tag{51}$$

where $[\phi_B^L]$ represents the modes with frequencies less than the cut-off frequency and $[\phi_B^H]$ those with higher frequencies. At this point one could neglect $[\phi_B^H]$ and calculate the response as a linear combination of the lower modes $[\phi_B^L]$ only. Usually this yields a poor accuracy in the response and the loads. The reason is that in most practical cases a significant part of the interface response is produced by the higher modes. Indeed, a typical interface is rather stiff and has little mass, i.e., that locally the interface has a high frequency content so that it responds significantly in the high frequency range. In truncating the higher modes the model does not include an adequate representation of that interface. The residual mass and stiffness method now, proposes to retain the static contribution to the response of these higher modes. This leads to a much better representation of the interface. The static contribution can be obtained from the following static equation

$$\left[K_B\right] \left\{x_B\right\} = \left\{\begin{matrix} F_N^B \\ R_I^B \end{matrix}\right\} \tag{52}$$

derived from Equation (3). Substituting Equation (50) into Equation (52) premultiplying by $[\phi_B]^T$ and recalling Equation (34) yields:

$$\left[\omega_B^2\right] \left\{q_B\right\} = \left[\phi_B\right]^T \left\{\begin{matrix} F_N^B \\ R_I^B \end{matrix}\right\} \tag{53}$$

Because we are only interested in the high frequency part, let us write Equation (43) as

$$\left[\begin{array}{c|c} \left[\omega_B^{L^2}\right] & \\ \hline 0 & \left[\omega_B^{H^2}\right] \end{array}\right] \left\{\begin{matrix} q_B^L \\ \hline q_B^H \end{matrix}\right\} = \left[\begin{matrix} \phi_B^{L^T} \\ \hline \phi_B^{H^T} \end{matrix}\right] \left\{\begin{matrix} F_N^B \\ R_I^B \end{matrix}\right\} \tag{54}$$

So that from the bottom row in Equation (54) we have

$$\left[\omega_B^{H^2}\right] \left\{q_B^H\right\} = \left[\phi_B^H\right]^T \left\{\begin{matrix} F_N^B \\ R_I^B \end{matrix}\right\} \tag{55}$$

Finally, let us partition $[\phi_B^H]$ in non-interface and interface partitions,

$$\left[\phi_B^H\right] = \left[\begin{matrix} \phi_{BN}^H \\ \hline \phi_{BI}^H \end{matrix}\right] \tag{56}$$

Substituting Equation (56) into Equation (55) we obtain,

$$\left[\omega_B^{H\,2}\right]\left\{q_B^H\right\} = \left[\phi_{BN}^H\right]^T\left\{F_N^B\right\} + \left[\phi_{BI}^H\right]^T\left\{R_I^B\right\} \tag{57}$$

In principal we can use Equation (55) as it is and solve for $\{q_B^H\}$,

$$\left\{q_B^H\right\} = \left[\omega_B^{H\,-2}\right]\left[\phi_B^H\right]^T\begin{Bmatrix} F_N^B \\ R_I^B \end{Bmatrix} \tag{58}$$

which can be substituted in Equation (51), yielding

$$\left\{x_B\right\} = \left[\phi_B^L \;\vdots\; \left[\phi_B^H\right]\left[\omega_B^{H\,-2}\right]\left[\phi_B^H\right]^T\right]\begin{Bmatrix} q_B^L \\ \hdashline F_N^B \\ R_I^B \end{Bmatrix} \tag{59}$$

However, it should be noted that for every force component we keep, we add a degree-of-freedom to the problem. If for example, $\{F_N^B\}$ contains many elements (i.e., many points of application) it may not pay off to use Equation (59), i.e., we may as well keep all the modes in Equation (50). If however $\{F_N^B\}$ contains a small number of elements (for example, in case of a landing or a rocket motor ignition) we can use Equation (59) as it is, and obtain a better response for few added degrees of freedom. However, because the cut-off frequency was defined in such a way that all significant frequencies of $\{F_N^B\}$ are contained in the lower frequency range L, we can state that the booster model will adequately respond to $\{F_N^B\}$ and no significant portion of the response will be lost. Therefore, we can omit the term in $\{F_N^B\}$ in Equation (57) altogether and just keep the interface part in $\{R_I^B\}$. The latter part in $\{R_I^B\}$ is important because $\{R_I^B\}$ will usually have a significant high frequency content (after all $\{R_I^B\}$ represents the effect of the payload on the booster and as such contains a wide range of frequencies). Because the interface usually has a high frequency content (as explained before) $\{R_I^B\}$ will induce a response at the interface primarily in the high frequency range which in turn will be, transmitted to the rest of the booster.

On the other hand if $\{F_N^B\}$ contains reaction elements due to some external constraints (e.g., a dock) we wish to retain these elements as well because they are equivalent to elements of $\{R_I^B\}$ in the sense that they represent the unknown effects of the constraints and also, the interface between the constraint and the booster usually has a high frequency content (e.g., connections between booster and dock).

Ignoring the term in $\{F_N^B\}$ in Equation (57) and solving for $\{q_B^H\}$ yields

$$\{q_B^H\} = [\omega_B^{H^{-2}}][\phi_{BI}^H]^T \{R_I^B\} \tag{60}$$

which can be substituted into Equation (51), yielding

$$\{x_B\} = \left[\phi_B^L \;\vdots\; [\phi_B^H][\omega_B^{H^{-2}}][\phi_{BI}^H]^T\right] \left\{\begin{array}{c} q_B^L \\ \hdashline R_I^B \end{array}\right\} \tag{61}$$

The term $[\phi_B^H][\omega_B^{H^{-2}}][\phi_{BI}^H]^T$ represents the residual modes and they eplace $[\Phi_B^H]$. Also, note that these modes only involve booster quantities which makes it a one-time computational effort.

Let us now derive the modally coupled equations of motion for the booster/payload system. First, we substitute Equation (61) into the top row of Equation (3) and then we premultiply by $\left[\phi_B^L \;\vdots\; [\phi_B^H][\omega_B^{H^{-2}}][\phi_{BI}^H]\right]^T$ yielding

$$\left[\begin{array}{c|c} I & 0 \\ \hdashline 0 & \underbrace{[\phi_{BI}^H][\omega_B^{H^{-4}}][\phi_{BI}^H]^T}_{\text{residual mass}} \end{array}\right] \left\{\begin{array}{c} \ddot{q}_B^L \\ \hdashline \ddot{R}_I^B \end{array}\right\} + \left[\begin{array}{c|c} [\omega_B^{L^2}] & 0 \\ \hdashline 0 & \underbrace{[\phi_{BI}^H][\omega_B^{H^{-2}}][\phi_{BI}^H]^T}_{\text{residual flexibility}} \end{array}\right] \left\{\begin{array}{c} q_B^L \\ \hdashline R_I^B \end{array}\right\}$$

$$= \left[\begin{array}{c} [\phi_B^L]^T \\ \hdashline [\phi_{BI}^H][\omega_B^{H^{-2}}][\phi_B^H]^T \end{array}\right] \left\{\begin{array}{c} F_N^B \\ \hdashline R_I^B \end{array}\right\} \tag{62}$$

Before proceeding, let us consider the homogeneous equation extracted from the lower half of Equation (62)

$$[\phi_{BI}^H][\omega_B^{H^{-4}}][\phi_{BI}^H]^T \{\ddot{R}_I^B\} + [\phi_{BI}^H][\omega_B^{H^{-2}}][\phi_{BI}^H]^T \{R_I^B\} = 0 \tag{63}$$

and solve the following eigenvalue problem

$$\left(-\omega_R^2 [\phi_{BI}^H][\omega_B^{H^{-4}}][\phi_{BI}^H]^T + [\phi_{BI}^H][\omega_B^{H^{-2}}][\phi_{BI}^H]^T\right) \{\phi_R\} = \{0\} \tag{64}$$

leading to the modal transformation

$$[R_I^B] = [\phi_R]\{q_R\} \tag{65}$$

and the properties

$$\left[\phi_R\right]^T \left[\phi_{BI}^H\right]\left[\omega_B^H\right]^{-4}\left[\phi_{BI}^H\right]^T\left[\phi_R\right] = \left[I\right], \left[\phi_R\right]^T\left[\phi_{BI}^H\right]\left[\omega_B^{H^{-2}}\right]\left[\phi_{BI}^H\right]^T\left[\phi_R\right] = \left[\omega_R^2\right] \tag{66}$$

We shall make use of these properties in deriving the modally coupled equations of motion of the booster/payload system. To this end let us write Equation (25),

$$\left[\begin{array}{c|c} M_B + T_P^T M_P T_P & T_P^T M_P I_P \\ \hline I_P^T M_P T_P & I_P^T M_P I_P \end{array}\right]\left\{\begin{array}{c} \ddot{x}_B \\ \hline \ddot{x}_N^P \end{array}\right\} + \left[\begin{array}{c|c} K_B + T_P^T K_P T_P & 0 \\ \hline 0 & I_P^T K_P I_P \end{array}\right]\left\{\begin{array}{c} x_B \\ \hline x_N^P \end{array}\right\} = \left\{\begin{array}{c} F_N^B \\ 0 \\ \hline 0 \end{array}\right\} \tag{67}$$

Let us now introduce the following notations

$$\left\{q_B\right\} = \left\{\begin{array}{c} q_B^L \\ \hline q_R \end{array}\right\}, \quad \left[\phi_B\right] = \left[\phi_B^L \,\middle|\, \left[\phi_B^H\right]\left[\omega_B^H\right]^{-2}\left[\phi_{BI}^H\right]^T\left[\phi_R\right]\right] \tag{68}$$

so that, combining Equations (61), (65) and (68) we can write,

$$\left\{x_B\right\} = \left[\phi_B\right]\left\{q_B\right\} \tag{69}$$

We now define a transformation similar to Equation (42)

$$\left\{\begin{array}{c} x_B \\ \hline x_n^P \end{array}\right\} = \left[\begin{array}{c|c} \phi_B & \\ \hline & \phi_N^P \end{array}\right]\left\{\begin{array}{c} q_B \\ \hline q_N^P \end{array}\right\} \tag{70}$$

where this time $\{q_B\}$ and $[\Phi_B]$ are given by Equation (68)

Applying this transformation to Equation (67) and premultiplying by $\left[\begin{array}{c|c} \phi_B & 0 \\ \hline 0 & \phi_N^P \end{array}\right]^T$ yields

$$\left[\begin{array}{c|c} \phi_B^T M_B \phi_B + \phi_B^T T_P^T M_P T_P \phi_B & \phi_B^T T_P^T M_P I_P \phi_N^P \\ \hline \phi_N^{P^T} I_P^T M_P T_P \phi_B & \phi_N^{P^T} I_P^T M_P I_P \phi_N^P \end{array}\right]\left\{\begin{array}{c} \ddot{q}_B \\ \hline \ddot{q}_N^P \end{array}\right\} + \left[\begin{array}{c|c} \phi_B^T K_B \phi_B + \phi_B^T T_P^T K_P T_P \phi_B & \\ \hline & \phi_N^{P^T} I_P^T K_P I_P \phi_N^P \end{array}\right]\left\{\begin{array}{c} q_B \\ \hline q_N^P \end{array}\right\} = \left\{\begin{array}{c} \phi_B^T \left\{\begin{array}{c} F_N^B \\ 0 \end{array}\right\} \\ \hline 0 \end{array}\right\} \tag{71}$$

Using Equations (34), (39) and (66) we can show that

$$\left[\phi_B\right]^T\left[M_B\right]\left[\phi_B\right] = \begin{bmatrix} I & 0 \\ 0 & I \end{bmatrix}, \quad \left[\phi_B\right]^T\left[K_B\right]\left[\phi_B\right] = \begin{bmatrix} \left[\frac{1}{\omega_B^2}\right] & \\ 0 & \left[\omega_R^2\right] \end{bmatrix} \tag{72}$$

and

$$\left[\phi_N^P\right]^T\left[I_P\right]^T\left[M_P\right]\left[I_P\right]\left[\phi_N^P\right] = \left[I\right], \quad \left[\phi_N^P\right]^T\left[I_P\right]^T\left[K_P\right]\left[I_P\right]\left[\phi_N^P\right] = \left[\omega_P^2\right] \tag{73}$$

so that Equation (71) becomes

$$\left[\begin{array}{c|c} \begin{bmatrix} I & 0 \\ 0 & I \end{bmatrix} + \phi_B^T I_P^T M_P I_P \phi_B & \phi_B^T I_P^T M_P I_P \phi_N^P \\ \hline \phi_N^{P^T} I_P^T M_P I_P \phi_B & I \end{array}\right] \left\{\begin{array}{c} \ddot{q}_B \\ \hline \ddot{q}_N^P \end{array}\right\} + \left[\begin{array}{c|c} \begin{bmatrix} \left[\frac{1}{\omega_B^2}\right] & \\ 0 & \left[\omega_R^2\right] \end{bmatrix} + \phi_B^T I_P^T K_P I_P \phi_B & 0 \\ \hline 0 & \left[\omega_P^2\right] \end{array}\right] \left\{\begin{array}{c} q_B \\ \hline q_N^P \end{array}\right\} = \left\{\begin{array}{c} \phi_B^T \begin{Bmatrix} F_N^B \\ 0 \end{Bmatrix} \\ \hline 0 \end{array}\right\} \tag{74}$$

The residual mass and stiffness technique essentially improves the interface representation in the model where the model is subjected to a frequency cut-off.

The result Equation (61) can then be used in any type of modal synthesis technique such as result Equation (74). Due to this interface improvement it is now possible to truncate the high booster modes while still obtaining an acceptable accuracy. In fact, inclusion of the residual mass and or stiffness into a modal synthesis technique seems to be the most efficient approach currently available. Another very good technique is discussed in the next section.

e. The Mass and Stiffness Loading Technique

Another way of improving the interface representation in the booster model subject to frequency cut-off is given by a technique developed by Hruda and Benfield and is based on Equation (25) which we repeat here for convenience,

$$\left[\begin{array}{c|c} M_B + T_P^T M_P T_P & T_P^T M_P I_P \\ \hline I_P^T M_P T_P & I_P^T M_P I_P \end{array}\right] \left\{\begin{array}{c} \ddot{x}_B \\ \hline \ddot{x}_N^P \end{array}\right\} + \left[\begin{array}{c|c} K_B + T_P^T K_P T_P & 0 \\ \hline 0 & I_P^T K_P I_P \end{array}\right] \left\{\begin{array}{c} x_B \\ \hline x_N^P \end{array}\right\} = \left\{\begin{array}{c} G_B \\ \hline 0 \end{array}\right\} \quad (75)$$

Instead of solving eigenvalue problem (31) Hruda and Benfield propose to solve the following eigenvalue problem,

$$\left(-\omega'^2_B \left[M_B + T_P^T M_P T_P\right] + \left[K_P + T_P^T K_P T_P\right]\right) \left\{\phi'_B\right\} = \left\{0\right\} \quad (76)$$

yielding the modal transformation

$$\left\{x_B\right\} = \left[\phi'_B\right] \left\{q'_B\right\} \quad (77)$$

Again, the modal transformations (39) and (77) can be combined in

$$\left\{\begin{array}{c} x_N^B \\ \hline x_I^B \\ \hline x_N^P \end{array}\right\} = \left\{\begin{array}{c} x_B \\ \hline x_N^P \end{array}\right\} = \left[\begin{array}{c|c} \phi'_B & 0 \\ \hline 0 & \phi_N^P \end{array}\right] \left\{\begin{array}{c} q'_B \\ \hline q_N^P \end{array}\right\} \quad (78)$$

Substituting Equation (78) into Equation (75) and premultiplying by $\left[\begin{array}{c|c} \phi'_B & \\ \hline 0 & \phi_N^P \end{array}\right]^T$ yields,

$$\left[\begin{array}{c|c} I & \phi'^T_B T_P^T M_P T_P \phi_N^P \\ \hline \phi_N^{PT} I_P^T M_P T_P \phi'_B & I \end{array}\right] \left\{\begin{array}{c} \ddot{q}'_B \\ \hline \ddot{q}_N^P \end{array}\right\} + \left[\begin{array}{c|c} \left[\omega'^2_B\right] & \\ \hline & \left[\omega_P^2\right] \end{array}\right] \left\{\begin{array}{c} q'_B \\ \hline q_N^P \end{array}\right\} = \left\{\begin{array}{c} \phi'^T_B G_B \\ \hline 0 \end{array}\right\} \quad (79)$$

where we used the properties

$$\left[\phi'_B\right]^T \left[M_B + T_P^T M_P T_P\right] \left[\phi'_B\right] = \left[I\right], \quad \left[\phi'_B\right]^T \left[K_B + T_P^T K_P T_P\right] \left[\phi'_B\right] = \left[\omega'^2_B\right] \tag{80}$$

Equation (79) now replaces Equation (43). The main difference lies in the fact that in solving eigenvalue problem (76), the booster interface is mass and stiffness loaded by $[T_P^T M_P T_P]$ and $[T_P^T K_P T_P]$ respectively; i.e., the booster interface is loaded with approximate dynamic effects of the payload. In doing so, the new modes $[\phi'_B]$ and frequencies $[\omega'^2_B]$ will include a good representation of the interface, and more resemble the system modes. This allows us to reduce the number of booster modes in Equation (79) according to the predetermined cut-off frequency. The disadvantage of this method in connection with the present study is that eigenvalue problem (76) is dependent on the payload. This means that for every change in the payload we must solve this eigenvalue problem again although the booster does not change. This makes the Hruda/Benfield technique less suitable for our purposes. However, if the changes in P are small, we can use the old booster modes as a first estimate to calculate the new booster modes in a Raleigh-Ritz type eigenvalue problem solver.

f. The Coupled Base Motion Technique

The coupled base motion technique as presented in this section is another way to obtain the response of a coupled booster/payload system. This section will give us the opportunity to develop an alternative set of equations for equation (43). Indeed, we shall not only use "cantilevered" displacements for the payload P but also for the booster B, while only the interface will be free. The derivation is very similar to the one in Secton b. Let us define a transformation similar to Equation (9) but now for the booster B

$$\left\{\begin{matrix} x_N^B \\ x_I^B \end{matrix}\right\} = \left[S_B\right] \left\{x_I^B\right\} + \left\{\begin{matrix} \bar{x}_N^B \\ 0 \end{matrix}\right\} \tag{81}$$

with

$$\left[S_B\right] = -\left[K_{NN}^B\right]^{-1} \left[K_{NI}^B\right] \tag{82}$$

Equation (11) can now be replaced by

$$\left\{\begin{matrix} x_N^B \\ x_I^B \\ \hline x_N^P \\ x_I^P \end{matrix}\right\} = \left[\begin{array}{c|c|c} I & S_B & 0 \\ \hline 0 & I & 0 \\ \hline 0 & S_P & I \\ \hline 0 & I & 0 \end{array}\right] \left\{\begin{matrix} \bar{x}_N^B \\ \hline x_I^B \\ \hline \bar{x}_N^P \end{matrix}\right\} \tag{83}$$

Again, this transformation will eliminate the redundant set of displacements $\{X_I^P\}$ in Equation (3) and in the process it will also eliminate the unknown reactions $\{R_I^B\}$ and $\{R_I^P\}$

Introducing the notations

$$\left[\begin{array}{c|c|c} I & S_B & 0 \\ 0 & I & 0 \\ \hline 0 & S_P & I \\ 0 & I & 0 \end{array}\right] = \left[\begin{array}{c|c|c} I_B & T_B & 0 \\ & & 0 \\ \hline 0 & & \\ 0 & T_P & I_P \end{array}\right] = A \tag{84}$$

where this time,

$$\left[T_B\right] = \begin{bmatrix} S_B \\ I \end{bmatrix}, \left[T_P\right] = \begin{bmatrix} S_P \\ I \end{bmatrix}, \left[I_B\right] = \begin{bmatrix} I \\ 0 \end{bmatrix}, \left[I_P\right] = \begin{bmatrix} I \\ 0 \end{bmatrix} \tag{85}$$

Note that $[I_B]$ and $[I_P]$ have different dimensions, namely (BXNB) and (PXNP).

Substituting transformation (83) into Equation (3) and premultiplying by A^T yields,

$$\left[\begin{array}{c|c|c} I_B^T M_B I_B & I_B^T M_B T_B & 0 \\ \hline T_B^T M_B I_B & T_B^T M_B T_B + T_P^T M_P T_P & T_P^T M_P I_P \\ \hline 0 & I_P^T M_P T_P & I_P^T M_P I_P \end{array}\right] \left\{\begin{array}{c} \ddot{x}_N^B \\ \hline \ddot{x}_I^B \\ \hline \ddot{x}_N^P \end{array}\right\} + \left[\begin{array}{c|c|c} I_B^T K_B I_B & 0 & 0 \\ \hline 0 & T_B^T K_B T_B + T_P^T K_P T_P & 0 \\ \hline 0 & 0 & I_P^T K_P I_P \end{array}\right] \left\{\begin{array}{c} x_N^B \\ \hline x_I^B \\ \hline x_N^P \end{array}\right\}$$

$$= \left\{\begin{array}{c} I_B^T F_B \\ \hline T_B^T F_B \\ \hline 0 \end{array}\right\} \tag{86}$$

Equation (86) replaces Equation (25).

The basic idea for a base drive method is the separation of the booster response into two separate parts

$$\begin{Bmatrix} \ddot{x}_N^B \\ x_I^B \end{Bmatrix} = \begin{Bmatrix} \ddot{x}_N^B \\ x_I^B \end{Bmatrix}^F + \begin{Bmatrix} \ddot{x}_N^B \\ x_I^B \end{Bmatrix}^R \tag{87}$$

where

$$\begin{Bmatrix} x_N^B \\ x_I^B \end{Bmatrix}^F = \text{part due to the action of } \{F_B\} \text{ only} \tag{89}$$

and

$$\begin{Bmatrix} x_N^B \\ x_I^B \end{Bmatrix}^R = \text{part due to the presence of the payload (=feedback)} \tag{89}$$

It is clear that vector (86) satisfies

$$\begin{bmatrix} I_B^T M_B I_B & I_B^T M_B T_B \\ T_B^T M_B I_B & T_B^T M_B T_B \end{bmatrix} \begin{Bmatrix} \ddot{x}_N^B \\ \ddot{x}_I^B \end{Bmatrix}^F + \begin{bmatrix} I_B^T K_B I_B & 0 \\ 0 & T_B^T K_B T_B \end{bmatrix} \begin{Bmatrix} x_N^B \\ x_I^B \end{Bmatrix}^F = \begin{Bmatrix} I_B^T F_B \\ T_B^T F_B \end{Bmatrix} \tag{90}$$

The solution of Equation (90) is a one-time computational effort because it only involves booster quantities. If we now substitute Equation (87) into Equation (86) and take into account Equation (90) we obtain the following new set of equations

$$\begin{bmatrix} I_B^T M_B I_B & I_B^T M_B T_B & 0 \\ T_B^T M_B I_B & T_B^T M_B T_B + T_P^T M_P T_P & T_P^T M_P I_P \\ 0 & I_P^T M_P T_P & I_P^T M_P I_P \end{bmatrix} \begin{Bmatrix} \ddot{x}_N^{BR} \\ \ddot{x}_I^{BR} \\ \ddot{\bar{x}}_N^{P} \end{Bmatrix} + \begin{bmatrix} I_B^T K_B I_B & 0 & 0 \\ 0 & T_B^T K_B T_B + T_P^T K_P T_P & 0 \\ 0 & 0 & I_P^T K_P I_P \end{bmatrix} \begin{Bmatrix} x_N^{BR} \\ x_I^{BR} \\ \bar{x}_N^{P} \end{Bmatrix}$$

$$= - \begin{Bmatrix} 0 \\ T_P^T M_P T_P \ddot{x}_I^{BF} \\ I_P^T M_P T_P \ddot{x}_I^{BF} \end{Bmatrix} - \begin{Bmatrix} 0 \\ T_P^T K_P T_P x_I^{BF} \\ 0 \end{Bmatrix} \qquad (91)$$

where $\{\ddot{x}_I^{BF}\}$ and $\{x_I^{BF}\}$ are known from Equation (90)

The second idea of a base drive method is to consider the bottom partition of Equation (91) and write it in the following form,

$$[I_P^T M_P I_P] \{\ddot{\bar{x}}_N^{P}\} + [I_P^T K_P I_P] \{\bar{x}_N^{P}\} = - [I_P^T M_P T_P] \left(\{\ddot{x}_I^{BF}\} + \{\ddot{x}_I^{BR}\} \right) \qquad (92)$$

If one is only interested in the design of the payload, Equations (92), (7) and (87) is all we need, to determine the response of the payload. If $\{\ddot{x}_I^{BR}\}$ is known we can "base drive" the payload by the terms on the right-hand side of Equation (92) to obtain $\{\bar{x}_N^{P}\}$. Of course, $\{\ddot{x}_I^{BR}\}$ is coupled into the booster equations in Equation (91).

Equation (91) can also be written in terms of normal coordinates. To this end let us introduce the following transformation :

$$\begin{Bmatrix} \bar{x}_N^{BR} \\ x_I^{BR} \\ \bar{x}_N^{P} \end{Bmatrix} = \begin{bmatrix} \bar{\phi}_N^{B} & 0 & 0 \\ 0 & \phi_I^{B} & 0 \\ 0 & 0 & \bar{\phi}_N^{P} \end{bmatrix} \begin{Bmatrix} \bar{q}_N^{BR} \\ q_I^{BR} \\ \bar{q}_N^{P} \end{Bmatrix} \qquad (93)$$

where $[\bar{\phi}_N^B]$ and $[\phi_I^B]$ are obtained from solving the following eigenvalue problems,

$$\left[-\bar{\omega}_B^2\,[I_B^T M_B I_B] + [I_B^T K_B I_B]\right]\{\phi_N^B\} = \{0\} \tag{94}$$

$$\left[-\omega_I^2\,[T_B^T M_B T_B + T_P^T M_P T_P] + [T_B^T K_B T_B + T_P^T K_P T_P]\right]\{\phi_I^B\} = \{0\} \tag{95}$$

with

$$[\bar{\phi}_N^B]^T [I_B^T M_B I_B][\bar{\phi}_N^B] = [I],\ [\bar{\phi}_N^B]^T [I_B^T K_B I_B][\bar{\phi}_N^B] = [\bar{\omega}_B^2] \tag{96}$$

$$[\phi_I^B]^T [T_B^T M_B T_B + T_P^T M_P T_P][\phi_I^B] = [I],\ [\phi_I^B]^T [T_B^T K_B T_B + T_P^T K_P T_P][\phi_I^B] = [\omega_I^2] \tag{97}$$

where again we used the simpler notations $[\bar{\omega}_B^2]$ and $[\omega_I^2]$ instead of $[\bar{\omega}_N^{B^2}]$ and $[\omega_I^{B^2}]$.

Substituting transformation (93) into Equation (91) and premultiplying by the transpose of the square transformation matrix in Equation (93) yields the modal form,

$$\begin{bmatrix} I & \bar{\phi}_N^{B^T} I_B^T M_B T_B \phi_I^B & 0 \\ \phi_I^{B^T} T_B^T M_B I_B \bar{\phi}_N^B & I & \phi_I^{B^T} T_P^T M_P I_P \bar{\phi}_N^P \\ 0 & \bar{\phi}_N^{P^T} I_P^T M_P T_P \phi_I^B & I \end{bmatrix} \begin{Bmatrix} \ddot{\bar{q}}_N^{BR} \\ \ddot{q}_I^{BR} \\ \ddot{\bar{q}}_N^P \end{Bmatrix} + \begin{bmatrix} [\bar{\omega}_B^2] & 0 & 0 \\ 0 & [\omega_I^2] & 0 \\ 0 & 0 & [\bar{\omega}_P^2] \end{bmatrix} \begin{Bmatrix} \bar{q}_N^{BR} \\ q_I^{BR} \\ \bar{q}_N^P \end{Bmatrix} = - \begin{Bmatrix} 0 \\ \phi_I^{B^T} T_P^T M_P T_P \ddot{x}_I^{BF} \\ \bar{\phi}_N^{P^T} I_P^T M_P T_P \ddot{x}_I^{BF} \end{Bmatrix} - \begin{Bmatrix} 0 \\ \phi_I^{B^T} T_P^T K_P T_P x_I^{BF} \\ 0 \end{Bmatrix} \tag{98}$$

Equation (98) represents the coupled base drive equations of motion in modal coordinates. The main advantage of equations (98) lies in the force term of the righthand side. If many different payload configurations must be investigated, then the force term is easier to evaluate than for example the force term in equation (43). This assumes of course that the booster and its interface remains the same so that the solution of Equation (90) remains the same.

The main advantage of Equation (90) is that it is written in a form that can be used as a starting point for several short-cut methods. This will be discussed in the next chapter.

4. The Load Calculation

As discussed in Section 3, the reason for solving the equations of motion of the booster/payload system is the determination of the displacement vector $\{x_P\}$ so that we can substitute this vector into

$$\{L_e^P\} = [k_e][T_e]\{x_P\} \tag{99}$$

in order to obtain the internal structural loads $\{L_e^P\}$ on an individual member e of the payload P. In principal Equation (99) could be used as is, but this "displacement" approach turns out to be very sensitive to inaccuracies in $\{x_P\}$; e.g., truncating high frequency modes as we did in Section 3b could very easily lead to erratic loads $\{L_e^P\}$. Heuristically speaking, $\{x_P\}$ contains three parts, the static displacement, the rigid body displacement and the "vibrational" displacement.

Therefore, if one has an error in $\{x_P\}$ one necessarily affect the accuracy of all three parts. For this reason one prefers the so called "acceleration method". Basically this approach is capable of separating the static and rigid body parts from the "vibrational" displacement. As a consequence one only makes errors in the "vibrational" part which often is the smallest part of the displacement vector $\{x_P\}$. Such an "acceleration" approach which is consistent with modal synthesis techniques was developed by Hruda and Jones.[53]

Recalling Equation (83) we can write

$$\{x_P\} = [T_P]\{x_I^B\} + [I_P]\{\bar{x}_N^P\} \tag{100}$$

so that from Equation (99) we obtain

$$\{L_e^P\} = [k_e][T_e][T_P]\{x_I^B\} + [k_e][T_e][I_P]\{\bar{x}_N^P\} \tag{101}$$

From the bottom row of Equation (86) we obtain

$$\{\bar{x}_N^P\} = [I_P^T K_P I_P]^{-1}\left(-[I_P^T M_P T_P]\{\ddot{x}_I^B\} - [I_P^T M_P I_P]\{\ddot{\bar{x}}_N^P\}\right) \tag{102}$$

and from the second row Equation (86) we obtain

$$\{x_I^B\} = [T_B^T K_B T_B + T_P^T K_P T_P]^{-1}\left([T_B]^T\{F_B\} - [T_B^T M_B T_B]\{\ddot{\bar{x}}_N^B\} - [T_P^T M_P T_P]\{\ddot{\bar{x}}_N^P\}\right) \tag{103}$$

Expressions (102) and (103) can now be substituted into Equation (101) yielding an equation for $\{L_e^P\}$ in terms of accelerations. Many of the matrix multiplications involved in Equations (101-103) can be simplified by using a unit load solution, which is a feature of most finite element programs

After this, it is possible to introduce cantilevered modes for the booster and the payload(s) and truncate these modes according to a preset cut-off frequency. In Chapter II we shall discuss the load calculation procedure in more detail.

5. Assessment

There are very few publications dealing with the comparison of the different full-scale payload integration methods. In this section we shall discuss two such studies. A study by R. Hruda shows that the residual mass and flexibility approach is one of the most effective in terms of cost, convenience and accuracy. The Craig/Bampton technique using interface payload(s) is also one of the best techniques.

As a test structure, Hruda used two planar trusses coupled together by a statically indeterminate interface (Figure 2). Five different techniques were compared to the exact solution, i.e., the solution in the discrete time domain as discussed in Section 3a.:

1. Hruda/Benfield Technique - (Section 3e.): inertial coupling of truss-2 constrained modes onto free-free modes of truss-1 which was mass and stiffness loaded at its truss-2 interface degrees-of-freedom by the interface properties of truss-2. (IMSL)

2. Craig/Bampton Technique (modal verson of Equation (86)): inertial coupling of truss-1 and truss-2 constrained modes onto a free-free modal representation of the interface degrees-of-freedom. (I/F)

3. MacNeal Technique: residual flexibility approach of coupling truss-2 constrained modes onto free-free modes of truss-1 which creates stiffness coupling (residual mass not included). (RFSWOM)

4. Rubin Technique: (the residual mass and flexibility technique - secton 3d.): coupling of truss-2 constrained modes onto free-free modes of truss-1 which yields only inertial coupling, and, by consistent application to the mass and stiffness terms in the equations of motion, yields both residual stiffness and residual mass terms. (RFIWM)

5. Rubin Technique but without residual mass constribution for truss-1.

The truss problem as illustrated in Figure 2 represents a planar problem with three rigid body degrees of freedom (two translational, one rotational). Each pinned joint has two translational degrees of freedom. The interface is statically indeterminate because there are six interface degrees of freedom. The heavy masses (asymmetric with respect to interface) are added to produce interface distortion. The forcing function is a ramp function. (RFIWOM)

The "exact" results, against which all comparisons were made, were obtained by extracting eigenvalues, eigenvectors, and loads directly from a finite element discrete/physical model using no modes at all.

Five different cases we investigated

EXACT: Discrete modal 70 DOF

CASE A: Modally coupled, 70 modes retained (=100%)

CASE B: Modally coupled, 50 modes retained (=71%)

CASE C: Modally coupled, 32 modes retained (=46%)

CASE F: Modally coupled, 19 modes retained (=27%)

Hruda used the following comparison values:

Frequencies: Percent error against the "exact" solution

Modes: An error vector is formed($\phi_N - \phi_E$) and its norm is calculated (which is defined as the Root Square Sum of the the elements of the vector); the comparison value is then defined as the norm of the error divided by the norm of the base/exact mode. Note that the norms are based on the modal amplitudes of all degrees of freedom from the coupled system.

Loads: Loads were calculated at the truss interface on both the truss-1 and truss-2 joints. A percent error of the absolute value of the largest (either maximum or minimum) value from a given case against the absolute value of the largest value from the exact solution.

i.e.

$$\text{Frequency comparison value} = \frac{\omega_N - \omega_E}{\omega_E} \times 100$$

$$\text{Mode comparison value} = \frac{\text{RSS}\ (\ \phi_N - \phi_E\ )}{\text{RSS}\ \phi_E} \times 100$$

$$\text{Load comparison value} = \frac{L_N - L_E}{L_E} \times 100$$

where E = Exact, and N = Case being compared.

The results are presented in Tables 1-12

For the 100% case-A, the MacNeal technique requires the inversion of the residual flexibility matrix to obtain a "residual stiffness". When attempting to retain all (100%) of the modes, this residual flexibility matrix is a function of the interface highest frequency modal amplitudes which can cause an ill-conditioned matrix (as in the present case). Since this is an unrepresentative case, it should not be deduced that this is an unacceptable technique. As can be seen in succeeding cases, where more residual modes are available, the MacNeal technique falls into line with other techniques. Note that in cases B, C, and F, in both the frequency and mode shape comparisons, that the MacNeal and the Rubin technique without residual mass are identical, thereby numerically supporting R. Coppolino's contention that these two techniques are equivalent for modal synthesis. In comparing the loads it is seen that the MacNeal column for case-A reflects the propagation of the ill-conditioning mentioned earlier. Loads were calculated by the modal acceleration technique (Section 4) for all methods except for the MacNeal technique.

Due to the stiffness coupling involved in the MacNeal method, a complete modal acceleration technique for calculating loads could not be used, therefore, the modal displacement techniques of calculating loads was used. Because of this, the larger loads inaccuracies for this method must be attributed to the method of loads calculation and not to the method itself.

In conclusion we can state that methods 1 through 5 are acceptable. However, the Rubin Technique (Residual Mass and Stiffness Approach) seems to outweigh the other approaches in terms of cost and convenience. Again, it should be noted that this method does not require any knowledge of payload properties which makes it very valuable for analysis of STS-applications.

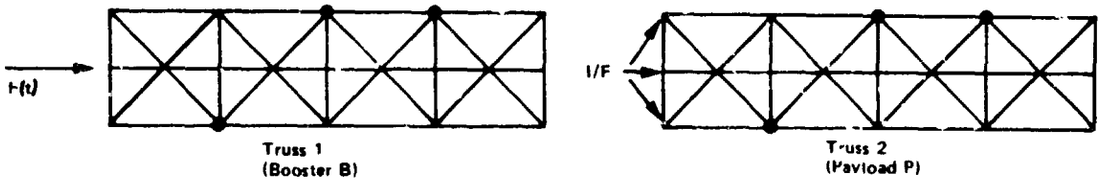

Figure 2 Structure Used for Comparing Coupling Techniques

Table 1: Frequency Comparison
Case A = 100% of Available Modes
% Diff for Various Modal Coupling Tech

Mode No	Exact Freq (Hz)	IMSL	1/F	RFSWOM	RFIWM	RFIWOM
4	.76	-.00	-.00	-49.17	-.00	-.00
5	1.75	-.00	-.00	6.75	-.00	.00
6	2.84	-.00	-.00	-21.81	-.00	-.00
7	3.08	-.00	-.00	-3.63	-.00	.00
8	3.80	-.00	-.00	-9.24	-.00	.00
9	4.62	-.00	-.00	-16.35	-.00	.00
10	5.11	-.00	-.00	-24.08	-.00	.00
11	5.50	-.00	-.00	-6.02	-.00	.00
12	5.81	-.00	-.00	-3.31	-.00	.00
13	7.69	.00	-.00	-6.08	-.00	.00
14	8.69	-.00	-.00	-.60	-.00	.00
15	9.14	-.00	-.00	-3.32	-.00	.00
16	9.42	-.00	-.00	-1.76	-.00	.00
17	9.73	-.00	-.00	-.92	-.00	.00
18	9.85	-.00	-.00	-.98	-.00	-.00
19	10.36	-.00	-.00	-1.36	-.00	.00
20	10.43	-.00	-.00	-.33	-.00	.00
21	10.79	-.00	-.00	-2.99	-.00	.00
22	10.90	-.00	-.00	-2.55	-.00	.00
23	11.37	-.00	-.00	-1.85	-.00	.00
24	11.49	-.00	-.00	.80	-.00	.00
25	11.78	-.00	-.00	.39	-.00	.00
26	11.96	-.00	-.00	-.12	-.00	.00
27	12.03	-.00	-.00	.19	-.00	.00
28	12.20	-.00	-.00	.40	-.00	.00
29	12.43	-.00	-.00	.12	-.00	.00
0	12.50	-.00	-.00	5.58	-.00	.00
31	12.75	-.00	-.00	4.00	-.00	.00
32	13.29	-.00	-.00	2.54	-.00	.00
33	13.51	-.00	-.00	3.12	-.00	.00
34	14.22	-.00	-.00	-.19	-.00	.00
35	14.53	-.00	-.00	.31	-.00	.00
36	14.86	-.00	-.00	-.11	-.00	.00
37	15.19	-.00	-.00	1.59	-.00	.00
38	15.54	-.00	-.00	1.23	-.00	.00
39	15.69	-.00	-.00	2.50	-.00	.00
40	16.16	-.00	-.00	.55	-.00	.00
41	16.17	-.00	-.00	.66	-.00	00
42	16.28	-.00	-.00	3.34	-.00	.00
43	16.86	-.00	-.00	.46	-.00	.00
44	17.07	-.00	-.00	.21	-.00	.00
45	17.17	-.00	-.00	5.12	-.00	.00
46	18.17	-.00	-.00	.03	-.00	.00
47	18.17	-.00	-.00	10.47	-.00	.00

Table 1: Frequency Comparison (Concl)
Case A = 100% of Available Modes
% Diff for Various Modal Coupling Tech

Mode No	Exact Freq (Hz)	IMSL	I/F	RFSWOM	RFIWM	RFIWOM
48	20.11	-.00	-.00	.81	-.00	.00
49	20.27	-.00	-.00	3.02	-.00	.00
50	21.11	-.00	-.00	.14	-.00	.00
51	21.15	-.00	-.00	.08	-.00	.00
52	21.26	-.00	-.00	.07	-.00	.00
53	21.29	-.00	-.00	.53	-.00	.00
54	21.45	-.00	-.00	.02	-.00	.00
55	21.47	-.00	-.00	2.91	-.00	.00
56	22.06	-.00	-.00	.45	-.00	.00
57	22.15	-.00	-.00	2.18	-.00	.00
58	22.63	-.00	-.00	5.09	-.00	.00

Table 2: Fr uency Comparison
Case B = 71% Available Modes
% Diff for Vario., Modal Coupling Tech

Mode No	Exact Freq (Hz)	IMSL	I/F	RFSWOM	RFIWM	RFIWOM
4	.76	.00	.00	.00	.00	.00
5	1.75	.00	.0C	.00	.00	.00
6	2.84	.00	.00	.00	.00	.02
7	3.08	.00	.00	.00	.00	.06
8	3.80	.00	.00	.00	.00	.00
9	4.62	.00	.00	.04	.00	.04
10	5.11	.00	.00	.00	.00	.00
11	5.50	.00	.00	.05	.00	.05
12	5.81	.04	.05	.03	.03	.03
13	7.60	.00	.00	.21	.00	.21
14	8.69	.02	.02	.03	.01	.03
15	9.14	.04	.06	.12	.04	.12
16	9.42	.01	.01	.01	.00	.01
17	9.73	.01	.02	.02	.01	.02
18	9.85	.03	.04	.03	.03	.03
19	10.36	.01	.01	.06	.01	.06
20	10.43	.00	.00	.01	.00	.01
21	10.79	.03	.05	.04	.02	.04
33	10.90	.03	.03	.04	.02	.04
23	11.37	.00	.00	.03	.00	.03
24	11.49	.00	.01	.05	.00	.05
25	11.78	.03	.03	.08	.03	.08
26	11.96	.08	.09	.08	.07	.08
27	12.03	.02	.03	.04	.02	.04
28	12.20	.13	.13	.10	.10	.10
29	12.43	.01	.01	.02	.00	.02
30	12.50	.03	.09	.07	.03	.07
31	12.75	.07	.07	.08	.06	.08
32	13.29	.04	.05	.06	.02	.06
33	13.51	.0E	.07	.07	.05	.07
34	14.22	.13	.13	.78	.09	.78
35	14.53	.09	.13	.29	.07	.29
36	14.86	.01	.01	.17	.01	.17
37	15.19	.06	.07	.11	.05	.11
38	15.54	.01	.03	1.17	.04	1.17
39	15.69	.02	.02	1.61	.03	1.61
40	16.16	.01	.02	.13	.09	.13
41	16.17	.07	.08	2.68	.12	2.68
42	16.28	.37	.44	3.88	.34	3.88
43	16.86	.13.	.12	7.73	.25	7.73
44	17.07	.06	.10	18.51	1.52	18.51
45	17.17	1.00	1.00	66.94	5.86	66.94
46	18.17	.02	.02	72.29	9.54	72.29

Table 2: Frequency Comparison (Concl)
Case B = 71% of Available Modes
% Diff for Various Modal Coupling Tech

Mode No	Exact Freq (Hz)	IMSL	I/F	RFSWOM	RFIWM	RFIWOM
47	18.17	.03	.04	122.22	11.51	122.22
48	20.11	.07	.09	473.05	7.55	473.05
49	20.27	.31	.3	962.70	8.65	902.70
50	21.11	4.07	4.20	536.67	19.40	536.67

Table 3: Frequency Comparison
Case C = 46% of Available Modes
% Diff for Various Modal Coupling Tech

Mode No	Exact Freq (Hz)	IMSL	I/F	RFSWOM	RFIWM	RFIWOM
4	.76	.00	.00	.02	.00	.02
5	1.75	.02	.00	.00	.00	.00
6	2.84	.04	.02	.12	.01	.12
7	3.08	.01	.00	.28	.00	.28
8	3.80	.02	.00	.00	.00	.00
9	4.62	.12	.05	.26	.02	.28
10	5.11	.02	.01	.01	.00	.01
11	5.50	.26	.10	.35	.05	.35
12	5.81	.16	.24	.12	.08	.12
13	7.69	.03	.04	1.55	.06	1.55
14	8.69	.14	.22	.17	.08	.17
15	9.14	.32	.33	.41	.17	.41
16	9.42	.05	.07	.07	.01	.07
17	9.73	.13	.18	.34	.08	.34
18	9.85	.30	.27	.31	.18	.31
19	10.36	.11	.11	.51	.12	.51
20	10.43	.09	.04	.45	.02	.45
21	10.79	.17	.33	.73	.11	.73
22	10.90	.41	.42	3.43	.55	3.43
23	11.37	.06	.04	3.23	1.49	3.23
24	11.49	.04	.11	5.14	3.66	5.14
25	11.78	.17	.17	5.52	2.76	5.52
26	11.96	.40	.90	4.79	3.70	4.79
27	12.03	.30	3.16	53.65	4.71	53.65
28	12.20	1.73	2.35	77.63	3.91	77.63
29	12.43	.41	4.66	80.30	14.58	80.30
30	12.50	1.94	12.32	143.04	22.38	143.04
31	12.75	3.52	14.90	167.76	29.91	167.76
32	13.29	11.88	61.19	630.91	63.27	630.19

Table 4: Frequency Comparison
Case F = 27% of Available Modes
% Diff for Various Modal Coupling Tech

Mode No	Exact Freq (Hz)	IMSL	I/F	RFSWOM	RFIWM	RFIWOM
4	.76	.00	.00	.05	.00	.05
5	1.75	.02	.00	.02	.00	.02
6	2.84	.06	.06	.31	.03	.31
7	3.08	.07	.00	4.32	.19	4.32
8	3.80	.03	.01	.03	.00	.03
9	4.62	.18	.14	.71	.08	.71
10	5.11	.05	.03	.03	.01	.03
11	5.50	.46	.34	1.64	.49	1.64
12	5.81	1.03	1.13	23.29	4.70	23.29
13	7.69	.14	.16	15.39	8.20	15.39
14	8.69	1.05	1.14	45.28	1.30	45.28
15	9.14	1.20	6.85	84.43	8.49	84.48
16	9.42	.37	27.17	98.00	27.57	98.00
17	9.73	2.23	36.67	97.08	36.41	97.08
18	9.85	18.25	37.17	203.74	37.43	203.74
19	10.36	22.07	103.62	279.52	105.23	279.52

Table 5: Mode Shape Comparison
Case A = 100% of Available Modes
% Diff for Various Modal Coupling Tech.

Mode No	Exact Freq (HZ)	IMSL	I/F	RFSWOM	RFIWM	RFIWOM
4	14.84	.00	.00	104.09	.00	.00
5	13.95	.00	.00	92.76	.00	.01
6	13.45	.00	.00	104.91	.00	.01
7	13.70	.00	.00	94.49	.00	.02
8	12.23	.00	.00	132.95	.00	.02
9	11.21	.00	.00	100.73	.00	.03
10	9.54	.00	.00	153.35	.00	.05
11	8.75	.00	.00	104.39	.00	.12
12	13.25	.00	.00	129.05	.00	.08
13	10.51	.00	.00	186.06	.00	.18
14	11.49	.00	.00	96.78	.00	.04
15	11.24	.00	.00	102.21	.00	.16
16	14.5	.00	.00	71.19	.00	.07
17	13.16	.00	.00	141.80	.00	.09
18	13.99	.00	.00	90.01	.00	.02
19	15.47	.00	.00	81.01	.00	.12
20	13.49	.00	.00	99.38	.00	.05
21	12.74	.00	.00	136.40	.00	.13
22	15.25	.00	.00	138.19	.00	.15
23	16.56	.00	.00	132.20	.00	.15
24	18.06	.00	.00	100.18	.00	.25
25	17.70	.00	.00	132.72	.00	.18
26	17.29	.00	.00	142.58	.00	.17
27	16.94	.00	.00	68.01	.00	.09
28	17.58	.00	.00	69.89	.00	.03
29	17.06	.00	.00	41.89	.00	.19
30	16.31	.00	.00	138.22	.00	.28
31	15.86	.00	.00	149.30	.00	.01
32	18.16	.00	.00	138.85	.00	.08
33	16.92	.00	.00	148.49	.00	.11
34	15.21	.00	.00	91.84	.00	.84
35	18.67	.00	.00	75.41	.00	.52
36	18.48	.00	.00	49.75	.00	.36
37	17.23	.00	.00	89.32	.00	.16
38	18.14	.00	.00	145.84	.00	1.36
39	18.12	.00	.00	146.47	.00	.72
40	18.82	.00	.00	160.19	.00	.51
41	19.22	.00	.00	126.88	.00	.56
42	15.63	.00	.00	162.42	.00	.90
43	18.47	.00	.00	124.22	.00	1.12
44	19.44	.00	.00	61.05	.00	.45
45	16.54	.00	.00	135.41	.00	.84
46	18.17	.00	.00	54.79	.00	.52

Table 5: Mode Shape Comparison (Concl)
Case A = 100% of Available Modes
% Diff for Various Modal Coupling Tech.

Mode No	Exact Freq (HZ)	IMSL	I/F	RFSWOM	RFIWM	RFIWOM
47	18.33	.00	.00	142.35	.00	.30
48	18.25	.00	.00	145.79	.00	2.22
49	19.16	.00	.00	139.28	.00	.27
50	19.29	.00	.00	65.342	.00	2.16
51	19.51	.00	.00	62.72	.00	1.22
52	19.17	.00	.00	52.42	.00	3.43
53	18.89	.00	.00	105.50	.00	4.69
54	19.52	.00	.00	38.21	.00	1.48
55	19.13	.00	.00	103.39	.00	2.35
56	11.17	.00	.00	161.11	.00	5.68
57	19.81	.00	.00	11.29	.00	.17
58	19.81	.00	.00	135.33	.00	.09

Table 6: Mode Shape Comparison
Case B = 71% of Available Modes
% Diff for Various Modal Coupling Tech.

Mode No	Exact Freq (HZ)	IMSL	I/F	RFSWOM	RFIWM	RFIWOM
4	14.84	.00	.00	.00	.00	.00
5	13.05	.02	.01	.01	.01	.01
6	13.45	.04	.03	.18	.02	.18
7	13.70	.07	.01	.23	.01	.23
8	12.23	.08	.06	.06	.05	.06
9	11.21	.12	.08	.33	.06	.33
10	9.54	.16	.18	.16	.15	.16
11	8.75	.22	.22	.66	.14	.66
12	13.25	.80	.89	.76	.70	.76
13	10.51	.30	.41	1.78	.27	1.78
14	11.49	.91	1.21	.88	.57	.88
15	11.24	1.75	2.05	2.53	1.67	2.53
16	14.55	.61	.71	.95	.34	.95
17	13.16	1.02	1.10	1.02	.70	1.02
18	13.99	1.52	1.67	1.63	1.50	1.63
19	15.47	1.28	1.03	1.86	.77	1.86
20	13.49	1.30	1.03	1.21	.75	1.21
21	12.74	1.54	2.02	2.20	1.23	2.20
22	15.25	1.93	1.84	1.98	1.50	1.98
23	16.56	.38	.62	3.31	.12	3.31
24	18.06	.32	.81	3.56	.31	3.56
25	17.70	3.44	3.63	4.94	3.43	4.94
26	17.29	9.71	9.84	8.91	8.36	8.91
27	16.94	8.37	8.24	7.18	7.04	7.18
28	17.58	7.16	7.15	6.09	5.94	6.09
29	17.06	1.11	2.22	3.50	.79	3.50
30	16.31	3.83	5.48	5.80	3.52	5.80
31	15.88	3.90	3.89	4.95	3.86	4.95
32	18.16	2.81	2.72	4.45	2.02	4.45
33	16.92	4.06	3.29	3.91	2.92	3.91
34	15.21	6.36	4.34	25.34	4.43	25.34
35	18.67	5.53	5.12	22.71	.42	22.71
36	18.48	1.64	1.62	16.67	1.79	16.67
37	17.23	4.65	5.05	12.42	3.98	12.42
38	18.14	1.43	2.71	71.43	6.38	71.43
39	18.12	2.45	2.06	189.04	4.32	189.04
40	18.82	35.48	19.60	104.85	60.42	104.85
41	19.22	39.52	27.36	128.81	60.10	128.81
42	15.63	26.78	27.93	126.75	28.17	126.75
43	18.47	9.51	9.90	140.52	38.29	140.52
44	19.44	14.36	15.85	144.04	126.68	144.04
45	16.54	24.08	24.65	213.55	142.78	213.55
46	18.17	3.25	4.86	150.22	123.17	150.22

Table 6: Mode Shape Comparison (Concl)
Case B = 71% of Available Modes
% Diff for Various Modal Coupling Tech.

Mode No	Exact Freq (HZ)	IMSL	I/F	RFSWOM	RFIWM	RFIWOM
47	18.33	4.54	5.77	250.51	144.13	250.51
48	18.25	62.46	70.50	553.15	77.72	553.15
49	19.16	57.97	66.55	965.00	130.07	985.90
50	19.29	114.23	116.94	930.68	128.01	930.68

Table 7: Mode Shape Comparison
Case C = 46% of Available Modes
% Diff for Various Modal Coupling Tech.

Mode No	Exact Freq (HZ)	IMSL	I/F	RFSWOM	RFIWM	RFIWOM
4	14.84	.02	.02	.03	.02	.03
5	13.95	.18	.04	.03	.03	.03
6	13.45	.47	.45	.49	.31	.49
7	13.70	.31	.10	.55	.13	.55
8	12.23	.54	.23	.18	.16	.18
9	11.21	.1.59	1.30	2.00	.90	2.00
10	9.54	1.10	.74	.41	.36	.41
11	8.75	2.79	3.01	3.61	1.79	3.61
12	13.25	2.50	3.48	2.42	1.79	2.42
13	10.51	1.92	2.35	9.62	2.83	9.62
14	11.49	4.84	7.14	5.19	3.88	5.19
15	11.24	8.72	9.37	8.63	5.92	8.63
16	14.55	3.33	4.77	3.71	1.62	3.71
17	13.16	9.03	90.46	13.85	5.90	13.85
18	13.99	11.17	10.37	13.28	7.67	13.28
19	15.47	12.62	11.13	68.73	9.12	68.73
20	13.49	13.23	10.81	81.34	7.28	81.34
21	12.74	7.56	16.01	46.68	10.40	46.68
22	14.25	16.60	19.11	54.62	20.68	54.62
23	16.56	6.01	5.57	123.28	97.95	123.28
24	18.06	4.87	9.79	129.15	145.42	129.15
25	17.70	17.82	16.45	135.79	155.65	135.79
26	17.29	68.71	127.43	150.09	124.74	150.09
27	16.94	72.98	144.11	134.45	120.45	134.45
28	17.58	103.74	98.65	152.44	150.49	152.44
29	17.06	81.82	139.33	166.49	128.91	166.49
30	16.31	110.88	130.70	145.30	111.59	145.30
31	15.86	95.31	153.24	243.62	141.77	243.62
32	18.16	101.15	122.19	695.80	128.54	695.89

Table 8: Mode Shape Comparison
Case F = 27% of Available Modes
% Diff for Various Modal Coupling Tech.

Mode No	Exact Freq (HZ)	IMSL	I/F	RFSWOM	RFIWM	RFIWOM
4	14.84	.04	.05	.06	.03	.06
5	13.95	.24	.07	.26	.06	.26
6	13.45	.71	.89	2.63	.71	2.63
7	13.70	1.02	.20	8.69	2.36	8.69
8	12.23	.74	.39	1.48	.42	1.48
9	11.21	2.58	2.75	4.62	1.96	4.62
10	9.54	2.84	2.19	1.40	.98	1.40
11	8.75	10.05	9.34	38.19	23.43	38.19
12	13.25	10.96	11.05	65.52	28.35	65.52
13	10.51	7.03	7.59	128.49	53.35	128.49
14	11.49	29.41	33.79	159.45	43.11	159.45
15	11.24	33.59	66.95	167.22	88.27	167.22
16	14.55	30.24	113.08	161.12	119.44	161.12
17	13.16	111.59	138.72	161.33	140.08	161.33
18	13.99	123.87	130.93	148.55	132.90	148.55
19	15.47	148.78	127.29	379.09	127.01	379.09

Table 9
Comparisons of Maximum Absolute Values of Interface Loads
Case A = 100% of Available Modes

Load No.	Exact Load (lbs)	Percent Difference - ABS. Max. Loads				
		IMSL	I/F	RFSWOM	RFIWM	RFIWOM
1	-481.999	0.	-.00	3419.56	.00	-.05
3	-202.138	0.	-.00	10154.67	.00	-.08
5	-498.819	0.	.00	3957.31	-.00	.11
7	474.713	0.	-.00	2208.71	.00	-.03
9	191.901	0.	-.00	22733.86	.00	-.02
11	486.870	0.	.00	17322.92	.00	.03

IMSL = Inertial Coupling W/ Mass and Stiffness Loading
I/F = Interface Method of Inertial Coupling
RFSWOM = Residual Flexibility with Stiffness Coupling, without Residual Mass
RFIWM = Residual Flexibility with Inertial Coupling, with Residual Mass
RFIWOM = Residual Flexibility with Inertial Coupling, without Residual Mass

Table 10
Comparisons of Maximum Absolute Values of Interface Loads
Case B = 71% of Available Modes

		Percent Difference - ABS. Max. Loads				
Load No.	Exact Load (lbs)	IMSL	I/F	RFSWOM	RFIWM	RFIWOM
1	-481.999	.10	-.00	2.08	.10	-.38
3	-202.138	.26	.27	2.62	.27	.26
5	-498.819	.12	.13	-.13	.14	-.20
7	474.713	.17	.15	-1.36	.18	.22
9	191.901	.15	.18	.26	.13	-.24
11	486.870	.19	.19	2.00	.24	-.10

*MSL = Inertial Coupling W/ Mass and Stiffness Loading
I/F = Interface Method of Inertial Coupling
RFSWOM = Residual Flexibility with Stiffness Coupling- without Residual Mass
RFIWM = Residual Flexibility with Inertial Coupling, with Residual Mass
RFIWOM = Residual Flexibility with Inertial Coupling, without Residual Mass

Table 11
Comparisons of Maximum Absolute Values of Interface Loads
Case C = 46% of Available Modes

Load No.	Exact Load (lbs)	Percent Difference - ABS. Max. Loads IMSL	I/F	RFSWOM	RFIWM	RFIWOM
1	-481.999	-1.32	-1.29	-4.07	-1.09	.29
3	-202.138	2.34	2.33	3.10	2.43	3.19
5	-498.819	.25	.39	-7.33	.45	.17
7	474.713	-1.48	-1.43	2.93	-1.36	-.34
9	191.901	.00	-.12	-25.44	-.07	-1.48
11	486.870	-.85	-.77	-3.83	-.78	-.73

IMSL = Inertial Coupling W/ Mass and Stiffness Loading
I/F = Interface Method of Inertial Coupling
RFSWOM = Residual Flexibility with Stiffness Coupling, without Residual Mass
RFIWM = Residual Flexibility with Inertial Coupling, with Residual Mass
RFIWOM = Residual Flexibility with Inertial Coupling, without Residual Mass

Table 12
Comparisons of Maximum Absolute Values of Interface Loads
Case F = 27% of Available Modes

Load No.	Exact Load (lbs)	Percent Difference - ABS. Max. Loads IMSL	I/F	RFSWOM	RFIWM	RFIWOM
1	-481.999	-2.45	-2.88	6.38	-6.66	-2.60
3	-202.138	3.04	-2.85	5.68	-10.99	.27
5	-498.819	-2.24	-2.61	8.02	-4.49	-1.85
7	474.713	-3.82	-4.44	10.81	-8.79	-10.31
9	191.901	-2.79	-.54	21.52	-7.54	-14.78
11	486.870	-.08	-.48	17.06	-4.28	-7.60

IMSL = Inertial Coupling W/ Mass and Stiffness Loading
I/F = Interface Method of Inertial Coupling
RFSWOM = Residual Flexibility with Stiffness Coupling, without Residual Mass
RFIWM = Residual Flexibility with Inertial Coupling, with Residual Mass
RFIWOM = Residual Flexibility with Inertial Coupling, without Residual Mass

Another comparison study of modal synthesis methods was conducted by W. Benfield, C. Bodley and G. Morosow. Here are a few extracts from that publication.

Some of the earliest formal documentation on modal synthesis is accredited to Hunn and Gladwell. Although their methods yield good accuracy, they are restricted to structures with statically determinate interfaces and have been somewhat overshadowed by more recent developments. In this paper, only methods applicable to redundant interface connections are compared.

Hurty developed the first modal synthesis method capable of analyzing structures with redundant interface connections. In this method, the component vibration modes are determined with all interface coordinates fixed, and are thus callled fixed-constraint modes, and fixed-constraint, natural vibration modes are used as the generalized coordinates to determine the modes of the system.

Bajan and Feng and Craig and Bampton introduced the concept of using only constraint modes, thus eliminating the need to distinguish rigid-body modes and redundant constraint modes. The fixed-constraint, natural-vibration modes of each component are determined in the same manner as in Hurty's method. The constraint modes and fixed-constraint, natural-vibration modes are then used as the generalized coordinates to determine the system modes.

Goldman developed a method of vibration analysis using dynamic participating. In his method, the component vibration modes are free-free, rather than fixed-constraint modes. Rigid body modes and selected component vibration modes are used to solve the interconnection problem. This eliminates the need for constraint modes. The component free-free vibration modes are then used as generalized coordinates to determine the modes of the system.

Hou has described a method for modal synthesis that also uses free-free component vibration modes. Constraint modes are not used. Selected component modes are used to connect the components together. These modes then become dependent coordinates thus reducing the number of independent, generalized coordinates by an amount equal to the number of system interface coordinates.

Benfield and Hruda presented a method of component mode substitution using either free-free or constrained component modes called branch modes. Constraint modes are used for constrained components, but these are reduced to dependent coordinates rather than carried in the solution as independent coordinates. Only the component vibration modes are used as generalized coordinates to determine the system modes. In addition they also presented the concept of using interface-loaded component modes to improve the accuracy of the solution.

In general, the methods that used constrained-component vibration modes produced more accurate results than those that used free-free vibration modes. Furthermore, methods that used component mass and stiffness matrices were more accurate than those that did not.

The features of the methods can be summarized as follows.

Method 1 - Benfield and Hruda, Free-Free Component Modes

- Less accurate
- Uses free-free component modes
- Easy to use, since no constraint modes or matrix inversions are used.
- Requires mass and stiffness matrices for the components.

Method 2 - Benfield and Hruda, Free-Free Component Modes, with Interface Loading

- Good accuracy
- Uses free-free, interface-loaded component modes
- Requires constraint modes or reducing transformations for each component.
- Requires mass and stiffness matrices for the components.
- Requires interface loading of component modes. As a result, other attached components affect the component modes.

Method 3 - Benfield and Hruda, Constrained Component Modes

- Good accuracy
- Uses constrained-component branch modes.
- More difficult to set up for many components
- Requires constraint modes for each component
- Requires mass and stiffness matrices for the components

Method 4 - Benfield and Hrude, Constrained Component Modes with Interface Loading

- One of the most accurate
- Uses constrained-component branch modes
- More difficult to set up for many components
- Requires constraint modes for each component
- Requires mass and stiffness matrices for the components
- Requires interface loading of component modes. As a result, other attached components affect the component modes.

Method 5 - Hurty

- One of the most accurate
- Uses fixed interface component modes
- Requires mass and stifness matrices for the components
- System rigid-body and redundant interface generalized coordinates must be retained as additional degrees of freedom in the modal solution. For structures having a large number of interface coordinates, the number of component modes used may be limited.

Method 6 - Bajan and Feng, and Craig and Bampton

- One of the most accurate
- Uses fixed-interface component modes
- Requires constraint modes. This method is more convenient to use since it is not necessary to identify statically determinate and redundant interface coordinates.
- Requires mass and stiffness matrices for the components.
- System interface generalized coordinates must be retained as additional degrees of freedom in the modal solution. For structures having a large number of interface connections, the number of component modes used may be limited.

Method 7 - Goldman

- One of the least accurate.

- Uses free-free component modes.

- Modal selection is important. A matrix inversion is required, and the matrix must have the same size as the number of interface coordinates. Since an ill-conditioned inversion may result from improperly selecting the component modes, it is desirable to have as few interface coordinates as possible.

- The modal stiffness matrix is nonsymmetric

- Does not require mass and stiffness matrices for the components. Thus, system modes may be synthesized using only the component modes.

- The first n modes in the system eigenvalue-eigenvector solution are not usable. (Here n is equal to the number of system interface connections).

Method 8 - Hou

- One of the least accurate

- Uses free-free component modes

- Modal selection is important. A nonsymmetric matrix inversion is required, and the matrix must have the same size as the number of interface connections. An ill-conditioned inversion may result from improperly selecting component modes. Thus, it is desirable to have as few interface coordinates as possible.

- Does not require mass and stiffness matrices for the components. Therefore, system modes may be synthesized using only the component modes.

- The number of component modal coordinates used in the system modal solution is reduced by n (where n is equal to the number of system interface coordinates).

B. SHORT-CUT TECHNIQUES

1. Introduction

In Section A we discussed several techniques to obtain the response of a booster/payload system. All these techniques necessitate the solution of the coupled booster/payload equations, i.e., they are "full-scale" methods. As we pointed out before, this solution is quite expensive, especially if it has to be repeated several times, for example during a design effort. Although mass and stiffness changes during a design effort are often small, current practices used to design payload structures require a new "full-scale" solution every time such small changes in the payload are made. A similar situation exists in the case of payloads that are designed for multiple flights with moderate configuration changes.

A need exists for the development of "short-cut" methods. The term "short-cut" method implies that the method should be able to evaluate small changes in the payload in a relatively short time. First, a short-cut method should avoid the direct solution of the coupled equations of the booster/payload system. Secondly, it should avoid as much as possible the interfacing between different organizations. This means that one should strive towards as much independence for the payload design organization as possible.

The objective then of Section B is to present several of the most promising of these short-cut methods. The first of these methods will be discussed in the next section.

2. The Perturbation Technique

In this section we shall discuss a short-cut method which is based on a well known perturbation technique. We shall first discuss the perturbation technique in general terms and then apply it to the particular problem of a booster/payload system.

Let us consider a set of equations of motion of a certain structure,

$$[M_0]\{\ddot{x}\} + [K_0]\{x\} = \{F\} \tag{104}$$

where $[M_0]$ and $[K_0]$ are the mass and stiffness matrix of the structure, respectively. The vectors $\{x\}$ and $\{F\}$ are the generalized discrete displacement and force vectors. The eigenvalue problem associated with Equation (104) can be written as

$$\left(-\omega_0^2\ [M_0] + [K_0]\right)\{\phi_0\} = \{0\} \tag{105}$$

The solution of this eigenvalue problem yields a modal matrix $[\phi_0]$ and a diagonal eigenvalue matrix $[\omega_0^2]$ satisfying

$$[\phi_0]^T [M_0][\phi_0] = [I], \quad [\phi_0]^T [K_0][\phi_0] = [\omega_0^2] \tag{106}$$

Next, let us assume that the elements of $[M_0]$ and $[K_0]$ undergo small changes, so that the new system of equations can be written as follows

$$[M]\{\ddot{x}\} + [K]\{x\} = \{F\} \tag{107}$$

with

$$[M] = [M_0] + \varepsilon[M_1], \quad [K] = [K_0] + \varepsilon[K_1] \tag{108}$$

where ε is a small parameter such that

$$\varepsilon[M_1] = [M] - [M_0], \quad \varepsilon[K_1] = [K] - [K_0] \tag{109}$$

Note that the matrix differences on the right-hand sides of Equations (109) are small, so that it is easy to determine a small ε so that $[M_1]$ and $[K_1]$ are of the same order of magnitude as $[M]$, $[M_0]$ and $[K]$, $[K_0]$.

The objective of the perturbation technique is to obtain a solution for the new eigenvalue problem associated with Equation (107).

$$\left(-\omega^2 [M] + [K]\right)\{\phi\} = \{0\} \tag{110}$$

without actually solving Equation (110). To this end, let us write

$$\{x\} = \{x_0\} + \varepsilon\{x_1\} + \varepsilon^2\{x_2\} + \ldots \tag{111}$$

$$\{\phi\} = \{\phi_0\} + \varepsilon\{\phi_1\} + \varepsilon^2\{\phi_2\} + \ldots \tag{112}$$

$$\omega = \omega_0 + \varepsilon\omega_1 + \varepsilon^2\omega_2 + \ldots \tag{113}$$

This can be done because of the small changes in $[M_0]$ and $[K_0]$ as expressed in Equation (108). Also,

$$\{q\} = \{q_0\} + \varepsilon \{q_1\} + \varepsilon^2 \{q_2\} + \ldots \tag{114}$$

where $\{q_0\}$ and $\{q\}$ are the normal coordinate vectors of the unperturbed and perturbed system, respectively, i.e.

$$\{x\} = [\phi]\{q\} \tag{115}$$

$$\{x_0\} = [\phi_0]\{q_0\} \tag{116}$$

with

$$[\phi]^T[M][\phi] = [I], \quad [\phi]^T[K][\phi]^T[K][\phi] = [\omega^2] \tag{117}$$

First, let us substitute Equation (116) into Equation (107) and premultiply by $[\Phi]^T$ yielding

$$\{\ddot{q}\} + [\omega^2]\{q\} = [\phi]^T\{F\} \tag{118}$$

Substituting Equations (112), (113) and (114) into Equation (118) and equating coefficients of like powers of ε, we can write,

$$\{\ddot{q}_0\} + [\omega_0^2]\{q_0\} = [\phi_0]^T\{F\} \tag{119}$$

$$\{\ddot{q}_1\} + [\omega_0^2]\{q_1\} = [\phi_1]^T\{F\} - 2[\omega_0][\omega_1]\{q_0\} \tag{120}$$

It is now possible to solve Equations (119, 120, etc.) in sequence. The first of Equations (119) represents the unperturbed equation of motion, i.e., the modal form of Equation (104). This solution is available or can be determined.

Once the vector $\{q_0\}$ is determined one can solve Equation (120) if $[\Phi_1]$ and $[\omega_1]$ are known. The determination of these matrices is the subject of the next paragraph.

First, it is always possible to write $[\Phi_1]$ as a linear combination of the eigenvectors $[\Phi_0]$,

$$[\phi_1] = [\phi_0]\ [\alpha] \tag{121}$$

because $[\Phi_0]$ is a complete set of vectors (i.e., they can be used as a basis for a vector space). Note that $[\alpha]$ represents the coefficient matrix of $[\Phi_0]$ in the linear combination and must still be determined. To this end, let us introduce Equations (108), (112), (113) and (121) into Equation (117), and only keep terms in ε^0 and ε^1,

$$\left([\phi_0] + \varepsilon [\phi_0]\ [\alpha]\right)^T \left([M_0] + \varepsilon [M_1]\right) \left([\phi_0] + \varepsilon [\phi_0][\alpha]\right) = [I] \tag{122}$$

$$\left([\phi_0] + \varepsilon [\phi_0]\ [\alpha]\right)^T \left([K_0] + \varepsilon [K_1]\right) \left([\phi_0] + \varepsilon [\phi_0]\ [\alpha]\right) = \left([\omega_0] + \varepsilon [\omega_1]\right)^2 \tag{123}$$

Equating coefficients of like powers in ε^0 and ε^1 we obtain from Equations (122-123)

$$[\alpha] + [\alpha]^T = -[\phi_0]^T [M_1]\ [\phi_0] \tag{124}$$

$$2\ [\omega_0]\ [\omega_1] = [\omega_0^2][\alpha] + [\alpha]^T [\omega_0^2] + [\phi_0]^T [K_1]\ [\phi_0] \tag{125}$$

Equations (124-125) can now be solved for $[\Phi_1]$ and $[\omega_1]$. This enables use to solve Equation (120) for $\{q_1\}$, so that from Equation (114) we obtain the first order approximation

$$\{q\} = \{q_0\} + \varepsilon\ \{q_1\} \tag{126}$$

and from Equation (116) we obtain $\{x\}$ where we use

$$[\phi] = [\phi_0] + \varepsilon [\phi_1] \tag{127}$$

This perturbation technique can now be applied to a booster/payload situation. The assumption is that only changes of order ε are made in the payload, i.e.,

$$[M_P] = [M_{P0}] + \varepsilon [M_{P1}]\ ,\ [K_P] = [K_{P0}] + \varepsilon [K_{P1}] \tag{128}$$

where $[M_{PO}]$ and $[K_{PO}]$ are the mass and stiffness matrices of the unperturbed payload P_O. Let us write the mass and stiffness matrices in Equation (25) for the perturbed payload P.

$$\left[\begin{array}{c|c} M_B + T_P^T M_P T_P & T_P^T M_P I_P \\ \hline I_P^T M_P T_P & I_P^T M_P I_P \end{array}\right] , \left[\begin{array}{c|c} K_B + T_P^T K_P T_P & 0 \\ \hline 0 & I_P^T K_P I_P \end{array}\right] \tag{129}$$

with

$$[T_P] = \begin{bmatrix} 0 & S_P \\ 0 & I \end{bmatrix} , \quad [S_P] = -\left[K_{NN}^P\right]^{-1}\left[K_{NI}^P\right] \tag{130}$$

Using Equation (128) we can write $[S_P]$ as

$$[S_P] = -\left(\left[K_{NN}^{PO}\right] + \varepsilon\left[K_{NN}^{P1}\right]\right)^{-1}\left(\left[K_{NI}^{PO}\right] + \varepsilon\left[K_{NI}^{P1}\right]\right) \tag{131}$$

and, keeping terms in ε only, we obtain

$$\begin{aligned}[S_P] &= -\left(\left[K_{NN}^{PO}\right]^{-1} - \varepsilon\left[K_{NN}^{PO}\right]^{-1}\left[K_{NN}^{P1}\right]\left[K_{NN}^{PO}\right]\right)\left(\left[K_{NN}^{PO}\right] + \varepsilon\left[K_{NI}^{P1}\right]\right) \qquad (132)\\ &= -\left[K_{NN}^{PO}\right]^{-1}\left[K_{NI}^{PO}\right] - \varepsilon\left(\left[K_{NN}^{PO}\right]^{-1}\left[K_{NI}^{P1}\right] - \left[K_{NN}^{PO}\right]^{-1}\left[K_{NN}^{P1}\right]\left[K_{NN}^{PO}\right]^{-1}\left[K_{NI}^{PO}\right]\right)\end{aligned}$$

or

$$[S_P] = [S_{PO}] + \varepsilon[S_{P1}] \tag{133}$$

with

$$[S_{PO}] = -\left[K_{NN}^{PO}\right]^{-1}\left[K_{NI}^{PO}\right] \tag{134}$$

$$[S_{P1}] = -\left[K_{NN}^{PO}\right]^{-1}\left[K_{NI}^{P1}\right] + \left[K_{NN}^{PO}\right]^{-1}\left[K_{NN}^{P1}\right]\left[K_{NN}^{PO}\right]^{-1}\left[K_{NI}^{PO}\right] \tag{135}$$

It is now possible to write $[T_P]$ as

$$[T_P] = [T_{PO}] + \varepsilon[T_{P1}] \tag{136}$$

with

$$[T_{PO}] = \begin{bmatrix} 0 & S_{PO} \\ 0 & 0 \end{bmatrix} , \quad [T_{P1}] = \begin{bmatrix} 0 & S_{P1} \\ 0 & I \end{bmatrix} \tag{137}$$

Finally we can write the mass and stiffness matrices of the coupled booster/payload system as follows

$$[M_C] = [M_{CO}] + \varepsilon [M_{C1}] \, , \, [K_C] = [K_{CO}] + \varepsilon [K_{C1}] \qquad (138)$$

where C indicates Coupled. Matrices $[M_C]$ and $[K_C]$ are given by expressions (129). Taking into account Equations (128) and (136) we can write

$$[M_{CO}] = \begin{bmatrix} M_B + T_{PO}^T M_{PO} T_{PO} & T_{PO}^T M_{PO} I_{PO} \\ I_{PO}^T M_{PO} T_{PO} & I_{PO}^T M_{PO} I_{PO} \end{bmatrix}, \quad [K_{CO}] = \begin{bmatrix} K_B + T_{PO}^T K_{PO} T_{PO} & 0 \\ 0 & I_{PO}^T K_{PO} I_{PO} \end{bmatrix} \qquad (139)$$

and

$$[M_{C1}] = \begin{bmatrix} T_{PO}^T M_{PO} T_{P1} + T_{PO}^T M_{P1} T_{PO} + T_{P1}^T M_{PO} T_{PO} & (T_{PO}^T M_{P1} + T_{P1}^T M_{PO}) I_{PO} \\ I_{PO}^T (M_{PO} T_{P1} + M_{P1} T_{PO}) & I_{PO}^T M_{P1} I_{PO} \end{bmatrix} \qquad (140)$$

$$[K_{C1}] = \begin{bmatrix} T_{PO}^T K_{PO} T_{P1} + T_{PO}^T K_{P1} T_{PO} + T_{P1}^T K_{PO} T_{PO} & 0 \\ 0 & I_{PO}^T K_{P1} I_{PO} \end{bmatrix} \qquad (141)$$

where $[T_{PO}]$ and $[T_{P1}]$ are given by Equation (137). Equation (138) is now equivalent to Equation (108) and the perturbation technique can be applied.

Note that theoretically one can also obtain the higher-order perturbations ε^2, ε^3, etc. But for all pratical purposes only ε perturbations are included. The question then is, how important ε^2, ε^3, etc. terms are. It is evident that Equation (111) is only valid as long as the asymptotic expansion in ε does not break down, i.e., as long as $\varepsilon \{x_i\} \ll \{x_c\}$, etc. There are indeed cases where such an asymptotic expansion breaks down. It is then necessary to introduce other perturbation techniques (e.g. Lighthill, multiple scales, etc). In this connection it is important to recognize the fact that small changes in the mass and stiffness of the payload produce small changes in the eigenvalues but not necessarily in the modes.

3. The Base Drive Technique

In this section we shall discuss the Base Drive Technique as developed by A. Devers, et.al. Let us first recall Equation (91) in partitioned form,

$$\left[I_B^T M_B I_B\right]\left\{\ddot{x}_N^{BR}\right\} + \left[I_B^T K_B I_B\right]\left\{\bar{x}_N^{BR}\right\} = -\left[I_B^T M_B T_B\right]\left\{\ddot{x}_I^{BR}\right\} \tag{142}$$

$$\left[I_P^T M_P I_P\right]\left\{\ddot{\bar{x}}_N^{P}\right\} + \left[I_P^T K_P I_P\right]\left\{\bar{x}_N^{P}\right\} = -\left[T_P^T M_P T_P\right]\left(\left\{\ddot{x}_I^{BF}\right\} + \left\{\ddot{x}_I^{BR}\right\}\right) \tag{143}$$

$$\left\{\ddot{x}_I^{BR}\right\} = \left[T_B^T M_B T_B + T_P^T M_P T_P\right]^{-1}\left(-\left[T_P^T M_P T_P\right]\left\{\ddot{x}_I^{BF}\right\} - \left[T_P^T K_P T_P\right]\left\{x_I^{BF}\right\}\right.$$

$$\left. - \left[T_P^T M_P I_P\right]\left\{\ddot{\bar{x}}_N^{P}\right\} - \left[T_B^T M_B I_B\right]\left\{\ddot{\bar{x}}_N^{BR}\right\} - \left[T_B^T K_B T_B + T_P^T K_P T_P\right]\left\{x_I^{BR}\right\}\right) \tag{144}$$

where we solved for $\left\{\ddot{x}_I^{BR}\right\}$ in Equation (144)

The payload designer is primarily interested in predicting the response of the payload which is given by

$$\left\{\begin{array}{c} x_N^P \\ \hline x_I^P \end{array}\right\} = \left[\begin{array}{c|c} I & S_P \\ \hline 0 & I \end{array}\right]\left\{\begin{array}{c} \bar{x}_N^P \\ \hline \bar{x}_I^P \end{array}\right\} \tag{145}$$

with

$$\left\{\begin{array}{c} \bar{x}_N^P \\ \hline x_I^P \end{array}\right\} = \left\{\begin{array}{c} \bar{x}_N^P \\ \hline x_I^{BF} + x_I^{BR} \end{array}\right\} \tag{146}$$

where $\left\{\bar{x}_N^P\right\}$ and $\left\{x_I^{BR}\right\}$ must be computed from Equations (142-144) and $\left\{x_I^{BF}\right\}$ from Equation (90).

The idea of a base drive short-cut method is to approximate $\left\{\ddot{x}_I^R\right\}$ in Equation (144) in such a way as to avoid the solution of the complete set (142-144). To evaluate a particular short-cut method, the approximation of $\left\{\ddot{x}_I^R\right\}$ must be compared to the exact value given by Equation (144).

A significant simplification of Equation (144) occurs when the interface is statically determinate, i.e., when

$$\left[T_B^T K_B T_B\right] = \left[T_P^T K_P T_P\right] = \left[0\right] \tag{147}$$

This eliminates the dependence of $\left\{\ddot{x}_I^R\right\}$ on $\left\{x_I^{BR}\right\}$ and $\left\{x_I^{BF}\right\}$, and $\left\{\ddot{x}_I^R\right\}$ becomes,

$$\left\{\ddot{x}_I^{BR}\right\} = \left[T_B^T M_B T_B + T_P^T M_P T_P\right]^{-1}\left(-\left[T_P^T M_P T_P\right]\left\{\ddot{x}_I^{BF}\right\} - \left[T_P^T M_P I_P\right]\left\{\ddot{\bar{x}}_N^{P}\right\}\right.$$

$$\left. - \left[T_B^T M_B I_B\right]\left\{\ddot{\bar{x}}_N^{BR}\right\}\right) \tag{148}$$

A first possibility is to assume that the presence of the payload has no effect on the response of the booster, i.e. $\{\ddot{X}_I^{BR}\}=\{0\}$. This approach is called the Direct Base Drive Technique or Open Loop Base Drive. Indeed if $\{\ddot{X}_I^{BR}\}=\{0\}$ then Equation (143) becomes

$$\left[I_P^T M_P I_P\right]\{\ddot{x}_N^P\} + \left[I_P^T K_P I_P\right]\{x_N\} = -\left[I_P^T M_P T_P\right]\{\ddot{x}_I^{BF}\} \tag{149}$$

which means that the payload is "directly" driven at its base (i.e. its interface with the booster B) by the force on the right hand side of Equation (149). Theoretically, the Direct Base Drive Technique assumes there is no coupling at all between the booster and the payload. Practically, it means that $\{\ddot{X}_I^{BR}\}\ll\{\ddot{X}_I^{BF}\}$ or that the feedback of the payload is negligible. The conditions under which such an approximation is valid is still an unanswered question. The development of a criterion of validity of the use of the Direct Base Drive Technique should be considered.

4. The Impedance Technique

In this section we shall discuss yet another approach to the solution of the equations of motion of the booster/payload system. The Impedance Technique as developed by K. Payne is basically a full-scale method in the sense that it does not make any assumptions concerning the size of the payload nor the extent of the changes made in the payload. However, the method does avoid a full-scale solution of the coupled booster/payload equations of motion and is particularly suited to deal with small changes in the payload. The Impedance Technique is essentially a Base Drive method (see Section 3). It differs from the approach in Section 3. in the manner in which the interface accelerations $\{\ddot{x}_I^{BR}\}$ are computed. Indeed, the interface accelerations will be computed in the frequency domain instead of the discrete time domain thereby essentially converting a set of differential equations into a set of algebraic equations.

Let us now derive the necessary equations. First, recall equation (3).

$$\left[\begin{array}{c|c} M_B & 0 \\ \hline 0 & M_P \end{array}\right]\left\{\begin{array}{c} \ddot{x}_B \\ \hline \ddot{x}_P \end{array}\right\} + \left[\begin{array}{c|c} K_B & \\ \hline & K_P \end{array}\right]\left\{\begin{array}{c} x_B \\ \hline x_P \end{array}\right\} = \left\{\begin{array}{c} F_B \\ \hline F_P \end{array}\right\} + \left\{\begin{array}{c} 0 \\ R_I^B \\ \hline 0 \\ R_I^P \end{array}\right\} \tag{150}$$

and write the top and bottom partitions separately,

$$\left[M_B\right]\{\ddot{x}_B\} + \left[K_B\right]\{x_B\} = \{F_B\} + \left\{\begin{array}{c} 0 \\ R_I^B \end{array}\right\} \tag{151}$$

$$\left[M_P\right]\{\ddot{x}_P\} + \left[K_P\right]\{x_P\} = \left\{\begin{array}{c} 0 \\ -R_I^P \end{array}\right\} \tag{152}$$

where we invoked Equation (2) and assumed the external payload forces to be absent $\left(\{F_p\} = \{0\}\right)$. Next, we introduce an equation similar to Equation (87).

$$\{x_B\} = \{x_B\}^F + \{x_B\}^R \tag{153}$$

where the F-vector represents the booster response due to the externally applied force vector $\{F_B\}$ and therefore satisfies,

$$\left[M_B\right]\{\ddot{x}_B\}^F + \left[K_B\right]\{x_B\}^F = \{F_B\} \tag{154}$$

and the R-vector represents the response of the booster due to the feedback of the payload and satisfies

$$\left[M_B\right]\{\ddot{x}_B\}^R + \left[K_B\right]\{x_B\}^R = \begin{Bmatrix} 0 \\ -R_I^B \end{Bmatrix} \tag{155}$$

Applying transformation (32) to Equation (154) yields,

$$\{\ddot{q}_B\}^F + \left[\omega_B^2\right]\{q_B\}^F = \left[\phi_B\right]^T \{F_B\} \tag{156}$$

We now consider Equation (153) and recall Equation (4),

$$\begin{Bmatrix} x_N^B \\ \hline x_I^B \end{Bmatrix} = \begin{Bmatrix} x_N^B \\ \hline x_I^B \end{Bmatrix}^F + \begin{Bmatrix} x_N^B \\ \hline x_I^B \end{Bmatrix}^R \tag{157}$$

Keeping the bottom partition in Equation (157) yields

$$\{x_I^B(t)\} = \{x_I^B(t)\}^F + \{x_I^B(t)\}^R \tag{158}$$

where we now included the dependence of the vectors on the discrete time t. Taking the Laplace Transform (with zero initial conditions) of both sides of Equation (158) introducing the transformation $s = j\Omega$ (with s = Laplace variable; Ω_i = the ith input frequency; and $j = \sqrt{-1}$) we can write

$$\{x_I^B(j\Omega_i)\} = \{x_I^B(j\Omega_i)\}^F + \{x_I^B(j\Omega_i)\}^R, \quad i = 1,2,\ldots\ldots \tag{159}$$

which represents Equation (158) in the frequency domain. Taking the second time derivative of Equation (159) yields:

$$\left\{\ddot{x}_I^B\ (j\Omega_i)\right\} = \left\{\ddot{x}_I^B\ (j\Omega_i)\right\}^F + \left\{\ddot{x}_I^B\ (j\Omega_i)\right\}^R, \quad i = 1,2,... \tag{160}$$

The basic idea of the Impedance Technique is to calculate the interface accelerations $\{\ddot{x}_I^B(j\Omega_i)\}$ in the frequency domain and then transform them back to the discrete time domain. The two terms on the righthand side of Equation (160) will be replaced by algebraic matrix expressions so that the calculation of $\{\ddot{x}_I^B(j\Omega_i)\}$ does not involve the solution of a set of differential equations. Let us start with the first term on the right-hand side of Equation (160). To this end let us convert Equation (156) to the frequency domain

$$\left\{q_B\ (j\Omega_i)\right\}^F = \left[\frac{1}{\omega_B^2 - \Omega_i^2}\right] \left[\phi_B\right]^T \left\{F_B\ (j\Omega_i)\right\}, \quad i = 1,2,.... \tag{161}$$

or, taking the second time derivative,

$$\left\{\ddot{q}_B\ (j\Omega_i)\right\}^F = \left[\frac{\Omega_i^2}{\Omega_i^2 - \omega_B^2}\right] \left[\phi_B\right]^T \left\{F_B\ (j\Omega_i)\right\}, \quad i = 1,2,... \tag{162}$$

Let us write Equation (32)

$$\left\{\begin{matrix} x_N^B \\ \hline x_I^B \end{matrix}\right\} = \left[\begin{matrix} \phi_N^B \\ \hline \phi_I^B \end{matrix}\right] \left\{q_B\right\} \tag{163}$$

with

$$\left[\phi_B\right] = \left[\begin{matrix} \phi_N^B \\ \hline \phi_I^B \end{matrix}\right] \tag{164}$$

Then the bottom partition of Equation (163)

$$\left\{x_I^B\right\} = \left[\phi_I^B\right] \left\{q_B\right\} \tag{165}$$

Premultiply Equation (162) by $\left[\phi_I^B\right]$ and invoking Equation (165) yields

$$\left\{\ddot{x}_I^B\ (j\Omega_i)\right\}^F = \left[\phi_I^B\right]\left[\frac{\Omega_i^2}{\Omega_i^2 - \omega_B^2}\right]\left[\phi_B\right]^T \left\{F_B\ (j\Omega_i)\right\}, \quad i = 1,2,.... \tag{166}$$

or

$$\left\{\ddot{x}_I^B\ (j\Omega_i)\right\}^F = \left[A\ (j\Omega_i)\right]\ \left\{F_B\ (j\Omega_i)\right\}, \quad i = 1,2,.... \tag{167}$$

with

$$\left[A\ (j\Omega_i)\right] = \left[\phi_I^B\right]\left[\frac{\Omega_i^2}{\Omega_i^2 - \omega_B^2}\right]\left[\phi_B\right]^T, \quad i = 1,2,.... \tag{168}$$

Equation (167) then, yields the first term on the right-hand side of Equation (160). The matrix $A(j\Omega_i)$ in Equation (168) is the transfer admittance from the points of application of the external forces $\{F_B\}$ to the interface accelerations.

Similarly, Equation (155) can be transformed into

$$\left\{\ddot{x}_I\ (j\Omega_i)\right\}^R = \left[B\ (j\Omega_i)\right]\ \left\{R_I^P\ (j\Omega_i)\right\}, \quad i = 1,2,.... \tag{169}$$

where this time

$$\left[B\ (j\Omega_i)\right] = \left[\phi_I^B\right]\left[\frac{\Omega_i^2}{\Omega_i^2 - \omega_B^2}\right]\left[\phi_I^B\right]^T, \quad i = 1,2,.... \tag{170}$$

is the matrix of coefficients for the point admittance for the booster at the interface. Equation (169) yields the second term on the right-hand side of equation (160). However, the reaction vector $\{R_I^P(j\Omega_i)\}$ is not known a priori. To determine this vector let us consider Equation (152) which represents the payload equations of motion, and write it as

$$\left[\begin{array}{c|c} M_{NN}^P & M_{NI}^P \\ \hline M_{IN}^P & M_{II}^P \end{array}\right] \left\{\begin{array}{c} \ddot{x}_N^P \\ \hline \ddot{x}_I^P \end{array}\right\} + \left[\begin{array}{c|c} K_{NN}^P & K_{NI}^P \\ \hline K_{IN}^P & K_{II}^P \end{array}\right] \left\{\begin{array}{c} x_N^P \\ \hline x_I^P \end{array}\right\} = \left\{\begin{array}{c} 0 \\ \hline -R_I^P \end{array}\right\} \tag{171}$$

where we used Equations (5) and (7). Introducing the modal transformation (39) and taking into account the properties (40) we obtain from Equation (171),

$$\left[\begin{array}{c|c} I & \bar{\phi}_N^{PT} M_1^P \\ \hline M_1^{PT} \bar{\phi}_N^P & M_2^P \end{array}\right] \left\{\begin{array}{c} \ddot{q}_N^P \\ \hline \ddot{x}_I^P \end{array}\right\} + \left[\begin{array}{c|c} \bar{\omega}_P^2 & 0 \\ \hline 0 & K_2^P \end{array}\right] \left\{\begin{array}{c} \bar{q}_N^P \\ \hline x_I^P \end{array}\right\} = \left\{\begin{array}{c} 0 \\ \hline -R_I^P \end{array}\right\} \tag{172}$$

with

$$\left[M_1^P\right] = \left[M_{NN}^P\right] \left[S_P\right] + \left[M_{NI}^P\right] \tag{173}$$

$$\left[K_2^P\right] = \left[K_{IN}^P\right] \left[S_P\right] + \left[K_{II}^P\right] \tag{174}$$

and $\left[M_2^P\right]$ given by Equation (28). Note that $\left[K_2^P\right]$ is zero when the interface is statically determinate.

The top and bottom partitions of Equation (172) can be written as,

$$\left\{\ddot{q}_N^P\right\} + \left[\bar{\omega}_P^2\right] \left\{\bar{q}_N^P\right\} = -\left[\bar{\phi}_N^P\right]^T \left[M_1^P\right] \left\{\ddot{x}_I^P\right\} \tag{175}$$

$$\left[M_1^P\right]^T \left[\bar{\phi}_N^P\right] \left\{\ddot{q}_N^P\right\} + \left[M_2^P\right] \left\{\ddot{x}_I^P\right\} + \left[K_2^P\right] \left\{x_I^P\right\} = -\left\{R_I^P\right\} \tag{176}$$

We shall now assume that the interface is statically determinate ($[K_2^P] = [0]$) and calculate an expression for $\{R_I^P\}$ from Equations (175-176). First, we transform Equation (175) to the frequency domain.

$$\left\{ \ddot{q}_N^P \ (j\Omega_i) \right\} = - \left[\frac{\Omega_i^2}{\Omega_i^2 - \bar{\omega}_P^2} \right] \left[\bar{\phi}_N^P \right]^T \left[M_1^P \right] \left\{ \ddot{x}_I^P \ (j\Omega_i) \right\}, \quad i = 1,2,.... \tag{177}$$

and from Equation (176) we obtain,

$$\left[M_1^P \right]^T \left[\bar{\phi}_N^P \right] \left\{ \ddot{q}_N^P \ (j\Omega_i) \right\} + \left[M_2^P \right] \left\{ \ddot{x}_I^P \ (j\Omega_i) \right\} = - \left\{ R_I^P \ (j\Omega_i) \right\} \tag{178}$$

$$i = 1,2,.....$$

Substituting Equation (177) into Equation (178) yields :

$$-\left[M_1^P \right]^T \left[\bar{\phi}_N^P \right] \left[\frac{\Omega_i^2}{\Omega_i^2 - \bar{\omega}_P^2} \right] \left[\bar{\phi}_N^P \right]^T \left[M_1^P \right] \left\{ \ddot{x}_I^P \ (j\Omega_i) \right\}$$

$$+ \left[M_2^P \right] \left\{ \ddot{x}_I^P \ (j\Omega_i) \right\} = - \left\{ R_I^P \ (j\Omega_i) \right\}, \tag{179}$$

$$i = 1,2,...$$

from which we obtain the following expression for $\left\{ R_I^P \ (j\Omega_i) \right\}$

$$\left\{ R_I^P \ (j\Omega_i) \right\} = \left[C \ (j\Omega_i) \right] \left\{ \ddot{x}_I^P \ (j\Omega_i) \right\}, \quad i = 1,2,.... \tag{180}$$

where

$$\left[C \ (j\Omega_i) \right] = \left[M_1^P \right]^T \left[\bar{\phi}_N^P \right] \left[\frac{\Omega_i^2}{\Omega_i^2 - \bar{\omega}_P^2} \right] \left[\bar{\phi}_N^P \right]^T \left[M_1^P \right] - \left[M_2^P \right] \tag{181}$$

is the impedance matrix of the payload at the payload/booster interface. Finally, we substitute Equation (180) into Equation (169),

$$\left\{ \ddot{x}_I \ (j\Omega_i) \right\}^R = \left[B \ (j\Omega_i) \right] \left[C \ (j\Omega_i) \right] \left\{ \ddot{x}_I^P \ (j\Omega_i) \right\}, \ i = 1,2,... \tag{182}$$

Combining Equations (160), (167) and (182) yields

$$\left(\left[\Gamma_I \right] - \left[B \ (j\Omega_i) \right] \left[C \ (j\Omega_i) \right] \right) \left\{ \ddot{x}_I^B \ (j\Omega_i) \right\} = \left[A \ (j\Omega_i) \right] \left\{ F_b \ (j\Omega_i) \right\} \tag{183}$$

$$i = 1.2,...$$

where we also used Equation (1).

The coefficient matrix of $\{\ddot{X}_I^B(j\Omega_i)\}$ in Equation (183) represents the coupled impedance of the booster/payload system, and the right hand side represents a pseudo-generalized force. The interface acceleration can now be computed from Equation (183) with relative ease.

If we now consider a new payload on the same booster and with the same force $\{F_B\}$, the right-hand side of Equation (183) does not change so that,

$$\left\{\begin{matrix}\ddot{x}^B \\ x_I\end{matrix}(j\Omega_i)\right\}^{(2)} = \left(\left[I\right] - \left[B\ (j\Omega_i)\right]^{(2)}\left[C(j\ \Omega_i)\right]^{(2)}\right)^{-1}\left(\left[I\right] - \left[B\ (j\Omega_i)\right]^{(1)}\left[C(j\Omega_i)\right]^{(1)}\right)^{x}$$

provided the interface does not change. $$\left\{\begin{matrix}\ddot{x} \\ x_I\end{matrix}(j\Omega_i)\right\}^{(1)} \qquad (184)$$

The interface accelerations $\{\ddot{X}_I(t)\}$ in the discrete time domain can now be derived from equation (183) or Equation (184), using the inverse Laplace Transform. The payload response then follows from Equation (175).

The approximation involved in the Impedance Technique is imbedded in the transformation to and from the frequency domain. If these transformations were exact, the method of determining $\{\ddot{X}_I(t)\}$ would be exact. Therefore, a detailed investigation of these transformations is required. There are also some problems pertaining to the modal damping when working in the frequency domain.

Although Equations (183) and (184) were derived for an undamped statically determinate system, it is clear that damping and statically indeterminate interfaces can be included. For an indeterminate system it becomes necessary to keep track not only of the interface accelerations but also of the velocities and displacements at the interface. The use of the Fast Fourier Transform in obtaining the spectral data to be used in Equations (183-184) presents some problems. In general, however, enough correlation with the exact time domain solution is apparent to warrant further investigation into possible improvements.

5. The Generalized Shock Spectrum Technique

The approach presented in this section is a generalized version of the shock spectrum technique as developed by Bamford.

In order to explain the basic ideas underlying this technique let us recall Equation (43)

$$\left[\begin{array}{c|c} I+\phi_B^T T_P^T M_P T_P \phi_B & \phi_B^T T_P^T M_P I_P \bar{\phi}_N^P \\ \hline \bar{\phi}_N^{P\,T} I_P^T M_P T_P \phi_B & I \end{array}\right] \left\{\begin{array}{c} \ddot{q}_B \\ \hline \ddot{\bar{q}}_N^P \end{array}\right\} + \left[\begin{array}{c|c} \left[\omega_B^2\right] + \phi_B^T T_P^T K_P T_P \phi_B & 0 \\ \hline 0 & \left[\bar{\omega}_P^2\right] \end{array}\right] \left\{\begin{array}{c} q_B \\ \hline \bar{q}_N^P \end{array}\right\} = \left\{\begin{array}{c} \phi_B^T \left\{\begin{array}{c} F_N^B \\ 0 \end{array}\right\} \\ \hline 0 \end{array}\right\} \tag{185}$$

and let us assume we retained M modes for the booster (i.e. $[\phi_B]$ is an MxM matrix) and N modes for the payload (ie. $[\bar{\Phi}_N^P]$ is an NxN matrix)

The basic idea of the shock spectrum technique is to determine load maxima without having to solve Equation (185). To reach this goal, a new model both for the coupled system and the forcing function $\{F_B\}$ is introduced.

First, the (N + M) modally coupled Equations (185) are replaced by (N x M) sets of two simultaneous equations each of which represents the coupling of one payload mode with one booster mode, as follows:

$$\left[\begin{array}{c|c} 1 + \left\{\phi_B\right\}_i^T T_P^T M_P T_P \left\{\phi_B\right\}_i & \left\{\phi_B\right\}_i^T T_P^T M_P I_P \left\{\bar{\phi}_N^P\right\}_j \\ \hline \left\{\bar{\phi}_N^P\right\}_j^T I_P^T M_P T_P \left\{\phi_B\right\}_i & 1 \end{array}\right] \left\{\begin{array}{c} \ddot{q}_{Bi} \\ \hline \ddot{\bar{q}}_{Nj}^B \end{array}\right\} + \left[\begin{array}{c|c} \omega_{Bi}^2 & 0 \\ \hline 0 & \bar{\omega}_{Pj}^2 \end{array}\right] \left\{\begin{array}{c} q_{Bi} \\ \hline \bar{q}_{Nj}^B \end{array}\right\} = \left\{\begin{array}{c} \left\{\phi_B\right\}_i^T \left\{\begin{array}{c} F_N^B \\ 0 \end{array}\right\} \\ \hline 0 \end{array}\right\} \quad \begin{array}{l} i=1,2,\ldots.M \\ j=1,2,\ldots.N \end{array} \tag{186}$$

where we assumed that the interface is statically determinate (i.e. $[T_P^T K_P T_P] = [0]$)

Secondly, a bound q_{BP} on each of the (N x M) modal responses of the payload is established. This is done by introducing a new model for the forcing function in Equation (186). The rather complicated forcing function is replaced by a much simpler function (e.g., an impulsive force) which produces the same maximum response peak as the original force. Therefore an analytical solution for both the response and maximum response of Equation (186) is possible (after some additional simplifications). Finally, a bound q_P on the total payload response is constructed by summing over all the individual modal bounds q_{BP} (over absolute values or in a root-sum-square sense that allows for phase weighting). Payload member loads are obtained by adding the contributions of all payload modal loads.

As stated above, the forcing function in Equation (186) is replaced by a modal delta function of a certain magnitude F_B. This magnitude F_B is evaluated from an already existing transient analysis of the booster with or without a dummy payload.

The main objections that can be raised against the Shock Spectrum Approach are:

1) No critical evaluation is available on the validity of replacing model (185) by model (186). What effect does this replacement have on the load bounds? This change of model could not only result in a too conservative design but also in an unconservative one. Model (186) not only ignores the coupling between the B-modes due to rigid body feedback of P , but more importantly it ignores the effects that the coupling of one B-mode with one P-mode has on all the other P-modes.

2) The manner in which F_S is calculated again leaves the question of whether or not the envelope values are conservative or not and by how much.

3) The method appears rather complicated and is not simple to use. This can lead to misinterpretation and confusion when the method is applied. More rigor in the mathematical formulation is desirable.

The method can be of definite use in the first stages of a design effort. It leaves the payload designer the freedom of operating independently from the booster organization. This results in a quick turn around time. The method could then in the final stages be complimented by a more rigorous approach.

CHAPTER II. A PAYLOAD INTEGRATION TECHNIQUE - FULL-SCALE VERSION

1. Introduction

Present analytical techniques by which design loads are predicted are very costly and time consuming. The calendar turnaround time of a given cycle usually is lengthened when the payload design organization, the booster organization and the payload integration organization are different companies. Indeed, a fair amount of coordination is necessary to make the transfer of information between those three organizations optimal. Unfortunately, this coordination is very difficult to establish, resulting in considerable time delays. Moreover, these costs and delays repeat themselves for every load cycle (i.e., every time a change is made in the booster or payload). A typical example is the development of the Viking Orbiter System as mentioned in Chapter I.

The ever increasing number of modal coordinates necessary to model today's aerospace structures not only increases the cost of a load cycle, but also imposes greater demands on the analyst to keep the models within range of current computer capabilities.

The objective of the present chapter is to develop a "full-scale" payload integration method which reduces the cost of a load cycle and will be capable of handling very large systems. This new approach is a "full-scale" method in the sense that it actually solves the coupled booster/payload system equations and does not involve any additional approximations or assumptions as compared to the standard transient analysis.

The configuration of multiple payloads connected to the booster through separate interfaces is typical for most Shuttle missions. The fact that many of these payloads are not directly coupled allows for a significant simplification of the booster/payloads system equations. Superfluous interface degrees of freedom on the booster side can be accommodated within the formulation. Superfluous interface degrees of freedom are those interface degrees of freedom which are included in the launch vehicle model but are not connected to any payload. The superfluous interface degrees of freedom arise because the booster organization cannot afford to reconstruct a booster model every time the interface with payload(s) changes.

A numerical integration scheme used to obtain the booster/payload(s) system response is defined. The standard approach is to obtain the so-called "modal modes" i.e. the coupled system modes in order to decouple the system equations. The present approach avoids the solution of such a system eigenvalue problem. A Newmark-Chan-Beta numerical integration scheme is used to directly determine the system response.

This technique takes advantage of the peculiar structure of the equations of motion for the system. All zero entries of the system mass and stiffness matrices can be eliminated. In fact, a comparison feature can be implemented so that elements close to zero can be omitted, reducing the cost of the integration routine even more. The comparison feature makes the full-scale method a so-called short-cut method. A full-scale method can be defined as a method which yields "exact" results compared to the standard transient analysis technique, whereas a short-cut method introduces an approximation or assumption which leads to a more cost-effective but less accurate solution.

A Fortran computer program has been written and implemented on the CDC Cyber 172. The final remarks section discusses advantages and disadvantages of the proposed approach.

2. Derivation of the Basic Equations

The objective of this section is the derivation of the equations of motion of the launch vehicle/payload(s) system. Figure 3 shows the free body diagrams of the booster B and the payload P1 and P2. The booster and the payloads are connected to each other through the interface. We also consider superfluous interface coordinates. Indeed, often the booster interface contains more degrees of freedom than is necessary to attach the payloads. The reason for this is that the booster organization provides a set of interface restrained booster modes which can be used to accommodate many different payload configurations. It would be prohibitive to recalculate a set of cantilevered launch vehicle modes every time the interface with the payloads changes.

From the free body diagrams in Figure 3 we can easily write the uncoupled equations of motion for the booster B and the payloads P1 and P2 (This is similar to equation (3)):

$$\begin{bmatrix} M_B & & \\ & M_{P1} & \\ & & M_{P2} \end{bmatrix} \begin{Bmatrix} \ddot{x}_B \\ \ddot{x}_{P1} \\ \ddot{x}_{P2} \end{Bmatrix} + \begin{bmatrix} K_B & & \\ & K_{P1} & \\ & & K_{P2} \end{bmatrix} \begin{Bmatrix} x_B \\ x_{P1} \\ x_{P2} \end{Bmatrix} = \begin{Bmatrix} F_B \\ F_{P1} \\ F_{P2} \end{Bmatrix} + \begin{Bmatrix} R_B \\ R_{P1} \\ R_{P2} \end{Bmatrix} \tag{187}$$

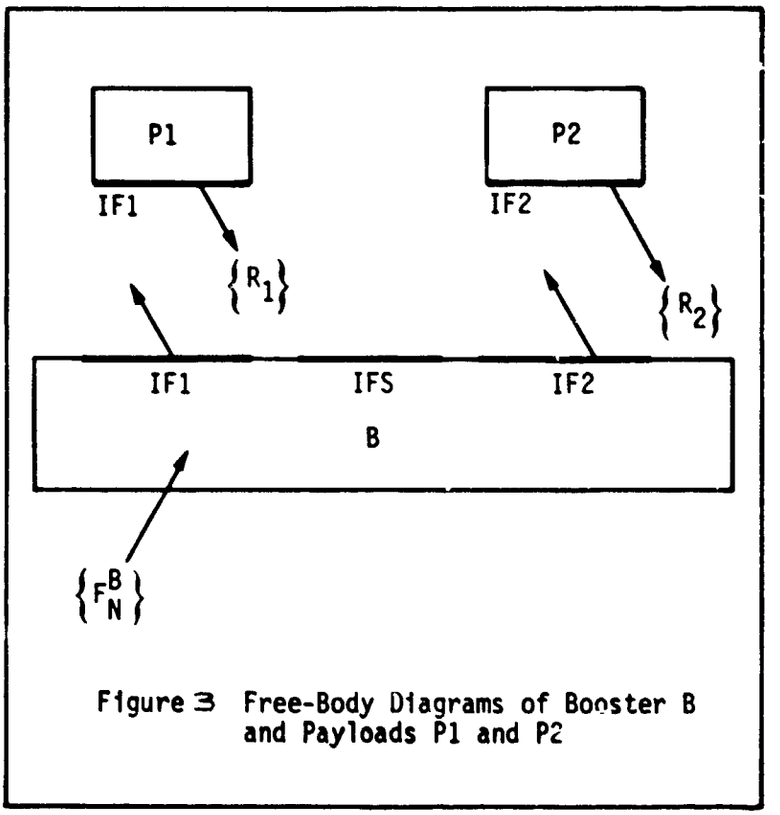

Figure 3 Free-Body Diagrams of Booster B and Payloads P1 and P2

Several well known procedures to couple the above three equations were discussed in part A of Chapter I. Again, the objective is to eliminate the redundant interface displacements and, in the process also, the unknown reaction vectors. One such technique uses so-called "cantilevered" booster and payload displacements. This technique was discussed in section A-3f of Chapter I. To set the stage, let us note that we can partition the vectors $\{x_B\}$, $\{x_{P1}\}$, $\{x_{P2}\}$, $\{F_B\}$, etc. as follows,

$$\{x_B\} = \begin{Bmatrix} x_N^B \\ \hline x_{I1}^B \\ \hline x_{I2}^B \\ \hline x_{IS}^B \end{Bmatrix} \quad , \quad \{x_{P1}\} = \begin{Bmatrix} x_N^{P1} \\ \hline x_{I1}^{P2} \end{Bmatrix}$$

$$\{x_{P2}\} = \begin{Bmatrix} x_N^{P2} \\ \hline x_{I2}^{P2} \end{Bmatrix} \quad , \quad \{F_B\} = \begin{Bmatrix} F_N^B \\ \hline 0 \\ \hline 0 \\ \hline 0 \end{Bmatrix}$$

$$\{F_{P1}\} = \begin{Bmatrix} 0 \\ \hline 0 \end{Bmatrix} \quad , \quad \{F_{P2}\} = \begin{Bmatrix} 0 \\ \hline 0 \end{Bmatrix} \qquad (18.)$$

$$\{R_B\} = \begin{Bmatrix} 0 \\ \hline R_1 \\ \hline R_2 \\ \hline 0 \end{Bmatrix} \quad , \quad \{R_{P1}\} = \begin{Bmatrix} 0 \\ \hline -R_1 \end{Bmatrix}$$

$$\{R_{P2}\} = \begin{Bmatrix} 0 \\ \hline -R_2 \end{Bmatrix}$$

Similar partitions can be written for the velocities and the accelerations. In the above equations we assumed that the external forces only act at the non-interface booster degrees of freedom. This assumption is only made for convenience. Also it should be noted that this development is not limited to two payloads.

Next, it is easy to show that $\{x_N^B\}$, $\{x_N^{P1}\}$, and $\{x_N^{P2}\}$ can be written as follows:

$$\begin{aligned}
\{x_N^B\} &= -[K_{NN}^B]^{-1}[K_{NI}^B]\{x_I^B\} + \{\bar{x}_N^B\} \\
\{x_N^{P1}\} &= -[K_{NN}^{P1}]^{-1}[K_{NI}^{P1}]\{x_{I1}^{P1}\} + \{\bar{x}_N^{P1}\} \\
\{x_N^{P1}\} &= -[K_{NN}^{P2}]^{-1}[K_{NI}^{P2}]\{x_{I2}^{P2}\} + \{\bar{x}_N^{P2}\}
\end{aligned} \tag{189}$$

These equations are similar to Equation (81).

Using Equation (189) and the fact that

$$\{x_{I1}^B\} = \{x_{I1}^{P1}\} \quad , \quad \{x_{I2}^B\} = \{x_{I2}^{P2}\} \tag{190}$$

we can form the following transformation,

$$\begin{Bmatrix} x_B \\ \hline x_{P1} \\ \hline x_{P2} \end{Bmatrix} = \left[\begin{array}{c|c|c|c} I_B & T_B & 0_1 & C_2 \\ \hline 0_5 & \begin{matrix} C_3 & 0_4 \\ T_{P1} & \\ 0_7 & 0_8 \end{matrix} & I_{P1} & 0_6 \\ \hline 0_{11} & \begin{matrix} 0_9 & 0_{10} \\ T_{P2} & \\ 0_{13} & 0_{14} \end{matrix} & 0_{12} & I_{P2} \end{array}\right] \begin{Bmatrix} \bar{x}_N^B \\ \hline x_I^B \\ \hline \bar{x}_N^{P1} \\ \hline \bar{x}_N^{P2} \end{Bmatrix} \tag{191}$$

where,

$$T_B = \begin{bmatrix} -K_{NN}^{B^{-1}} K_{NI}^B \\ \hline I \quad 0 \quad 0 \\ 0 \quad 1 \quad 0 \\ 0 \quad 0 \quad I \end{bmatrix} (BxIF) \quad , \quad x_I^B = \begin{Bmatrix} x_{I1}^B \\ \hline x_{I2}^B \\ \hline x_{IS}^B \end{Bmatrix} \begin{matrix} (1xIF1) \\ (1xIF2) \\ (1xIFS) \end{matrix} \tag{192}$$

$$T_{P1} = \begin{bmatrix} -K_{NN}^{P1^{-1}} K_{NI}^{P1} \\ \hline I \end{bmatrix} (P1xIF1), \quad I_{P1} = \begin{bmatrix} I \\ \hline 0 \end{bmatrix} \quad (P1xNP1)$$

$$T_{P2} = \begin{bmatrix} -K_{NN}^{P2^{-1}} K_{NI}^{P2} \\ \hline I \end{bmatrix} \text{(P2xIF2)}, \quad I_{P2} = \begin{bmatrix} I \\ \hline 0 \end{bmatrix} \text{(P2xNP2)}, \quad I_B = \begin{bmatrix} I \\ 0 \\ 0 \\ 0 \end{bmatrix} \text{(BxNB)}$$

NOTE:

$$\begin{aligned} IF &= IF1 + IF2 + IFS \\ B &= NB + IF \\ P1 &= NP1 + IF1 \\ P2 &= NP2 + IF2 \end{aligned}$$

also, 0_9, the zero matrices 0_1, 0_2, 0_3, 0_4, 0_5, 0_6, 0_7, 0_8, 0_9, 0_{10}, 0_{11}, 0_{12}, 0_{13}, and 0_{14} have dimensions BxNP1, BxNP2, NP1xIF2, NP1xIFS, P1xNB, P1xNP2, IF1xIF2, IF1xIFS, NP2xIF1, NP2xIFS, P2xNB, P2xNP1, IF2xIF1 and IF2xIF2 respectively.

Taking into account that the reactions between interfaces are equal but opposite we can substitute transformation (191) into Equation (187) and then premultiply by the transpose of the transformation matrix. This will eliminate the redundant interface displacement vectors as well as the reaction vectors. The resulting equations are the couple discrete equations of motion and can be written as:

$$\begin{bmatrix} I_B^T M_B I_B & I_B^T M_B T_P & 0 & 0 \\ T_B^T M_B I_B & M_{II} & T_{P1}^T M_{P1} I_{P1} \; 0 & 0 \; T_{T2}^T M_{P2} I_{P2} \\ & & 0 & 0 \\ 0 & I_{P1}^T M_{P1} T_{P1} \; 0 \; 0 & I_{P1}^T M_{P1} I_{P1} & 0 \\ 0 & 0 \; I_{P2}^T M_{P2} T_{P2} \; 0 & 0 & I_{P2}^T M_{T2} I_{P2} \end{bmatrix} \begin{Bmatrix} \ddot{x}_N^B \\ \ddot{x}_I^B \\ \ddot{x}_N^{P1} \\ \ddot{x}_N^{P2} \end{Bmatrix}$$

$$+ \begin{bmatrix} I_B^T K_B I_B & 0 & 0 & 0 \\ 0 & K_{II} & 0 & 0 \\ 0 & 0 & I_{P1}^T K_{P1} I_{P1} & 0 \\ 0 & 0 & 0 & I_{P2}^T K_{P2} I_{P2} \end{bmatrix} \begin{Bmatrix} \bar{x}_N^B \\ \bar{x}_I^B \\ \bar{v}^{P1} \\ \bar{x}_N^{P2} \end{Bmatrix} = \begin{Bmatrix} I_B^T F_B \\ T_B^T F_B \\ 0 \\ 0 \end{Bmatrix} \qquad (193)$$

where,

$$M_{II} = T_B^T M_B T_B + \begin{bmatrix} T_{P1}^T M_{P1} T_{P1} & 0 & 0 \\ 0 & T_{P2}^T M_{P2} T_{P2} & 0 \\ 0 & 0 & 0 \end{bmatrix}$$

$$K_{II} = T_B^T K_B T_B + \begin{bmatrix} T_{P1}^T K_{P1} T_{P1} & 0 & 0 \\ 0 & T_{P2}^T K_{P2} T_{P2} & 0 \\ 0 & 0 & 0 \end{bmatrix} \qquad (194)$$

and again, it can be shown that $[I_B^T K_B T_B]$, $[I_{P1}^T K_{P1} T_{P1}]$ and $[I_{P2}^T K_{P2} T_{P2}]$ always vanish and $[T_B^T K_B T_B]$, $[T_{P1}^T K_{P1} T_{P1}]$ and $[T_{P2}^T K_{P2} T_{P2}]$ vanish when the corresponding interface is determinate.

Next, we introduce the interface restrained modes, i.e.

$$[\bar{\phi}_N^B]\{\bar{q}_N^B\} = \{\bar{x}_N^B\} \quad ,$$

$$[\bar{\phi}_N^{P1}]\{\bar{q}_N^{P1}\} = \{\bar{x}_N^{P1}\} \quad , \qquad (195)$$

$$[\bar{\phi}_N^{P2}]\{\bar{q}_N^{P2}\} = \{\bar{x}_N^{P2}\}$$

These modes can be truncated according to a predetermined cut-off frequency, thereby reducing the size of Equation (193). Substituting Equations (195) into Equations (193) we obtain:

$$\begin{bmatrix} I & B^T & 0 \\ B & M_{II} & P \\ 0 & P^T & I \end{bmatrix} \begin{Bmatrix} \ddot{\bar{q}}_N^B \\ \ddot{x}_I^B \\ \ddot{\bar{q}}_N^P \end{Bmatrix} + \begin{bmatrix} 2\bar{\zeta}_B\bar{\omega}_B & & \\ & D_{II} & \\ & & 2\bar{\zeta}_P\bar{\omega}_P \end{bmatrix} \begin{Bmatrix} \dot{\bar{q}}_N^B \\ \dot{x}_I^B \\ \dot{\bar{q}}_N^P \end{Bmatrix} +$$

$$\begin{bmatrix} \bar{\omega}_B^2 & & \\ & K_{II} & \\ & & \bar{\omega}_P^2 \end{bmatrix} \begin{Bmatrix} \bar{q}_N^B \\ x_I^B \\ \bar{q}_N^P \end{Bmatrix} = \begin{Bmatrix} \bar{\phi}_N^{B^T} I_B^T F_B \\ T_B^T F_B \\ 0 \end{Bmatrix}, \qquad (196)$$

with

$$B = T_B^T M_B I_B \bar{\phi}_N^B$$

$$\bar{\omega}_N^2 = \begin{bmatrix} \bar{\omega}_{P1}^2 & \\ & \bar{\omega}_{P2}^2 \end{bmatrix} \qquad (197)$$

$$P = \begin{bmatrix} T_{P1}^T M_{P1} I_{P1} \bar{\phi}_N^{P1} & 0 \\ 0 & T_{P2}^T M_{P2} I_{P2} \bar{\phi}_N^{P2} \\ 0 & 0 \end{bmatrix}$$

D_{II} = Discrete Damping

$$\{\ddot{q}_N^P\} = \begin{Bmatrix} \ddot{q}_N^{P1} \\ \hline \ddot{q}_N^{P2} \end{Bmatrix}$$

Note that we introduced damping and that we kept the interface degrees of freedom in discrete form. This is recommended when DENSE Logic is used in programming the procedure. If PARTITION Logic is used, we actuall, introduce the interface modes $[\Phi_I]$,

$$\begin{aligned} [\Phi_I^T][M_{II}][\Phi_I] &= [I] \\ [\Phi_I^T][K_{II}][\Phi_I] &= [\omega_I^2] \end{aligned} \tag{198}$$

Although the booster and payload modes can be truncated, it is imperative not to truncate any interface definition. This is of special significance if one introduces the interface modes. The motivation for this will be explained in the load section.

Before proceeding with the next section, we wish to introduce the following notations:

$$[M] = \left[\begin{array}{c|c|c} I & B^T & 0 \\ \hline B & M_{II} & \Gamma \\ \hline 0 & P^T & I \end{array}\right], \qquad [K] = \left[\begin{array}{c|c|c} \bar{\omega}_B^2 & 0 & 0 \\ \hline 0 & K_{II} & 0 \\ \hline 0 & 0 & \bar{\omega}_P^2 \end{array}\right] \tag{199}$$

$$[C] = \left[\begin{array}{c|c|c} 2\bar{\zeta}_B \bar{\omega}_B & 0 & 0 \\ \hline 0 & D_{II} & 0 \\ \hline 0 & 0 & 2\bar{\zeta}_B \bar{\omega}_B \end{array}\right]$$

$$\{q\} = \begin{Bmatrix} \ddot{q}_N^B \\ \hline x_I^B \\ \hline \ddot{q}_N^P \end{Bmatrix}, \qquad \{F\} = \begin{Bmatrix} \Phi_N^{B^T} \Gamma_B^T F_B \\ \hline T_B^T F_B \\ \hline 0 \end{Bmatrix} \tag{200}$$

So that Equation (196) can be written as:

$$[M]\{\ddot{q}\} + [C]\{\dot{q}\} + [K]\{q\} = \{F\} \tag{201}$$

3. The Numerical Integration Scheme

The objective of this section is to choose a suitable integration scheme to directly integrate Equation (201). This is in contrast with the usual approach, where a new eigenvalue problem with [M] and [K] as mass and stiffness matrix is solved.

It is important to recognize that system (201) can have a frequency content much higher than the cut-off frequency of the forcing term. Usually, those higher frequencies will not produce significant responses. Therefore, a suitable numerical technique should be capable of using a stepsize h, which reflects only the highest frequency of interest but at the same time remains numerically stable. For example, a Runge-Kutta routine would not be suitable because it requires a time-step consistent with the highest frequency in the system, even though these high frequencies may not be of interest to the analyst. Although there are techniques to obtain a good estimate of the highest system frequency, using such a frequency to determine the stepsize would unnecessarily increased the cost of the response routine.

A method that satisfies above constraints is given by the Newmark-Chan-Beta integration method:

$$\{\dot{q}\}_{i+1} = \{\dot{q}\}_i + (1-\gamma)h\{\ddot{q}\}_i + \gamma h\{\ddot{q}\}_{i+1} \tag{202}$$

$$\{q\}_{i+1} = \{q\}_i + h\{\dot{q}\}_i + (0.5-\beta)h^2\{\ddot{q}\}_i + \beta h^2\{\ddot{q}\}_{i+1} \tag{203}$$

$$[M]\{\ddot{q}\}_{i+1} + [C]\{\dot{q}\}_{i+1} + [K]\{q\}_{i+1} = \{F\}_{i+1} \tag{204}$$

where the method is unconditionally stable if $\beta > (2\gamma+1)^2/16$. Artificial positive damping is introduced when $\gamma > 0.5$, and artificial negative damping if $\gamma < 0.5$. Good values for our purposes are $\gamma = 0.5$ and $\beta = 0.25$. Theoretically, the time step h can then be given any value while the scheme remains stable. In fact, for very large values of h, the scheme generates the static solution of Equation (201). Also, the scheme will damp out the highest (and least important) modes while preserving the lower ones. In addition, as we shall see shortly, the Newmark-Chan-Beta scheme is capable of taking advantage of the peculiar structure of the present equations of motion. Indeed, let us substitute Equations (202) and (203) into (205) and obtain

$$[M + \gamma hC + \beta h^2 K]\{\ddot{q}\}_{i+1} = \{F\}_{i+1} - [C + hK]\{\dot{q}\}_i$$

$$- [(1-\gamma)hC + (\tfrac{1}{2} - \beta)h^2 K]\{\ddot{q}\}_i - [K]\{q\}_i \qquad (205)$$

or, using Equation (199), we can write:

$$\left[\begin{array}{c|c|c} D_1 & B^T & 0 \\ \hline B & D_2 & P \\ \hline 0 & P^T & D_3 \end{array}\right] \left\{\begin{array}{c} \ddot{\bar{q}}^B_{Ni+1} \\ \hline \ddot{x}^B_{Ii+1} \\ \hline \ddot{\bar{q}}^P_{Ni+1} \end{array}\right\} = \left\{\begin{array}{c} f_{Bi} \\ \hline f_{Ii} \\ \hline f_{Pi} \end{array}\right\} \qquad (206)$$

with

$$f_{Bi} = \bar{\phi}^T_N I^T_B F_{Bi+1} - D_4 \dot{\bar{q}}^B_{Ni} - D_7 \ddot{\bar{q}}^B_{Ni} - \bar{\omega}^2_B \bar{q}^B_{Ni} \qquad (207)$$

$$f_{Ii} = T^T_B F_{Bi+1} - D_5 \dot{x}^B_{Ii} - D_8 \ddot{x}^B_{Ii} - K_{II} x^B_{Ii} \qquad (208)$$

$$f_{Pi} = - D_6 \dot{\bar{q}}^P_{Ni} - D_9 \ddot{\bar{q}}^P_{Ni} - \bar{\omega}^2_P \bar{q}^P_{Ni} \qquad (209)$$

and

$$D_1 = I + 2\gamma h \bar{\zeta}_B \bar{\omega}_B + \beta h^2 \bar{\omega}^2_B \qquad D_2 = M_{II} + \gamma h D_{II} + \beta h^2 K_{II}$$

$$D_3 = I + 2\gamma h \bar{\zeta}_P \bar{\omega}_P + \beta h^2 \bar{\omega}^2_P \qquad D_4 = 2\bar{\zeta}_B \bar{\omega}_B + h \bar{\omega}^2_B$$

$$D_5 = D_{II} + hK_{II} \qquad D_6 = 2\bar{\zeta}_P \bar{\omega}_P + h\bar{\omega}^2_P \qquad (210)$$

$$D_7 = 2(1-\gamma)h\bar{\zeta}_B \bar{\omega}_B + (0.5-\beta)h^2 \bar{\omega}^2_B \qquad D_8 = (1-\gamma)hD_{II} + (0.5-\beta)h^2 K_{II}$$

$$D_9 = 2(1-\gamma)h\bar{\zeta}_P \bar{\omega}_P + (0.5-\beta)h^2 \bar{\omega}^2_P$$

are diagonal matrices, except D_2, D_5 and D_8 which are IFxIF matrices. Consequently, the evaluation of f_{Bi}, f_{Ii}, and f_{Pi}, are very cost-effective. Also, note that D_i (i=1,...,9) are one-time calculations.

Normally, the solution for $\{\ddot{q}\}_{i+1}$ in Equation (206) requires a triangular decomposition and must be repeated for every h. However, in this case the unique form of the coefficient matrix of $\{\ddot{q}\}_{i+1}$ makes it possible to avoid such decompositions. Moreover, it is possible to completely take advantage of the diagonal and zero partitions appearing in that coefficient matrix.

First, let us premultiply Equation (206) by $[-BD_1^{-1} \mid I \mid -PD_3^{-1}]$ which yields the following expression:

$$\{\ddot{x}^B_{Ii+1}\} = A_1\{A_2 f_{Bi} + f_{Ii} + A_3 f_{Pi}\} \tag{211}$$

with

$$A_1 = [D_2 + A_2 B^T + A_3 P^T]^{-1} \tag{212}$$

$$A_2 = -BD_1^{-1}, \quad A_3 = -PD_3^{-1} \tag{213}$$

Furthermore, from Equation (206), we easily obtain,

$$\bar{q}^B_{Ni+1} = D_1^{-1} f_{Bi} + A_2^T \ddot{x}^B_{Ii+1} \tag{214}$$

$$\bar{q}^P_{Ni+1} = D_3^{-1} f_{Pi} + A_3^T \ddot{x}^B_{Ii+1} \tag{215}$$

Equations (211), (214) and (215) represent the final set of recurrence relations replacing Equation (206). Note that Equation (212) represents the inversion of an IFxIF matrix where IF is relatively small in many applications. This effectively removes the problem of triangular decomposition of a large matrix. Also, note that the cost of the algorithm primarily comes from multiplications involving matrices A_1, A_2 and A_3. Note however, that their dimensions are IFxIF, IFxNB and IFxNP respectively. In addition, the routine requires much less core memory which allows for the solution of much larger problems.

4. The Load Transformation

The purpose of this section is to briefly review the "acceleration" approach to calculating loads and at the same time point out some possible savings. An elementary member load transformation can be written as:

$$\{L_j\} = [k\Psi]_j \{x_{Pj}\} \tag{216}$$

Note that such a member could be part of any payload. For example, if the member belongs to payload P1, then $\{x_{Pj}\} = \{x_{P1}\}$.

Therefore, once the system response is known, one can substitute the displacement vector $\{x_p\}$ into Equation (216) and obtain the member loads. This direct approach is called the "displacement" method. In many cases, this is a perfectly valid approach especially if all the modes in Equations (32) and (39) are kept. However, if modes are truncated according to a cut-off frequency, this procedure often leads to inaccurate results. This can be corrected by using the so-called "acceleration" method whereby $\{x_p\}$ is replaced in terms of applied forces and accelerations using the system equations of motion without damping.

Hruda and Jones introduced a load transformation consistent with modal synthesis techniques. In terms of the present notation, Equation (216) can be replaced by:

$$\{L_j\} = [LT1]_j \begin{Bmatrix} \ddot{q}_N^{Pj} \\ \hline \ddot{x}_{Ij}^B \end{Bmatrix} + [LT2]_j \{x_{Ij}^B\} \tag{217}$$

with

$$[LT1]_j = [k\Psi]_j [I_{Pj} E_{Pj} I_{Pj}^T][-M_{Pj}](I_{Pj}\Phi_N^{Pj} \mid T_{Pj}) \tag{218}$$

$$[LT2]_j = [k\Psi]_j [T_{Pj}] \tag{219}$$

Note that [LT2] = 0 when the interface is determinate.

Normally, the displacement vector $\{x_{Ij}^B\}$ in Equation (217) must be written in terms of forces and accelerations using the second partition in Equation (193). This not only increases the cost of the procedure, but also introduces the booster accelerations $\{\ddot{q}_N^B\}$ and forces $\{F_B\}$ into the problem. We shall now show that this is not necessary under certain conditions.

First, let us obtain the expression for $\{x_{Ij}^B\}$ which ordinarily should be used in Equation (217). From the second partition in the discrete Equation (193) we obtain for $\{x_I^B\}$:

$$\{x_I^B\} = [K_{II}]^{-1} ([T_B]^T \{F_B\} - [\tilde{B}]\{\ddot{x}_N^B\} - \tag{220}$$

$$- [\tilde{P}]\{\ddot{x}_N^P\} - [M_{II}]\{\ddot{x}_I^B\} - [D_{II}]\{\dot{x}_I^B\})$$

where

$$[\tilde{B}] = [T_B^T M_B I_B] \tag{221}$$

$$[\tilde{P}] = \begin{bmatrix} T_{P1}^T M_{P1} I_{P1} & 0 \\ 0 & T_{P2}^T M_{P2} I_{P2} \\ 0 & 0 \end{bmatrix} \tag{222}$$

This is the exact expression for the discrete interface displacement vector. The damping force $[D_{II}]\{\dot{x}_I^B\}$ possibly can be neglected, but we may also keep it. Next, the acceleration approach requires the introduction of the modal accelerations which then subsequently are truncated:

$$\{x_I^B\} = [K_{II}]^{-1} \left([T_B]^T \{F_B\} - [B]\{\ddot{q}_N^B\} - \right.$$
$$\left. - [P]\{\ddot{q}_N^P\} - [M_{II}]\{\ddot{x}_I^B\} - [D_{II}]\{\dot{x}_I^B\} \right) \tag{223}$$

This is the expression which ordinarily must be used in Equation (217), i.e., the $\{x_I^B\}$ as given by Equation (223) must be used to select out the appropriate $\{x_{Ij}^B\}$ partition.

On the other hand, the expression for $\{x_I^B\}$ as calculated by the response routine can be obtained from the second partition of Equation (196):

$$\{x_I^B\} = [K_{II}]^{-1} \left([T_B]^T \{F_B\} - [B]\{\ddot{q}_N^B\} - \right.$$
$$\left. - [P]\{\ddot{q}_N^P\} - [M_{II}]\{\ddot{x}_I^B\} - [D_{II}]\{\dot{x}_I^B\} \right) \tag{224}$$

which turns out to be identical to Equation (223). Therefore, we can use $\{x_{Ij}\}$ in Equation (217) as given by the response routine. No conversion is necessary.

In case interface modes are used in the response routine, i.e. if

$$\{x_I^B\} = [\Phi_I^B]\{q_I^B\} \tag{225}$$

then the calculated $\{q_I^B\}$ vector is given by:

$$\{q_I^B\} = [\omega_I^2]^{-1} \left([\Phi_I^B]^T [T_B]^T \{F_B\} \right.$$
$$- [\Phi_I^B{}^T T_B^T M_B I_B \bar{\Phi}_N^B] \{\ddot{\bar{q}}_N^B\} - [2\zeta_I \omega_I] \{\dot{q}_I^B\} \qquad (226)$$
$$\left. - [\Phi_I^B{}^T T_P^T M_P I_P \bar{\Phi}_N^P] \{\ddot{\bar{q}}_N^P\} - \{\ddot{q}_I^B\} \right)$$

The corresponding $\{x_I^B\}$ is given by:

$$\{x_I^B\} = [\Phi_I^B] [\omega_I^2]^{-1} \left([\Phi_I^B]^T [T_B]^T \{F_B\} \right.$$
$$- [\Phi_I^B]^T [B] \{\ddot{\bar{q}}_N^B\} - [2\zeta_I \omega_I] \{\dot{q}_I^B\} \qquad (227)$$
$$\left. - [\Phi_I^B]^T [P] \{\ddot{\bar{q}}_N^P\} - \{\ddot{q}_I^B\} \right)$$

where we used Equation (225).

Expression (227) will be identical to expression (223) if and only if <u>all</u> interface modes are kept. Indeed , considering the properties

$$[\Phi_I^B]^T [M_{II}] [\Phi_I^B] = [I], \quad [\Phi_I^B]^T [K_{II}] [\Phi_I^B] = [\omega_I^2] \qquad (228)$$

we can write

$$[K_{II}]^{-1} = [\Phi_I^B] [\omega_I^2]^{-1} [\Phi_I^B]^T \qquad (229)$$

only if we keep all interface modes. Conversely, if we do not keep all interface modes, then Equation (229) is not valid and the right-hand side of Equation (227) is different from the right-hand side of Equation (226). Substituting Equations (225), (228) and (229) into Equation (227) yields:

$$\{x_I^B\} = [\Phi_I^B] [\omega_I^2]^{-1} [\Phi_I^B]^T \left([T_B]^T \{F_B\} - [B] \{\ddot{\bar{q}}_N^B\} \right.$$
$$- [\Phi_I^B]^{-T} [2\zeta_I \omega_I] [\Phi_I^B]^{-1} \{\dot{x}_I^B\} \qquad (230)$$
$$\left. - [P] \{\ddot{\bar{q}}_N^P\} - [M_{II}] [\Phi_I^B] \{\ddot{q}_I^B\} \right)$$

or,

$$\{x_I^B\} = [K_{II}]^{-1} \left([T_B]^T \{F_B\} - [B]\{\ddot{\bar{q}}_N^B\} - \right.$$

$$\left. - [P]\{\ddot{\bar{q}}_N^P\} - [M_{II}]\{\ddot{x}_I^B\} - [D_{II}]\{\dot{x}_I^B\} \right) \tag{231}$$

which is identical to Equation (223)

Next, let us write Equation (218) as follows:

$$[LT1]_j = [k\Psi]_j [I_{Pj}] \left(- [E_{Pj}][I_{Pj}^T M_{Pj} I_{Pj}][\bar{\phi}_N^{Pj}] \right.$$

$$\left. - [E_{Pj}][I_{Pj}^T M_{Pj} T_{Pj}] \right) \tag{232}$$

It is now relatively easy to show that $[E_{Pj}][I_{Pj}^T M_{Pj} I_{Pj}][\bar{\phi}_N^{Pj}] = [\bar{\phi}_N^{Pj}][\bar{\omega}_{Pj}^2]^{-1}$ even when not all the payload modes are retained in $[\bar{\phi}_N^P]$. Therefore, Equation (234) can be written as:

$$[LT1]_j = [k\Psi]_j [I_{Pj}] \left(- [\bar{\phi}_N^{Pj}] [\bar{\omega}_{Pj}^2]^{-1} \right.$$

$$\left. - [E_{Pj}][I_{Pj}^T M_{Pj} T_{Pj}] \right) \tag{233}$$

Using Equations (217), (219) and (233) has several advantages over the approach outlined in Reference [53]. First, in case the interface is indeterminate (i.e. if LT2 = 0) it is not necessary to use Equation (223) for $\{x_I^B\}$, if and only if we keep all the interface modes $[\phi_I^B]$. This not only makes the evaluation of Equation (217) much simpler, but also reduces the amount of information to be stored in the course of the response calculations (i.e. only $\{\ddot{\bar{q}}_N^P\}$, $\{\ddot{x}_I^B\}$ and $\{x_I^B\}$ must be stored). Secondly, the rather expensive evaluation of $[\alpha]_j = -[k\Psi]_j [I_{Pj}][E_{Pj}][I_{Pj}^T M_{Pj} I_{Pj}][\bar{\phi}_N^{Pj}]$ as proposed in Reference [53] is now replaced by the more efficient computation of $[\beta]_j = [\bar{\phi}_N^{Pj}][\bar{\omega}_{Pj}^2]^{-1}$. Indeed, applying unit loads successively to each of the non-interface dofs., often becomes a rather expensive item, considering the potentially very large payload models. The other term in Equation (232), $[\gamma]_j = -[k\Psi]_j [I_{Pj}][E_{Pj}] \times [I_{Pj}^T M_{Pj} T_{Pj}]$ can be easily evaluated by first forming the product

$[I_{Pj}^T M_{Pj} T_{Pj}]$, the columns of which can be looked upon as inertial loads applied at the interface of the payload. The corresponding deflections are equal to $[\mathcal{E}]_j = [E_{Pj}][I_{Pj}^T M_{Pj} T_{Pj}]$. Finally, one must evaluate $[\mathcal{E}]_j = [T_{Pj}]$ in Equation (219) so that we obtain:

$$[LT1]_j = [k\Psi]_j([\beta]_j, [\delta]_j) \tag{234}$$

$$[LT2] = [k\Psi]_j[\mathcal{E}]_j \tag{235}$$

Observe that the payload organization can easily save $[\beta]_j$, $[\delta]_j$, and $[\mathcal{E}]_j$ so that any member in the payload can now be investigated without recalculating these matrices. Observe that Reference [53] requires the payload analyst to make the choice of members before the evaluation of Equations (234) and (235). If for some reason an additional member has to be investigated, a reevaluation of $[LT1]_j$ and $[LT2]_j$ is necessary.

Finally, it should also be noted that the loads calculation does not involve the "modal modes" which reduces the computational cost even more.

5. Conclusions and Summary

A numerical integration scheme has been presented. It is a "full-scale" approach in the sense that it does not introduce new assumptions or approximations compared to the conventional "exact" solution techniques. Improvements over the conventional techniques are introduced in both the response and loads calculations.

The response analysis uses an adaptation of the Newmark-Chan-Beta numerical integration technique. This integration scheme is directly applied to the coupled system equations (i.e. booster/payload system) thereby avoiding the expensive solution of a system eigenvalue problem. The Newmark-Chan-Beta technique has the convenient feature that the step size can be based on the "cut-off frequency" associated with the forcing function regardless of the highest system frequency. This particular feature is necessary in the present method because the highest system frequency is not known a priori. Although there are techniques to determine the highest frequency, it is very likely that this highest frequency will be much larger than the cut-off frequency which would lead to a much smaller time step. It should also be noted that the present approach allows for the solution of much larger systems.

Next, we derived a load transformation consistent with the above modal synthesis method. Several cost saving features were introduced. First, we showed that in the case of an indeterminate interface it is not necessary to write the interface displacements in terms of accelerations and forces, provided one keeps all the interface modes. As indicated, one could actually keep the discrete interface displacements instead of

introducing the interface modes. Secondly, it was shown that several simplifications can be affected in the calculation of [LT1] and [LT2] leading to a more efficient and convenient loads calculation. Finally, it should also be pointed out that we do not involve system modes which reduces the cost and simplifies the analysis.

It is estimated that the present approach will reduce the computer cost of a payload integration effort by a considerable amount. Considering the numerous load cases that must be considered in the course of a design effort, the present approach may prove to be of great value.

CHAPTER III. A PAYLOAD INTEGRATION TECHNIQUE - SHORT-CUT VERSION

1. Introduction

In Chapter II, we developed a numerical integration scheme which is capable of solving the set of coupled system equations as given by Equations (196). The method is a full-scale technique because no special assumptions or approximations are used. This means that the results are as accurate as those obtained from a standard full-scale approach. However, under the right circumstances, the cost of this approach is significantly lower.

In this chapter, we wish to adapt this full-scale direct integration technique to a short-cut version. The approach is based on estimating the size of the feedback from the payload response into the booster. First, we shall derive the so-called coupled base motion equations for the system. These equations still represent a set of accurate full-scale equations of motion. One possible approach is to completely neglect the feedback of the payload into the booster. This leads to a technique known as the direct base drive technique as discussed in Chapter I, section A3f and B3. In many cases this technique leads to acceptable results. Instead of completely neglecting the feedback, we shall subject the magnitude of this feedback to a criterion. The result will be a method which, depending on the nature of the structure at hand, will vasilate between a full-up coupled base motion technique and a direct base drive method.

In section 2, we shall derive the pertinent equations of motion.

2. The Equations of Motion

First, note that the equations of motion for the coupled base moti technique are derived in Chapter A3.f. Following that derivation, let us write down the coupled set of equations of motion as given by Equations (196):

$$\begin{bmatrix} I & B^T & 0 \\ B & M_{II} & P \\ 0 & P^T & I \end{bmatrix} \begin{Bmatrix} \ddot{q}_N^B \\ \ddot{x}_I^B \\ \ddot{q}_N^P \end{Bmatrix} + \begin{bmatrix} 2\tilde{\zeta}_B \tilde{\omega}_B & & \\ & D_{II} & \\ & & 2\zeta_P \omega_P \end{bmatrix} \begin{Bmatrix} \dot{q}_N^B \\ \dot{x}_I^B \\ \dot{q}_N^P \end{Bmatrix} + \begin{bmatrix} \tilde{\omega}_B^2 & & \\ & K_{II} & \\ & & \omega_P^2 \end{bmatrix} \begin{Bmatrix} q_N^B \\ x_I^B \\ q_N^P \end{Bmatrix} = \begin{Bmatrix} \tilde{\zeta}_N^B I_B^T F_B \\ T_B^T F_B \\ 0 \end{Bmatrix}, \tag{236}$$

where

$$M_{II} = T_B^T M_B T_B + \begin{bmatrix} T_{P1}^T M_{P1} T_{P1} & 0 & 0 \\ 0 & T_{P2}^T M_{P2} T_{P2} & 0 \\ 0 & 0 & 0 \end{bmatrix},$$

$$K_{II} = T_B^T K_B T_B + \begin{bmatrix} T_{P1}^T K_{P1} T_{P1} & 0 & 0 \\ 0 & T_{P2}^T K_{P2} T_{P2} & 0 \\ 0 & 0 & 0 \end{bmatrix}, \qquad (237)$$

$$P = \left[\begin{array}{c|c} T_{P1}^T M_{P1} I_{P1} \bar{\phi}_N^{P1} & 0 \\ \hline 0 & T_{P2}^T M_{P2} I_{P2} \bar{\phi}_N^{P2} \\ \hline 0 & 0 \end{array}\right], \qquad \{\bar{\sigma}_N^P\} = \left\{\begin{array}{c} \bar{q}_N^{P1} \\ \hline \bar{q}_N^{P2} \end{array}\right\}$$

$$B = T_B^T M_B I_B \bar{\phi}_N^B, \qquad \bar{\omega}_N^2 = \left[\begin{array}{c|c} \bar{\omega}_{P1}^2 & \\ \hline & \bar{\omega}_{P2}^2 \end{array}\right]$$

Following the philosophy of a base motion technique we first solve the following set of equations,

$$\left[\begin{array}{c|c} I & B^T \\ \hline B & T_B^T M_B T_B \end{array}\right] \left\{\begin{array}{c} \ddot{\bar{q}}_{N0}^B \\ \hline \ddot{x}_{I0}^B \end{array}\right\} + \left[\begin{array}{c|c} 2\bar{\zeta}_E \bar{\omega}_B & 0 \\ \hline 0 & 0 \end{array}\right] \left\{\begin{array}{c} \dot{\bar{q}}_{N0}^B \\ \hline \dot{x}_{I0}^B \end{array}\right\}$$

$$+ \left[\begin{array}{c|c} \bar{\omega}_B^2 & 0 \\ \hline 0 & T_B^T K_E T_B \end{array}\right] \left\{\begin{array}{c} \bar{q}_{N0}^B \\ \hline x_{I0}^B \end{array}\right\} = \left\{\begin{array}{c} \bar{\phi}_N^{B^T} I_B^T F_B \\ \hline T_B^T F_B \end{array}\right\} \qquad (238)$$

This set of equations represent the equations of motion for the booster without payload(s). Note that one could also load the booster with a standard payload which would represent a kind of average payload.

The solution of Equation (238) is the same for all payload configurations and does not change as long as the forcing function and the booster model do not change. A modified Newmark-Chan-Beta numerical integration scheme can be used to obtain the solution of (238):

$$\{\dot{q}\}_{0i+1} = \{\dot{q}\}_{0i} + (1-\gamma)h\{\ddot{q}\}_{0i} + \gamma h\{\ddot{q}\}_{0i+1}$$

$$\{q\}_{0i+1} = \{q\}_{0i} + h\{\dot{q}\}_{0i} + (0.5-\beta)h^2\{\ddot{q}\}_{0i} + h^2\beta\{\ddot{q}\}_{0i+1} \tag{239}$$

$$\begin{bmatrix} D_1 & B^T \\ B & D_2 \end{bmatrix} \begin{Bmatrix} \ddot{\bar{q}}^B_{NOi+1} \\ \ddot{x}^B_{IOi+1} \end{Bmatrix} = \begin{Bmatrix} f_{Bi} \\ f_{Ii} \end{Bmatrix} \tag{240}$$

where

$$f_{Bi} = \bar{\Phi}^{B^T}_N I^T_B F_{Bi+1} - D_3\dot{\bar{q}}^B_{NOi} - D_5\ddot{\bar{q}}^B_{NOi} - \bar{\omega}^2_B\,\bar{q}^B_{NOi} \tag{241}$$

$$f_{Ii} = T^T_B F_{Bi+1} - D_4\dot{x}^B_{IOi} - D_6\ddot{x}^B_{NOi} - T^T_B K_B T_B x^B_{NOi}$$

Also,

$$D_1 = I + 2\gamma h\bar{\zeta}_B\bar{\omega}_B + \beta h^2\bar{\omega}^2_B$$

$$D_1 = T^T_B M_B T_B + T^T_B K_B T_B h^2\beta \tag{242}$$

$$D_3 = 2\bar{\zeta}_B\bar{\omega}_B + \bar{\omega}^2_B h^2$$

C-2

$$D_4 = T_B^T K_B T_B h^2$$

$$D_5 = 2\bar{\zeta}_B \bar{\omega}_B (1-\gamma)h + (0.5-\beta)h^2 \bar{\omega}_B^2 \qquad (242)$$

$$D_6 = T_B^T K_B T_B (0.5-\beta)h^2$$

Premultiplying (240) by $[\ -BD_1^{-1} \mid I]$ yields

$$\ddot{x}^B_{ICi+1} = A_1 [\ f_{Ii} + A_2 f_{Bi}\ ] \qquad (243)$$

with

$$A_2 = -B\ D_1^{-1}$$

$$A_1 = [\ D_2 + A_2\ B^T\ ]^{-1}$$

also,

$$\ddot{q}^B_{NOi+1} = D_1^{-1}\ f_{Bi} - A_2^T\ \ddot{x}^B_{NOi+1} \qquad (244)$$

The equations to use then are Equations (239, 241, 243, 244). The quantities to save are $\{x_{IO}\}$, $\{\dot{x}_{IO}\}$ and $\{\ddot{x}_{IO}\}$.

Returning to Equation (236) we can write:

$$\left\{\bar{q}_N^B\right\} = \left\{\bar{q}_{NO}^B\right\} + \left\{\bar{q}_{NR}^B\right\}$$

$$\left\{x_I^B\right\} = \left\{x_{IO}^B\right\} + \left\{x_{IR}^B\right\} \qquad (245)$$

The residual quantities $\left\{\bar{q}_{NR}^B\right\}$ and $\left\{x_{IR}^B\right\}$ are clearly due to the presence of the payload(s), i.e. they are the feedback of the payload(s) back into the booster. Let us write the following vector equation,

$$\begin{Bmatrix} \bar{q}_N^B \\ x_I^B \\ \bar{q}_N^P \end{Bmatrix} = \begin{Bmatrix} \bar{q}_{NO}^B \\ x_{IO}^B \\ 0 \end{Bmatrix} + \begin{Bmatrix} \bar{q}_{NR}^B \\ x_{IR}^B \\ \bar{q}_N^P \end{Bmatrix} \qquad (246)$$

Substituting Equation (246) into Equation (236) and taking into account Equations (237-238) leads to the coupled base motion equations,

$$\left[\begin{array}{c|c|c} I & B^T & 0 \\ \hline B & M_{II} & P \\ \hline 0 & P^T & I \end{array}\right] \begin{Bmatrix} \ddot{\bar{q}}_{NR}^B \\ \ddot{x}_{IR}^B \\ \ddot{\bar{q}}_N^P \end{Bmatrix} + \left[\begin{array}{c|c|c} 2\bar{\zeta}_B\bar{\omega}_B & 0 & 0 \\ \hline 0 & D_{II} & 0 \\ \hline 0 & 0 & 2\bar{\zeta}_P\bar{\omega}_P \end{array}\right] \begin{Bmatrix} \dot{\bar{q}}_{NR}^B \\ \dot{x}_{IR}^B \\ \dot{\bar{q}}_N^P \end{Bmatrix}$$

$$+ \left[\begin{array}{c|c|c} \bar{\omega}_B^2 & 0 & 0 \\ \hline 0 & K_{II} & 0 \\ \hline 0 & 0 & \bar{\omega}_P^2 \end{array}\right] \begin{Bmatrix} \bar{q}_{NR}^B \\ x_{IR}^B \\ \bar{q}_N^P \end{Bmatrix} = \begin{Bmatrix} 0 \\ \hline -MP_{II}\ddot{x}_{IO}^B - D_{II}\dot{x}_{IO}^B - KP_{II}x_{IO}^B \\ \hline -P^T\ddot{x}_{IO}^B \end{Bmatrix} \qquad (247)$$

where

$$[MP_{II}] = \begin{bmatrix} T_{P1}^T M_{P1} T_{P1} & 0 & 0 \\ 0 & T_{P2}^T M_{P2} T_{P2} & 0 \\ 0 & 0 & 0 \end{bmatrix}$$

$$[KP_{II}] = \begin{bmatrix} T_{P1}^T K_{P1} T_{P1} & 0 & 0 \\ 0 & T_{P2}^T K_{P2} T_{P2} & 0 \\ 0 & 0 & 0 \end{bmatrix} \qquad (248)$$

This set of Equations (247) could be solved resulting in a full-scale accurate solution. However, physically it is possible that the feedback vector $\{\ddot{x}_{IR}^{B}\}$ is small (note that we need not have $\{\dot{x}_{IR}^{B}\}$ and $\{x_{IR}^{B}\}$ small), i.e. $\{\ddot{x}_{IR}^{B}\} \approx 0$ for all times t. Then from the third partition of Equation (247) we obtain a decoupled equation for $\{\bar{q}_N^P\}$,

$$\{\ddot{\bar{q}}_N^P\} + [2\bar{\zeta}_P\bar{\omega}_P]\{\dot{\bar{q}}_N^P\} + [\bar{\omega}_P^2]\{\bar{q}_N^P\} = -\{P^T x_{I0}^B\} \qquad (249)$$

which can be easily solved, because $\{\ddot{x}^B_{IO}\}$ is known. This approach is called the direct base drive technique and has been used successfully.

The problem however is that the magnitude of $\{\ddot{x}^B_{IR}\}$ is not known in advance and may not always be small. In that case, Equation (247) should be solved retaining the coupling terms. Again, a Newmark-Chan-Beta technique can be used as follows,

$$\{\dot{q}\}_{i+1} = \{\dot{q}\}_i + (1-\gamma)h\{\ddot{q}\}_i + \gamma h\{\ddot{q}\}_{i+1} \tag{250}$$

$$\{q\}_{i+1} = \{q\}_i + h\{\dot{q}\}_i + (0.5-\beta)h^2\{\ddot{q}\}_i + h^2\beta\{\ddot{q}\}_{i+1}$$

and

$$f_{Bi} = -D_4 \dot{\bar{q}}^B_{NRi} - D_7 \ddot{\bar{q}}^B_{NRi} - \bar{\omega}_B^2 \bar{q}^B_{NRi}$$

$$f_{Ii} = -MP_{II} \ddot{x}^B_{IOi+1} - D_{II} \dot{x}^B_{IOi+1} - KP_{II} x^B_{IOi+1}$$

$$- D_5 \dot{x}^B_{IRi} - D_8 \ddot{x}^B_{IRi} - K_{II} x^B_{IRi} \tag{251}$$

$$f_{Pi} = -P^T \ddot{x}^B_{IOi+1} - D_6 \dot{\bar{q}}^P_{Ni} - D_9 \ddot{\bar{q}}^P_{Ni} - \bar{\omega}_P^2 \bar{q}^P_{Ni}$$

Also,

$$\ddot{x}^B_{IRi+1} = A_1(A_2 f_{Bi} + f_{Ii} + A_3 f_{Pi}) \tag{252}$$

$$\ddot{\bar{q}}^B_{NRi+1} = D_1^{-1} f_{Bi} + A_2^T \ddot{x}^B_{IRi+1}$$

$$\ddot{\bar{q}}^P_{Ni+1} = D_3^{-1} f_{Pi} + A_3^T \ddot{x}^B_{IRi+1} \tag{253}$$

where

$$A_1 = [\ D_2 + A_2 B^T + A_3 P^T\ ]^{-1}$$

$$A_2 = -\ B\ D_1^{-1} \quad , \quad A_3 = -\ P\ D_3^{-1} \tag{254}$$

and

$$D_1 = I + 2\gamma h \bar{\zeta}_B \bar{\omega}_B + \beta h^2 \bar{\omega}_B^2$$

$$D_2 = M_{II} + \gamma h D_{II} + \beta h^2 K_{II}$$

$$D_3 = I + 2\gamma h \bar{\zeta}_P \bar{\omega}_P + \beta h^2 \bar{\omega}_P^2$$

$$D_4 = 2\bar{\zeta}_B \bar{\omega}_B + h\bar{\omega}_B^2 \quad , \quad D_5 = D_{II} + h K_{II}$$

$$D_6 = 2\bar{\zeta}_P \bar{\omega}_P + h\bar{\omega}_P^2$$

$$D_7 = 2(1-\gamma) h \bar{\zeta}_B \bar{\omega}_B + (0.5-\beta) h^2 \bar{\omega}_B^2 \tag{255}$$

$$D_8 = (1-\gamma) h D_{II} + (0.5-\beta) h^2 K_{II}$$

$$D_9 = 2(1-\gamma) h \bar{\zeta}_P \bar{\omega}_P + (0.5-\beta) h^2 \bar{\omega}_P^2$$

At this point, it is possible to introduce a criterion which checks the magnitude of say $\{\ddot{x}^B_{IRi}\}$. If this magnitude is smaller than a certain preset ε then the quantities $A_2^T\{\ddot{x}^B_{IRi+1}\}$ and $A_3^T\{\ddot{x}^B_{IRi+1}\}$ in Equations (253) are not calculated. A possible criterion could be of the following form :

$$\|\ddot{x}^B_{IRi}\| \leq \varepsilon \|\ddot{x}^B_{IOi}\| \tag{256}$$

where ε is a preset percentage (e.g. 0.01).

This criterion could partially avoid the premultiplications by A_2^T and A_3^T in Equation (253). There are two more cost generating premultiplications by A_2 and A_3 in Equation (252). These could possibly also be avoided when the feedback acceleration is small. This would mean a direct base drive at that particular time step. Both these approaches were implemented and will be discussed in the next chapter.

The main problem with this kind of approaches is to find an answer to the question: What constitutes a small feedback? This question is still not answered even with an equation like Equation (256). Even though encouraging results were obtained, it is recognized that additional research and development is necessary.

CHAPTER IV. THE SOFTWARE PACKAGE - IMPLEMENTATION

1. Introduction

This chapter discusses in general terms the software package associated with a complete booster/payload response and loads analysis. An attempt will be made to clearly link the theory of Chapter I with the specific program and subroutine descriptions. This will give us the opportunity to touch upon some of the constraints and difficulties invariably associated with the development of a practical payload integration software package. Some factors to consider are: computer core usage; convergence; available data; the separation of booster, payload and integration organizations; work schedules; engineering time; ease of program usage; computer cost and related efficiency of algorithms; reuse of existing information; required accuracy versus cost; handling of potentially large models; etc.

Section 2 of this chapter presents a general description of the organization and components of the software package. In particular, we explain the purpose and contents of the components and how they relate to each other.

Section 3 presents a simple sample problem and shows how it is analyzed and evaluated. Also, the case of the STS-ST-OMS Kit is discussed in addition to some other sample problems. Finally, we shall also discuss some of the results related to the short-cut version developed in Chapter III.

2. Organization - General Description

This section outlines the organization of the software package. Figure 4 represents a flow diagram of a complete booster/payload integration problem. Each of the flow diagram blocks has a program associated with it. Therefore, there are six programs: PROGRAM BOOSTER, PROGRAM PAYLOAD, PROGRAM INTFACE, PROGRAM FORCE, PROGRAM RESPONS AND PROGRAM LOADS. Each of these programs draws on a pool of subroutines called FORMA (Fortran Matrix Analysis). FORMA is a library of subroutines coded in FORTRAN IV for the efficient solution of structural dynamics problems. These subroutines are in the form of building blocks that can be put together to solve a large variety of structural dynamics problems. The FORMA library was developed by the Dynamics and Loads Section at Martin Marietta Aerospace and is being updated and expanded whenever the need occurs.

It should be pointed out that other libraries can be used and that the proposed integration method does in no way inherently depend on the FORMA library. However, in this report, the software is built around the FORMA subroutine library (in particular, the Partition-Logic version) and therefore, the reader is assumed to have a working knowledge of that library.

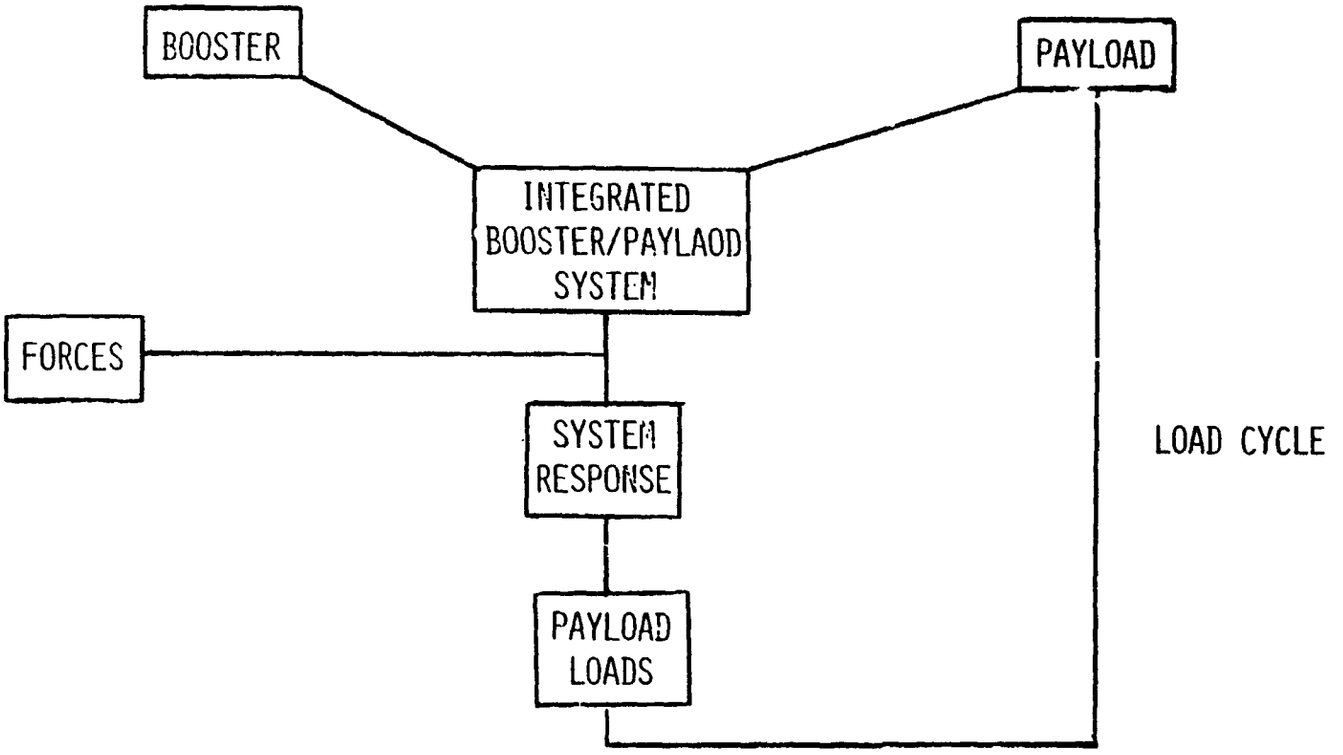

Figure 4: PAYLOAD INTEGRATION PROBLEM

There are several reasons motivating the PROGRAM approach. Because all FORMA routines are written in terms of variable dimensions, it is possible to write each PROGRAM for the specific dimensions of the problem at hand, thereby optimizing computer core usage. Also, the user often has at his/her disposal data already generated by other means. The PROGRAM approach allows the user to omit the recalculation of that particular data. For example, a set of so-called expanded modes could be available. The user then can directly read those expanded modes into the PROGRAM and omit the use of a subroutine which calculates those expanded modes. Furthermore, the PROGRAM approach allows for the separation of data generated by the booster, payload and integration organizations. Indeed, very often these three organizations are physically at different locations and data peculiar to one organization often is not readily available to the other organizations. PROGRAM BOOSTER for example, only deals with data pertaining to the booster and, therefore, works independent of the payload. Also, sometimes the data generated by PROGRAM BOOSTER can be used in analyses of different payloads and therefore has not to be recalculated.

Finally, the PROGRAM approach also allows for better check-out and control of the data generated at several points in the process of a load cycle. Indeed, the user can put in his/her own checks if desired.

PROGRAM RESPONS represents the hub around which the other five programs are centered. The purpose of PROGRAM RESPONS is to generate the coupled booster/payload system response. The most important subroutine called by PROGRAM RESPONS is SUBROUTINE ZRESP, which implements the integration scheme as outlined in Chapter II. The INPUT to PROGRAM RESPONS consists of all the quantities necessary to run SUBROUTINE ZRESP. The OUTPUT of PROGRAM RESPONS is the system response i.e. displacements, velocities and accelerations. These quantities can be written on paper and tape. In particular, the payload accelerations and the booster/payload interface displacements at each time step are written on tape so that they can be used in PROGRAM LOADS for the calculation of member loads.

Much of the INPUT to PROGRAM RESPONS is not directly given and therefore must be created in advance. PROGRAM BOOSTER, PROGRAM PAYLOAD and PROGRAM FORCE were composed to serve this purpose. PROGRAM BOOSTER generates all booster data necessary to run PROGRAM RESPONSE. The booster organization can use this PROGRAM independently of any other organization. Enough subroutines were developed so that all booster data can be generated starting with the free mass and stiffness matrices $[M_B]$ and $[K_B]$ and the interface restrained modes and frequencies $[\Phi^B_N]$ and $[\bar{\omega}^2_B]$. It is reasonable to expect that these INPUT quantities are available. If not, the user is expected to provide this information before running PROGRAM BOOSTER. It would not be wise to "can" the construction of $[M_B]$, $[K_B]$, $[\Phi^B_N]$ and $[\bar{\omega}^2_B]$ because of

the multitude of ways these quantities can be generated. Furthermore, PROGRAM BOOSTER contains a number of "flags" which allow for user flexibility of INPUT. Indeed, often times certain quantities are already available and need not to be regenerated. The same is true for PROGRAM PAYLOAD which is very similar to PROGRAM BOOSTER except that it generates payload quantities necessary to run PROGRAM RESPONS. In addition, it also generates parts of load transformations if desired. Again, much flexibility is possible depending on the case at hand. PROGRAM INTFACE collects some of the data generated by PROGRAM BOOSTER and PROGRAM PAYLOAD and produces quantities that involve both booster and payload data. Again, these quantities are needed in PROGRAM RESPONS and PROGRAM LOADS. PROGRAM INTFACE reflects the coupling between booster and payload through the interface. For example, it calculates the interface modes $[\Phi_I^B]$. PROGRAM FORCE essentially converts the force data into the right format to be used in the integration program PROGRAM RESPONS. PROGRAM FORCE also contains a number of "flags" which allows for more flexibility. Finally, as mentioned above, PROGRAM LOADS generates member loads and draws on PROGRAM PAYLOAD for load transformation INPUT and on PROGRAM RESPONS for payload response INPUT.

Each of the six PROGRAMS are independent components of the software package. PROGRAM BOOSTER can be used by an independent booster organization. Similarly, PROGRAM PAYLOAD can be used by an independent payload organization. PROGRAM INTFACE, PROGRAM FORCE and PROGRAM RESPONS can be used by an independent integration organization while PROGRAM LOADS can be used by any organization that is responsible for loads calculations. Because each of the PROGRAMS is compatible with the other PROGRAMS, it is also possible for one organization to use the entire package in sequence.

This section was intended to give the reader a general idea of how the software package is structured. It is not intended to be a detailed user guide. The Final Report of this contract will be accompanied by a detailed user guide as well as the actual listings of all the PROGRAMS and associated SUBROUTINES.

3. Numerical Examples

In this section we shall discuss several simple sample problems which were used to check out the internal correctness of the software package. Furthermore, we shall briefly present the results of two realistic analyses namely, the analysis of the STS-ST-OMS Kit system and the analysis of a defense booster/payload system.

The first example is depicted in Figure 5. The booster B consists of 18 pipe segments. The mass of each segment is equally divided between the end points of the segment. If we only keep translational dofs, then the free booster has 57 dofs and the "cantilevered" booster has NB = 54 dofs. Similarly, the payload P consists of 7 pipe segments and NP = 21. Because there are 3 rigid body modes, we have a determinate interface and IF = 3. The parameters for a booster pipe segment are:

$$E=6.89\times10^{6}\,kN/m^2,\ \rho=2.77\times10^{2}\,kg/m^3,\ A_{body}=1.93\times10^{-2}m^2,$$

$$A_{wing}=4.17\times10^{-3}m^2,\ L=0.762m\ \ J_o=8.325\times10^{-4}m^4$$

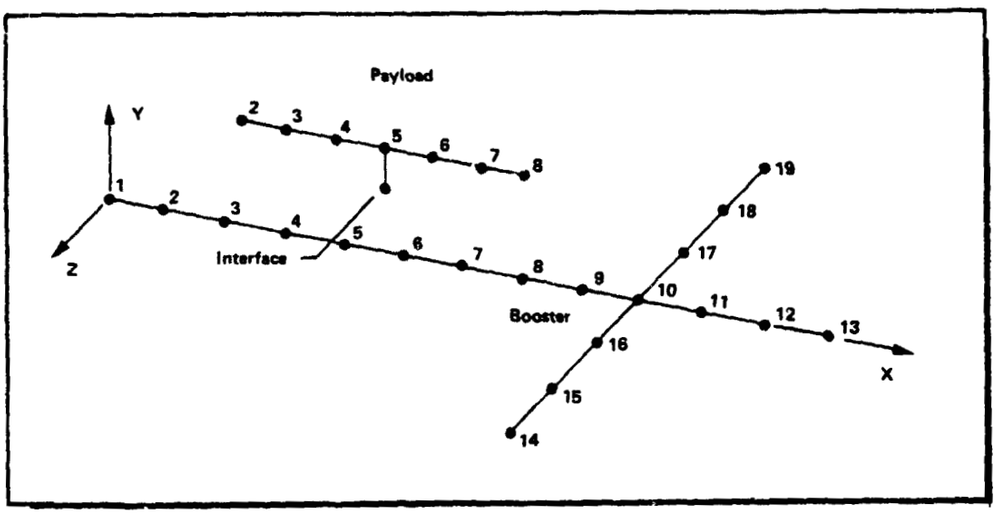

Figure 5 Sample Problem: Booster and Payload

Similarly, for a payload pipe segment:

$E=6.89\times10^{6}kN/m^{2}$, $=2.77\times10^{2}kg/m^{3}$, $A=4.05\times10^{-3}m^{2}$,

$L=0.762m$, $J_{o}=1.249\times10^{-6}m^{4}$

Using the above data, a finite element model was derived for both the cantilevered booster and the cantilevered payload. Solving the eigenvalue problem yields booster frequencies ranging from 1 Hz to 106 Hz and payload frequencies from 1 Hz to 104 Hz. In this particular example we used zero initial conditions and applied loads to stations 16 to 17 in the x, y and z-directions ($444822\times\cos(i50t)N, i=1,6$).

The accuracy of the adapted Newmark-Chan-Beta routine was checked by comparing the response results from PROGRAM RESPONS with those obtained from a fourth order Runge-Kutta (Gill modification) routine using the same step size. The results compare very well. Table I shows some of the results for a step size h = 0.001 seconds. It should be pointed out that a phase shift in the response was observed. This is to be expected and is inherent to the numerical technique used. However, this phase shift does not affect the value of the maximum or minimum loads in an element. It may slightly affect the time at which this minimum occurs, but this is of little consequence. Indeed, it is fair to say that in practice every numerical integration technique produces a phase shift when a time step is used consistent with a cut-off frequency.

Next, we compared computer cost of the present method with that of the conventional approach. The conventional "full-scale" approach first calculates the so-called "modal modes and frequencies" (i.e. the system modes from Equation(196)). Then, a numerical scheme (e.g. Runge-Kutta) is used to determine the response from the uncoupled system equations. For the present example, the cost of the direct integration routine to determine the response is less by a factor of 5 compared to the conventional approach.

We also compared the cost of the load calculations. The improved technique decreases the cost by a factor of 6. It is hard to tell how this factor will change when the booster/payload system represents a more realistic configuration. Also, it may be hard to compare cost factors for large systems from a logistic point of view. Indeed, payload organizations currently deliver load transformations which are not consistent with the present improved approach. Therefore, it is often impossible to generate the appropriate quantities required for use in the present approach, for lack of certain information. It should be noted that this is only a logistics problem and changes could easily be accommodated.

Table II lists some of the load results obtained for this example.

TABLE I
COMPARISON OF FOURTH-ORDER
RUNGE-KUTTA TECHNIQUE AND
NEWMARK-CHAN-BETA TECHNIQUE

DOF	Time (sec)		Runge-Kutta	Newmark-Chan-Beta	Relative Error (%)
21	0.01	Acc. (cm/sec^2)	156.5	155.8	0.46
		Vel. (cm/sec)	-0.5626	-0.5686	1.06
		Dis. (cm)	-6.126^{-3}	$-6.094\ 10^{-3}$	0.52
3	0.01	Acc.	$-6.112\ 10^{4}$	-6.112^{4}	$4.16\ 10^{-6}$
		Vel.	$-2/746\ 10^{2}$	$-2.746\ 10^{2}$	$9.25\ 10^{-6}$
		Dis.	-0.787	-0.792	0.65

TABLE II
COMPARISON OF CLASSICAL AND IMPROVED LOADS CALCULATION TECHNIQUES

Element	Time (sec)	DOF	Loads (N) Classical Method	Loads (N) Improved Method	Relative Error (%)
Interface 1-5	0.01	1	0.646	0.646	0
		2	-0.646	-0.646	0
		3	0	0	0
		4	0	0	0
		5	$-3.929\ 10^{-2}$	$-3.929\ 10^{-2}$	0
		6	$3.929\ 10^{-2}$	$3.929\ 10^{-2}$	0
		7	-0.589	-0.589	0
		8	-0.589	-0.589	0
		9	1.060	1.060	0
		10	-1.060	-1.060	0
		11	-15.90	-15.90	0
		12	-15.90	-15.90	0

The next sample problem consists of a booster plate model to be integrated with two truss-like payloads. The finite element code FINEL (a finite element program developed by the Martin Marietta Aerospace Dynamics Section) was used to develop the three models for the booster and the two payloads.

The booster as shown in Figure 6 is a hexagonal cylinder consisting of 24 quadrilateral plate sections. The material properties for these plates are:

$$\rho = 0.025 \text{ lb/in}^2 \quad , \quad E = 10.6 \times 10^4 \text{ lb/in}^2$$
$$\nu = 0.334 \quad , \quad t \text{ (thickness)} = 0.1 \text{ in}$$

The 24 elements were joined at 30 nodes as described in Table 1. Each of these 30 nodes were assigned three translational degrees of freedom. The geometry and dof. numbering scheme for this booster model are shown in Table 2. Twelve nodes (numbers 8, 9, 11, 12, 14, 15, 17, 18, 20, 21, 23 and 24) and all of their corresponding dofs. were designated to make up the interface for possible coupling with payloads. Thus, for the booster, we have 36 interface dofs. (IF = 36) and 54 non-interface dofs. ($\overline{NB}$ = 54). The booster model was forced in the x-direction at nodes 26, 27, 29 and 30 (dofs. 78, 81, 87 and 90) as follows:

$$F_{78} = 150000 * \text{SIN}[2\pi (0.5) (t-0.001)]$$

$$F_{82} = 160000 * \text{SIN}[2\pi (0.45) (t-0.002)]$$

$$F_{87} = 125000 * \text{SIN}[2\pi (0.6) (t-0.02)]$$

$$F_{90} = 17000 * \text{SIN}[2\pi (0.55) (t-0.01)]$$

i.e. NF = 4.

Figure 7 shows the first payload P1, which is made up of 18 bar elements. The bars are joined at 8 nodes to form this truss. The geometry of the structure is given in Table 4 and the material properties in Table 5. All nodes are assigned translational degrees of freedom only. The four corner nodes make up the interface. We have: ND = 12, IF = 12, NP = 12 and the interface dofs. are 1, 2, 3, 4, 5, 6, 10, 11, 12, 13, 14 and 15.

The model of payload P2 is shown in Figure 8 . It consists of 28 bars joined at 12 nodes forming a truss. The geometry and the degree of freedom table for the model are given in Table 7 and the material properties and connections in Table 8. Again, only translational dofs. are considered. The parameters are: ND = 36, IF = 12, NP = 24 and the interface dofs. are 7, 8, 9, 10, 11, 12, 19, 20, 21, 22, 23 and 24.

A total description of how to use the software package for this sample problem is given in the User Guide MCR-82-002 .

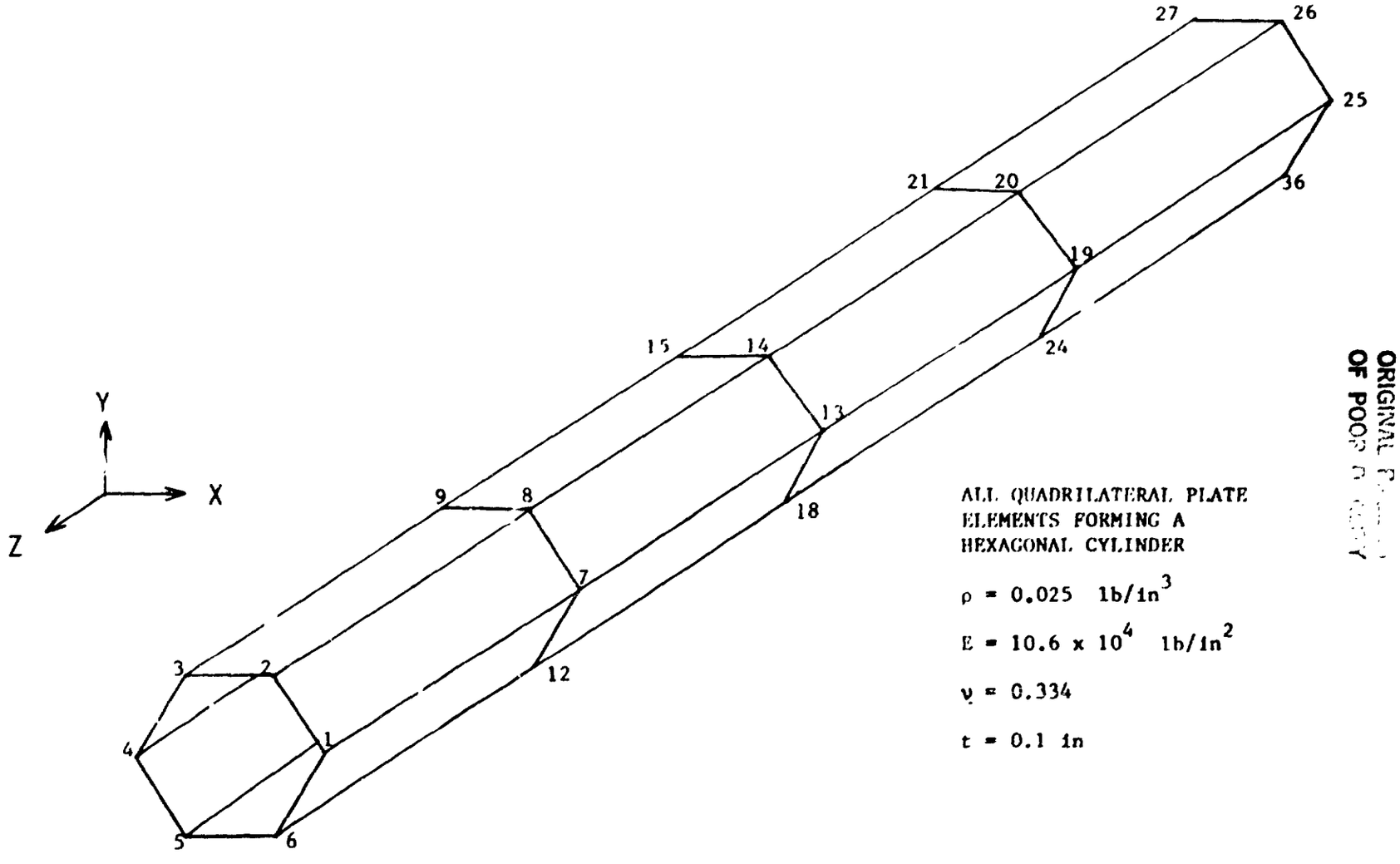

Figure 6 . Booster model for Sample Problem 2

INPUT DATA FOR COMBINED MEMBRANE-BENDING QUADRILATERAL PLATE ELEMENTS

MASS = M1		STIF = K1	
RO = .250E-01		E = .106E+06	
T(MASS) = .100E+00		NU = .334E+00	
		T(MEMBRANE) = .100E+00	
		T(BENDING) = .100E+00	

ELEMENT NUMBER	JOINT 1	JOINT 2	JOINT 3	JOINT 4
1	1	2	8	7
2	2	3	9	8
3	3	4	10	9
4	4	5	11	10
5	5	6	12	11
6	6	1	7	12
7	7	8	14	13
8	8	9	15	14
9	9	10	16	15
10	10	11	17	16
11	11	12	18	17
12	12	7	13	18
13	13	14	20	19
14	14	15	21	20
15	15	16	22	21
16	16	17	23	22
17	17	18	24	23
18	18	13	19	24
19	19	20	26	25
20	20	21	27	26
21	21	22	28	27
22	22	23	29	28
23	23	24	30	29
24	24	19	25	30

Table 1. Description of quadrilateral plate elements for the booster model used in sample problem 2

JOINT DATA USED IN SUBROUTINE FEMKA

JOINT	DEGREES OF FREEDOM TRANSLATION U	V	W	ROTATION P	Q	R	GLOBAL CARTESIAN COORDINATES X	Y	Z
1	1	2	3	0	0	0	5.0000	0.0000	50.0000
2	4	5	6	0	0	0	2.5000	4.3300	50.0000
3	7	8	9	0	0	0	-2.5000	4.3300	50.0000
4	10	11	12	0	0	0	-5.0000	0.0000	50.0000
5	13	14	15	0	0	0	-2.5000	-4.3300	50.0000
6	16	17	18	0	0	0	2.5000	-4.3300	50.0000
7	19	20	21	0	0	0	5.0000	0.0000	25.0000
8	22	23	24	0	0	0	2.5000	4.3300	25.0000
9	25	26	27	0	0	0	-2.5000	4.3300	25.0000
10	28	29	30	0	0	0	-5.0000	0.0000	25.0000
11	31	32	33	0	0	0	-2.5000	-4.3300	25.0000
12	34	35	36	0	0	0	2.5000	-4.3300	25.0000
13	37	38	39	0	0	0	5.0000	0.0000	0.0000
14	40	41	42	0	0	0	2.5000	4.3300	0.0000
15	43	44	45	0	0	0	-2.5000	4.3300	0.0000
16	46	47	48	0	0	0	-5.0000	0.0000	0.0000
17	49	50	51	0	0	0	-2.5000	-4.3300	0.0000
18	52	53	54	0	0	0	2.5000	-4.3300	0.0000
19	55	56	57	0	0	0	5.0000	0.0000	-25.0000
20	58	59	60	0	0	0	2.5000	4.3300	-25.0000
21	61	62	63	0	0	0	-2.5000	4.3300	-25.0000
22	64	65	66	0	0	0	-5.0000	0.0000	-25.0000
23	67	68	69	0	0	0	-2.5000	-4.3300	-25.0000
24	70	71	72	0	0	0	2.5000	-4.3300	-25.0000
25	73	74	75	0	0	0	5.0000	0.0000	-50.0000
26	76	77	78	0	0	0	2.5000	4.3300	-50.0000
27	79	80	81	0	0	0	-2.5000	4.3300	-50.0000
28	82	83	84	0	0	0	-5.0000	0.0000	-50.0000
29	85	86	87	0	0	0	-2.5000	-4.3300	-50.0000
30	88	89	90	0	0	0	2.5000	-4.3300	-50.0000

Table 2. Geometry desciption and degree of freedom table for the booster model used in sample problem 2

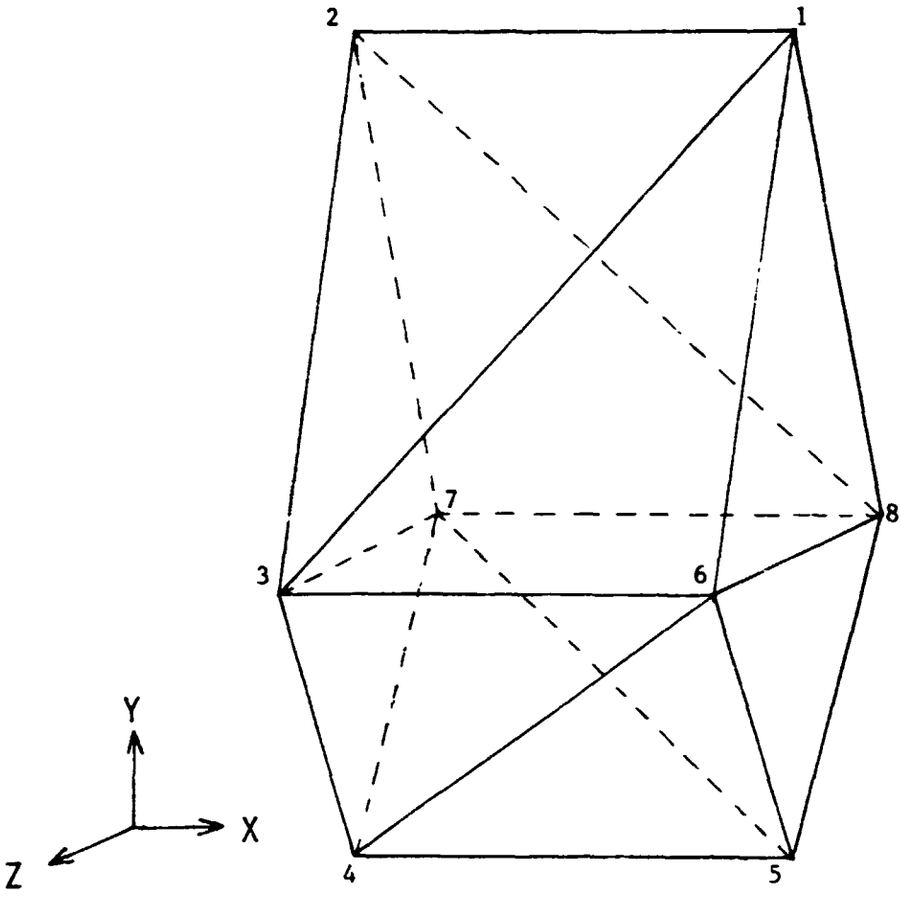

ALL BAR ELEMENTS

$\rho = 0.0025 \quad lb/in^3$

$E = 10.6 \times 10^3 \quad lb/in^2$

$G = 3.84 \times 10^6 \quad lb/in^2$

$A = 0.01 \quad in^2$

$J_0 = 1.67 \times 10^{-5} \quad in^4$

Figure 7 . Payload 1

JOINT DATA USED IN SUBROUTINE FEMKA

JOINT	DEGREES OF FREEDOM TRANSLATION U	V	W	ROTATION P	Q	R	GLOBAL CARTESIAN COORDINATES X	Y	Z
1	1	2	3	0	0	0	2.5000	4.3300	0.0000
2	4	5	6	0	0	0	-2.5000	4.3300	0.0000
3	7	8	9	0	0	0	-2.5000	-1.0000	1.0000
4	10	11	12	0	0	0	-2.5000	-4.3300	0.0000
5	13	14	15	0	0	0	2.5000	-4.3300	0.0000
6	16	17	18	0	0	0	2.5000	-1.0000	1.0000
7	19	20	21	0	0	0	-2.5000	-1.0000	-1.0000
8	22	23	24	0	0	0	2.5000	-1.0000	-1.0000

Table 4. Geometry and degree of freedom table for payload 1

INPUT DATA FOR BAR ELEMENTS

MASS = M1 STIF = K1 KODEK = KODEB =
RO = .250E-02 E = .106E+05 LOAD TRANS = PAYLT STRESS TRANS = ALPHA = 0.
G = 384E+07

ELEMENT NUMBER	JOINT 1	JOINT 2	REF POINT	AREA	POLAR INERTIA	TORSION CONST	Z BENDING INERTIA	Y BENDING INERTIA	SHEAR FACTOR
1	6	1	2	.100E-01	.167E-04	.141E-04	.833E-05	.833E-05	.833
2	1	2	3	.100E-01	.167E-04	.141E-04	.833E-05	.833E-05	.833
3	2	3	1	.100E-01	.167E-04	.141E-04	.833E-05	.833E-05	.833
4	3	6	1	.100E-01	.167E-04	.141E-04	.833E-05	.833E-05	.833
5	3	1	2	.100E-01	.167E-04	.141E-04	.833E-05	.833E-05	.833
6	8	2	1	.100E-01	.167E-04	.141E-04	.833E-05	.833E-05	.833
7	3	4	6	.100E-01	.167E-04	.141E-04	.833E-05	.833E-05	.833
8	4	5	1	.100E-01	.167E-04	.141E-04	.833E-05	.833E-05	.833
9	5	6	3	.100E-01	.167E-04	.141E-04	.833E-05	.833E-05	.833
10	4	6	1	.100E-01	.167E-04	.141E-04	.833E-05	.833E-05	.833
11	7	5	4	.100E-01	.167E-04	.141E-04	.833E-05	.833E-05	.833
12	6	8	5	.100E-01	.167E-04	.141E-04	.833E-05	.833E-05	.833
13	3	7	4	.100E-01	.167E-04	.141E-04	.833E-05	.833E-05	.833
14	8	7	2	.100E-01	.167E-04	.141E-04	.833E-05	.833E-05	.833
15	5	8	6	.100E-01	.167E-04	.141E-04	.833E-05	.833E-05	.833
16	4	7	3	.100E-01	.167E-04	.141E-04	.833E-05	.833E-05	.833
17	1	8	6	.100E-01	.167E-04	.141E-04	.833E-05	.833E-05	.833
18	2	7	3	.100E-01	.167E-04	.141E-04	.833E-05	.833E-05	.833

Table 5. Payload 1 material properties

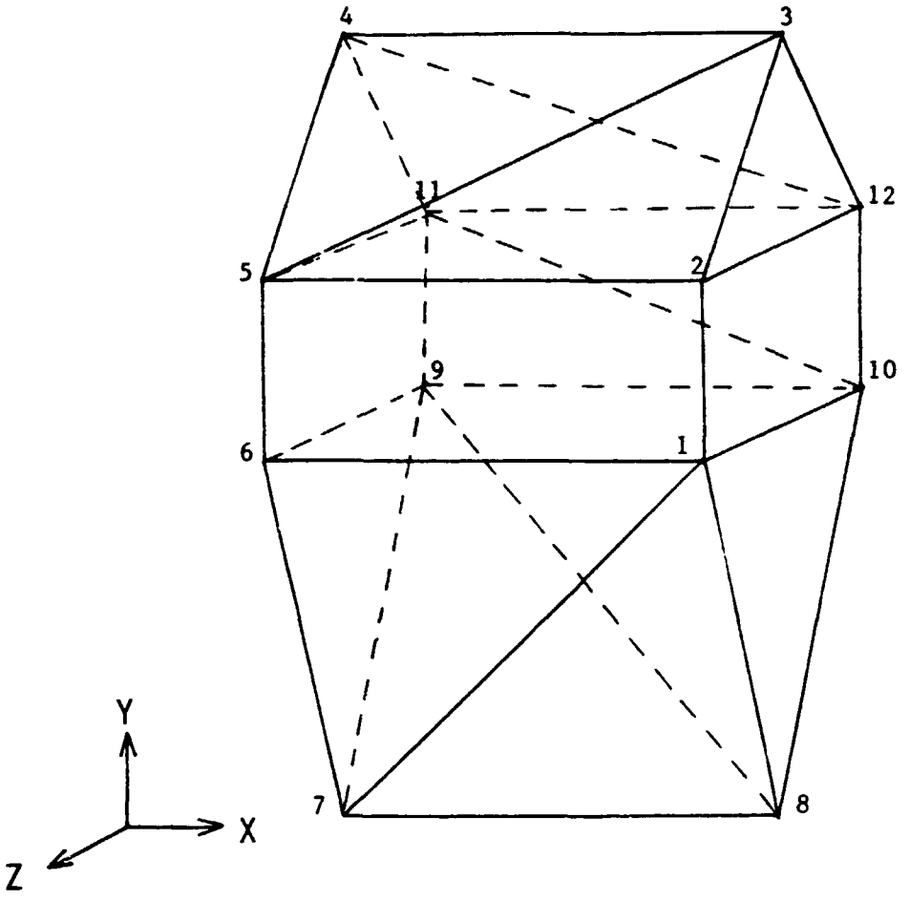

ALL BAR ELEMENTS

$\rho = 0.0025 \quad lb/in^3$

$E = 10.6 \times 10^3 \quad lb/in^2$

$G = 3.84 \times 10^6 \quad lb/in^2$

$A = 0.01 \quad in^2$

$J_0 = 1.67 \times 10^{-5} \quad in^4$

Figure 8 . Payload 2

JOINT DATA USED IN SUBROUTINE FEMKA

JOINT	DEGREES OF FREEDOM TRANSLATION U	V	W	ROTATION P	Q	R	GLOBAL CARTESIAN COORDINATES X	Y	Z
1	1	2	3	0	0	0	2.5000	0.0000	1.0000
	4	5	6	0	0	0	2.5000	2.0000	1.0000
3	7	8	9	0	0	0	2.5000	4.3300	0.0000
4	10	11	12	0	0	0	-2.5000	4.3300	0.0000
5	13	14	15	0	0	0	-2.5000	2.0000	1.0000
6	16	17	18	0	0	0	-2.5000	0.0000	1.0000
7	19	20	21	0	0	0	-2.5000	-4.3300	0.0000
8	22	23	24	0	0	0	2.5000	-4.3300	0.0000
9	25	26	27	0	0	0	-2.5000	0.0000	-1.0000
10	28	29	30	0	0	0	2.5000	0.0000	-1.0000
11	31	32	33	0	0	0	-2.5000	2.0000	-1.0000
12	34	35	36	0	0	0	2.5000	2.0000	-1.0000

Table 7. Geometry and degree of freedom table for payload 2

INPUT DATA FOR BAR ELEMENTS

MASS = M1 STIF = K1 KODEK = KODEB =
RO = .250E-02 E = .106E+05 LOAD TRANS = PAY4LT STRESS TRANS =
G = .384E+07 ALPHA = 0.

ELEMENT NUMBER	JOINT 1	JOINT 2	REF POINT	AREA	POLAR INERTIA	TORSION CONST	Z BENDING INERTIA	Y BENDING INERTIA	SHEAR FACTOR
1	1	2	4	.100E-01	.167E-04	.141E-04	.833E-05	.833E-05	.833
2	2	3	4	.100E-01	.167E-04	.141E-04	.833E-05	.833E-05	.833
3	3	4	2	.100E-01	.167E-04	.141E-04	.833E-05	.833E-05	.833
4	4	5	2	.100E-01	.167E-04	.141E-04	.833E-05	.833E-05	.833
5	5	6	1	.100E-01	.167E-04	.141E-04	.833E-05	.833E-05	.833
6	6	7	1	.100E-01	.167E-04	.141E-04	.833E-05	.833E-05	.833
7	7	8	1	.100E-01	.167E-04	.141E-04	.833E-05	.833E-05	.833
8	8	1	6	.100E-01	.167E-04	.141E-04	.833E-05	.833E-05	.833
9	5	2	3	.100E-01	.167E-04	.141E-04	.833E-05	.833E-05	.833
10	11	12	10	.100E-01	.167E-04	.141E-04	.833E-05	.833E-05	.833
11	5	3	2	.100E-01	.167E-04	.141E-04	.833E-05	.833E-05	.833
12	6	1	2	.100E-01	.167E-04	.141E-04	.833E-05	.833E-05	.833
13	6	2	1	.100E-01	.167E-04	.141E-04	.833E-05	.833E-05	.833
14	9	10	12	.100E-01	.167E-04	.141E-04	.833E-05	.833E-05	.833
15	7	1	8	.100E-01	.167E-04	.141E-04	.833E-05	.833E-05	.833
16	4	12	3	.100E-01	.167E-04	.141E-04	.833E-05	.833E-05	.833
17	11	10	9	.100E-01	.167E-04	.141E-04	.833E-05	.833E-05	.833
18	9	8	10	.100E-01	.167E-04	.141E-04	.833E-05	.833E-05	.833
19	1	10	12	.100E-01	.167E-04	.141E-04	.833E-05	.833E-05	.833
20	2	12	10	.100E-01	.167E-04	.141E-04	.833E-05	.833E-05	.833
21	6	9	11	.100E-01	.167E-04	.141E-04	.833E-05	.833E-05	.833
22	5	11	9	.100E-01	.167E-04	.141E-04	.833E-05	.833E-05	.833
23	8	10	1	.100E-01	.167E-04	.141E-04	.833E-05	.833E-05	.833
24	10	12	1	.100E-01	.167E-04	.141E-04	.833E-05	.833E-05	.833
25	12	3	2	.100E-01	.167E-04	.141E-04	.833E-05	.833E-05	.833
26	7	9	6	.100E-01	.167E-04	.141E-04	.833E-05	.833E-05	.833
27	9	11	6	.100E-01	.167E-04	.141E-04	.833E-05	.833E-05	.833
28	11	4	5	.100E-01	.167E-04	.141E-04	.833E-05	.833E-05	.833

Table 8. Payload 2 material properties

The integration was carried out over 0.9 seconds, i.e. STARTT = 0, ENDT = 0.9 and DELTAT = 0.01.

The results are encouraging. The cost per time step is equal to 0.00018 C.U. (C.U. = cost unit) in subroutine ZRESP whereas the cost per time step for the usual TRSP3 is 0.00017 C.U. It should be recognized, of course, that the usual TRSP3 route requires the solution of a 126 x 126 eigenvalue problem which costs 0.031 C.U. The accuracy of the response is the same for both approaches. The loads program ZLOADS requires on the average $4.\times 10^{-6}$ C.U. in order to track a maximum and minimum load at a particular station. This compares with $9.\times 10^{-6}$ C.U. for the conventional technique. Again, the maxima and minima compare well with the values generated by the conventional technique.

The theory as presented in Chapter III was also applied to the case of the MX missile. Indeed, the method lends itself very well to this case. The missile was basically modeled in two parts, an aft and front end. The number of interface dofs. is 6 being the ideal number for this integration technique. Also, a respectable number of load cases must be evaluated. In particular, several payload configurations have to be investigated. The conventional technique requires a new system eigenvalue problem for every new configuration of the Reentry Vehicles. This undertaking was conceived as a parallel effort to the regular techniques. Again, the results were encouraging. It should be noted that damping was included, resulting in slightly different results for the loads (difference $< 0.2\%$). This can be attributed to the difference in handling the modal damping. The model consisted of a 261 degree of freedom payload model and a 92 degree of freedom booster model. A cut-off frequency of 50 Hz was chosen, resulting in a coupled booster/payload model containing 27 cantilevered booster modes and 55 cantilevered payload modes. The entire analysis was performed on the VAX/VMS-11/780 computer sytem.

Another realistic sample problem is given by the Space Transportation System/Space Telescope/OMS Kit structure. Figure 9 represents the Space Telescope.

The payload for the Space Telescope (S.T.) mission consists of two cargo elements: (1) the Space Telescope and (2) the OMS Kit. These two structures are coupled to the Space Transportation System (S.T.S.). Together, these three structures form the lift off system. The S.T. itself is a modal synthesis of the System Support Module (S.S.M.) and the Orbital Telescope Assembly (O.T.A.) using interface restrained modes. A free S.T. mass and stiffness matrix of size 214 x 214 was formed and 175 cantilevered mode shapes and frequencies calculated. There are 6 interface degrees of freedom with the S.T.S. This means that the interface is determinate.

The OMS Kit is modeled with 36 degrees of freedom and has 7 degrees of freedom in common with the S.T.S.

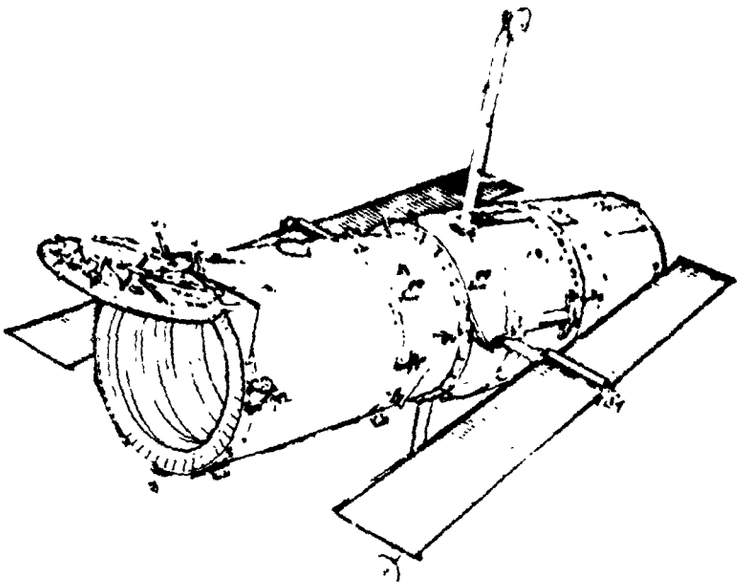

Figure 9 The Space Telescope.

The S.T.S. lift off dynamic model for the hot S.R.B. propellant condition is again provided in terms of interface restrained coordinates. The model has 759 degrees of freedom and 300 interface restrained modes and frequencies were calculated. The S.T.S. interface has 30 degrees of freedom. This means there are 30-7-6 = 20 superfluous interface coordinates on the booster side.

A modal synthesis of the lift off system (S.T.S. + S.T. + OMS Kit) was accomplished through a Craig-Bampton formulation and is used for comparison purposes. Finally, also provided was a lift off forcing function (L07201) which turns out to be a critical case for the Space Telescope.

At this point all necessary data are available to run the six program software package.

The number of booster restrained modes kept in the analys
NB = 300. Similarly for payloads 1 and 2 we have NP1 = 175. 36.
The interface dimensions are IF = 30, IF1 = 6, IF2 = 7, and I 0.
The number of non-zero applied forces on the booster is equal 9.

The possible cost savings occur in programs RESPONS and LOADS. For the current S.T.S.-S.T.-OMS Kit system we considered a start time equal to zero and an end time equal to 10 seconds. The integration step is equal to 0.005 seconds. Furthermore, the velocities and the elastic accelerations at time zero are chosen to be zero.

A CDC/CYBER 75C was used to execute all programs. In this particular case, program RESPONS required on the average 0.0015 C.U. (=realistic cost unit) per time step h. It should be noted that a phase shift was observed in the response compared to the conventional approach where system modes ("model modes") are used. This is typical for a Newmark-Chan-Beta numerical scheme. This phenomenon is no cause for concern if the only goal is to arrive at maximum and minimum member loads. Although it is hard to correctly compare different techniques, the authors feel that the cost to obtain the response compares favorably even with the conventional system modes approach where a set of decoupled system equations are solved. The average cost per time step here becomes 0.0017 C.U.'s. Note that when system modes are used, one has to perform an additional $[\phi]^T$ type multiplication on the right hand-side of the decoupled equations. In this case this results in a more expensive force term calculation than is the case in the present scheme.

The maximum and minimum member loads obtained from program LOADS are all within 1% of the corresponding loads obtained from the conventional approach. The gain in program LOADS is primarily due to the fact that no system modes and frequencies are involved in the computations. In addition, the term $[LT2]_j \{x_{Ij}\}$ can be evaluated directly without having to write $\{x_{Ij}\}$ in terms of accelerations and applied forces as should be done when system modes are used. The average cost in order to track the maximum and minimum load at a particular station is 0.00012 C.U. which compares with 0.00026 C.U.'s for the conventional technique.

Finally, we wish to discuss some of the results obtained for the short-cut versions as discussed in Chapter IV. We tried out two schemes based on Equation (256) in Chapter IV. The actual control statement used can be written as follows:

$$\| \ddot{q}^{B}_{IRi} \|^2 / \| \ddot{q}^{B}_{IOi} \|^2 \leq \varepsilon^2$$

where ε is a small quantity chosen by the user. The left-hand side of the inequality represents a normalized magnitude squared of the interface acceleration feedback. The first scheme checks this quantity against the chosen ε^2. If the inequality is fulfilled, then the calculations of the A_2 and A_3 terms in Equation (253) are by-passed. The second scheme follows the philosophy of a direct base drive approach. This means that if the inequality is fulfilled at time t, we assume that the feedback is small at that time, and a direct base drive solution is generated for that time. If the inequality is not fulfilled, a coupled solution is obtained for that time step. That means that this short-cut version vasilates between a full-scale and a direct base drive method.

The first scheme turned out to be expensive. The reason for this is that a coupled base motion technqiue requires a rather significant amount of bookkeeping .

The second scheme proved successful in the case where the feedback is indeed small. Again, because of the added bookkeeping, it is necessary that the ε-inequality is indeed fulfilled part of the time, because otherwise the method becomes more expensive. It is also realized that more research and checking is necessary before a final judgement can be given. Compared to the ZRESP routine, the second short-cut version vasilates anywhere between 40% slower (coupling at all times) and 30% faster (no coupling at all).

It should be noted that ZRESP (fully coupled) is already within the realm of reasonable cost and additional cost reduction, although possible, may complicate matters too much.

CHAPTER V: CONCLUSIONS AND SUGGESTIONS

1. Introduction

In Chapter I-A we reviewed and assessed a set of "full-scale" methodologies. This allowed us to introduce the necessary background material in terms of a unified nomenclature. All these methods have their merits. However, the Residual Mass and Stiffness Method appears to yield the most accurate results. It is the approach which best describes the booster structure in terms of a minimum number of modes, given a certain cut-off frequency for the externally applied force $\{F_B\}$. The fact that no payload information is required to obtain the booster model is a very convenient feature in connection with the present study. Therefore, the same booster model can be used as long as the booster does not change.

In Chapter I-B several short-cut methods have been discussed and evaluated. Although each of these methods has its own merits, it is believed that none of them is acceptable in their present stage of development to function as a standard short-cut method for general use. In fact, it would be very hard to develop an "ultimate" short-cut method. The main reason for this may be the multitude of different situations such a method would have to accommodate .

In Chapter II we attempted the development of a full-scale numerical integration scheme to obtain the response of a booster/payload(s) system. It is felt that under the right circumstances this method can be of certain value.

A short cut version of the above numerical scheme was developed in Chapter III. The method is designed to vasilate between a full-up coupled base motion approach and a direct base drive method. It is hoped that this technique will have the characteristics of both methods, i.e., the accuracy of the coupled base motion technique and the speed of a direct base drive.

In Chapter IV we discuss the implementation and programming of the above methods. A software package was developed and checked out on several sample problems.

In the remainder of this last chapter we shall discuss a few other suggestions for possible short-cut approaches.

2. Base Motion Techniques

The Coupled Base Motion Technique as explained in Chapter I-A, leads to a fundamental set of equations, which we repeat here for clarity of presentation,

$$\left[I_B^T M_B I_B\right] \left|\ddot{x}_N^{BR}\right| + \left[I_B^T K_B I_B\right] \left|\bar{x}_N^{BR}\right| = - \left[I_B^T M_B T_B\right] \left|\ddot{x}_I^{BR}\right| \quad (257)$$

$$\left[I_P^T M_P I_P\right] \left|\ddot{x}_N^{P}\right| + \left[I_P^T K_P I_P\right] \left|x_N^{P}\right| = - \left[I_P^T M_P T_P\right] \left(\left|\ddot{x}_I^{BF}\right| + \left|\ddot{x}_I^{BR}\right|\right) \quad (258)$$

$$\left|\ddot{x}_I^{BR}\right| = \left[T_B^T M_B T_B + T_P^T M_P T_P\right]^{-1} \left(- \left[T_P^T M_P T_P\right] \left|\ddot{x}_I^{BF}\right| - \left[T_P^T K_P T_P\right] \left|x_I^{BF}\right| \right.$$

$$\left. - \left[T_P^T M_P I_P\right] \left|\ddot{x}_N^{P}\right| - \left[T_B^T M_B I_B\right] \left|\ddot{x}_N^{BR}\right| - \left[T_B^T K_B T_B + T_P K_P T_P\right] \left|x_I^{BR}\right| \right) \quad (259)$$

As mentioned in Chapter I-A, the payload designer is primarily interested in the response of the payload i.e.,

$$\left\{\begin{array}{c} x_N^P \\ \hline x_I^P \end{array}\right\} = \left[\begin{array}{c|c} I & S_P \\ \hline 0 & I \end{array}\right] \left\{\begin{array}{c} \bar{x}_N^P \\ \hline x_I^P \end{array}\right\} \quad (260)$$

with

$$\left\{\begin{array}{c} \bar{x}_N^P \\ \hline x_I^P \end{array}\right\} = \left\{\begin{array}{c} \bar{x}_N^P \\ \hline x_I^{BF} + x_I^{BR} \end{array}\right\} \quad (261)$$

where $\{\ddot{X}_N^P\}$ and $\{X_I^{BR}\}$ must be computed from Equations (257-259) and from Equation (90). The base drive method focuses on Equation (258) which yields $\{\ddot{X}_N^P\}$ provided $\{\ddot{X}_I^{BR}\}$ on the right hand side of Equation (258) is known. The idea is to produce an expression for $\{\ddot{X}_I^{BR}\}$ without actually solving the coupled set of Equations (257-259).

First, consider the coefficients of $\{\ddot{X}_N^P\}$ and $\{\ddot{X}_I^{BF}\}$ in Equation (259). These coefficients represent the ratio of the payload mass and the total vehicle mass. In many STS applications this ratio will be rather small ($< 10\%$). Therefore, a first possibility is to ignore these terms in Equation (259). Secondly, in many applications we can assume a statically determinate interface, i.e. $[T_B^T K_B T_B] = [T_P^T K_P T_P] = [0]$, so that Equation (259) becomes

$$\left|\ddot{x}_I^{BR}\right| = - \left[T_B^T M_B T_B + T_P^T M_P T_P\right]^{-1} \left[T_B^T M_B I_B\right] \left|\ddot{x}_N^{BR}\right| \quad (262)$$

Ordinarily, the coefficient matrix of $\{\ddot{X}_N^{BR}\}$ in Equation (262) is not small and cannot be ignored. A first possibility is to assume that $\{\ddot{X}_N^{BR}\}$ is small and can be ignored. This means that the feedback of the payload is not important. This can be a realistic assumption because the payload is usually small compared to the booster. In this case we can completely ignore $\{\ddot{X}_I^{BR}\}$ in Equation (258) and write

$$\left[I_P^T M_P I_P\right]\left\{\ddot{x}_N^P\right\} + \left[I_P^T K_P I_P\right]\left\{x_N^P\right\} = -\left[I_P^T M_P T_P\right]\left\{\ddot{x}_I^{BF}\right\} \tag{263}$$

Equation (263) is now effectively decoupled from Equations (257) and (259). Physically, ignoring the feedback of the payload means that payload and booster are not modally coupled. Equation (263) is the direct base drive equation.

A second possibility is to scale the vector $\{\ddot{X}_N^{BR}\}$ in Equation (262). Indeed, let us assume a full-scale solution is available for some payload P_1. Now, some relatively small changes are made in the payload P_1 to generate payload P. The assumption now, is that $\{\ddot{X}_N^{BR}\}$ is not much different from $\{\ddot{X}_N^{BR}\}_1$ i.e.,

$$\left\{\ddot{x}_N^{BR}\right\} \simeq \left\{\ddot{x}_N^{BR}\right\}_1 \tag{264}$$

Equation (262) for payload P_1 can be written as

$$\left\{\ddot{x}_I^{BR}\right\}_1 = -\left[T_B^T M_B T_B + T_{P1}^T M_{P1} T_{P1}\right]^{-1}\left[T_B^T M_B I_B\right]\left\{\ddot{x}_N^{BR}\right\}_1 \tag{265}$$

or

$$\left[T_B^T M_B I_B\right]\left\{\ddot{x}_N^{BR}\right\}_1 = -\left[T_B^T M_B T_B + T_{P1}^T M_{P1} T_{P1}\right]\left\{\ddot{x}_I^{BR}\right\}_1 \tag{266}$$

Taking into account Equation (264) it follows from Equations (266) and (262) that

$$\left\{\ddot{x}_I^{BR}\right\} = \left[T_B^T M_B T_B + T_P^T M_P T_P\right]^{-1}\left[T_B^T M_B T_B + T_{P1}^T M_{P1} T_{P1}\right]\left\{\ddot{x}_I^{BR}\right\}_1 \tag{267}$$

which yields a scaled value for $\{\ddot{X}_I^{BR}\}$ to be used in Equation (258). Again, one should investigate when such an approach is valid.

3. Another Possible Approach

In the course of our investigation and evaluation of several short-cut methods it was noted that many methods involve assumptions and approximations leading to either doubtful or cumbersome results. In addition, it is often very difficult to assess the effects of those assumptions on the response and the loads of the booster/payload system.

The basic problem is to somehow deal with the coupling effects between booster B and payload P without solving an eigenvalue problem pertaining to the coupled booster/payload system. This is a difficult problem indeed. Each of the short-cut methods discussed in Chapter I-B addresses this problem in a different way. However, the proposed solutions invariably lead to cumbersome mathematics and program coding. This observation led us to the development of a more direct approach which we think shows great promise. This new approach is easy to understand and easy to implement. It is based on the work of C. W. White and B. D. Maytum [74].

Let us recall Equation (25) :

$$\left[\begin{array}{c|c} M_B+T_P^T M_P T_P & T_P^T M_P I_P \\ \hline I_P^T M_P T_P & I_P^T M_P I_P \end{array}\right]\left\{\begin{array}{c} \ddot{x}_B \\ \hline \ddot{\bar{x}}_N^P \end{array}\right\} + \left[\begin{array}{c|c} K_B+T_P^T K_P T_P & 0 \\ \hline 0 & I_P^T K_P I_P \end{array}\right]\left\{\begin{array}{c} x_B \\ \hline \bar{x}_N^P \end{array}\right\} = \left\{\begin{array}{c} F_N^B \\ \hline 0 \end{array}\right\} \qquad (268)$$

which represents the set of equations of motion of the coupled booster/payload system. It is now assumed that a cut-off frequency is defined based on a Fourier series expansion of $\{F_N^B\}$. Furthermore, we also assume that e.g. the Residual Mass and Stiffness Method was used to construct the following set of modally coupled equations.

$$\left[\begin{array}{c|c} I+\phi_B^T T_P^T M_P T_P \phi_B & \phi_B^T T_P^T M_P I_P \bar{\phi}_N^P \\ \hline \bar{\phi}_N^{P\,T} I_P^T M_P T_P \phi_B & I \end{array}\right]\left\{\begin{array}{c} \ddot{q}_B \\ \hline \ddot{\bar{q}}_N^P \end{array}\right\} + \left[\begin{array}{c|c} [\omega_B^2] + \phi_B^T T_P^T K_P T_P \phi_B & \\ \hline 0 & [\omega_P^2] \end{array}\right]\left\{\begin{array}{c} q_B \\ \hline \bar{q}_N^P \end{array}\right\}$$

where

$$= \left\{\begin{array}{c} \phi_B^T \left\{\begin{array}{c} F_N^B \\ 0 \end{array}\right\} \\ \hline 0 \end{array}\right\} \qquad (269)$$

$$\left\{x_B\right\} = \left[\phi_B\right]\left\{q_B\right\}, \quad \left\{\bar{x}_N^P\right\} = \left[\bar{\phi}_N^P\right]\left\{\bar{q}_N^P\right\} \qquad (270)$$

and the cut-off frequency was used to determine the size of $[\phi_B]$ and $[\phi_N^P]$. In other words, the size of Equation (269) is already much less than the size of Equation (268). Due to e.g. the Residual Mass and Stiffness Method, the reduced Equation (269) still represents an acceptable model for the coupled booster/payload system.

The first step of the present approach is to solve the eigenvalue problem associated with Equation (269), namely

$$\left(-\Omega^2 \left[\begin{array}{c|c} I+\phi_B^T T_P^T M_P T_P \phi_B & \phi_B^T T_P^T M_P I_P \phi_N^P \\ \hline \overline{\phi}_N^{P\,T} I_P^T M_P T_P \phi_B & I \end{array}\right] + \left[\begin{array}{c|c} [\omega_B^2] + \phi_B^T T_P^T K_P T_P \phi_B & \\ \hline 0 & [\overline{\omega}_B^{-2}] \end{array}\right]\right) [\Psi] = \{0\} \tag{271}$$

yielding a set of modes $[\Psi]$ and a set of frequencies $[\Omega^2]$ satisfying

$$\left\{\begin{array}{c} q_B \\ \hline \overline{q}_N^P \end{array}\right\} = [\Psi]\{u\} \tag{272}$$

and

$$[\Psi]^T \left[\begin{array}{c|c} I+\phi_B^T T_P^T M_P T_P \phi_B & \phi_B^T T_P^T M_P I_P \phi_N^P \\ \hline \overline{\phi}_N^{P\,T} I_P^T M_P T_P \phi_B & I \end{array}\right] [\Psi] = [I] \tag{273}$$

$$[\Psi]^T \left[\begin{array}{c|c} [\omega_B^2] + \phi_B^T T_P^T K_P T_P \phi_B & \\ \hline 0 & [\overline{\omega}_P^{-2}] \end{array}\right] [\Psi] = [\Omega^2] \tag{274}$$

where $\{u\}$ are the new normal coordinates. Substituting transformation (272) into Equation (269) and premultiplying by $[\Psi]^T$ and using Equations (273-274) we obtain the uncoupled set of equations,

$$\{\ddot{u}\} + [\Omega^2]\{u\} = [\Psi]^T \left\{\begin{array}{c} \phi_B^T \left\{\begin{array}{c} F_N^B \\ 0 \end{array}\right\} \\ \hline 0 \end{array}\right\} \tag{275}$$

The modal matrix $[\Psi]$ and the frequency matrix $[\Omega^2]$ represent the modal information of the coupled booster/payload system. The idea now is to change the payload and calculate the changes in $[\Psi]$ and $[\Omega^2]$. In other words, we use the full-scale solution of Equation (269) as a "start-solution". This approach is taken in most short-cut methods and as such does not detract from the present approach. For example, this full-scale solution could be determined at the beginning of a design effort and would stay the same for all subsequent design cycles of a particular payload.

Let us now consider the new payload P_1, with mass matrix $[K_{P1}]$ and stiffness matrix $[M_{P1}]$. This payload P_1 could be totally new or just a modification of the nominal payload P, as long as we have the same degrees of freedom for both payloads P and P_1. For this new payload P_1, we replace Equation (268).

$$\left[\begin{array}{c|c} M_B+T_{P1}^T M_{P1} T_{P1} & T_{P1}^T M_{P1} I_{P1} \\ \hline I_{P1}^T M_{P1} T_{P1} & I_{P1}^T M_{P1} I_{P1} \end{array}\right] \left\{\begin{array}{c} \ddot{x}_{B1} \\ \hline \ddot{x}_N^{P1} \end{array}\right\} + \left[\begin{array}{c|c} K_B+T_{P1}^T K_{P1} T_{P1} & 0 \\ \hline 0 & I_{P1}^T K_{p1} I_{P1} \end{array}\right] \left\{\begin{array}{c} x_{B1} \\ \hline x_N^{P1} \end{array}\right\} = \left\{\begin{array}{c} F_N^{B1} \\ 0 \\ \hline 0 \end{array}\right\} \tag{276}$$

where

$$\left[S_{P1}\right] = -\left[K_{NN}^{P1}\right]^{-1} \left[K_{NI}^{P1}\right] \tag{277}$$

is the new transformation matrix and

$$\left\{\begin{array}{c} x_{B1} \\ \hline x_N^{P1} \end{array}\right\} \tag{278}$$

is the new system displacement vector.

Let us now write Equation (276) as follows:

$$\left[\begin{array}{c|c} M_B+T_P^T M_P T_P+m_{BB} & T_P^T M_P I_P+m_{BP} \\ \hline I_P^T M_P T_P+m_{BP}^T & I_P^T M_P I_P+m_{PP} \end{array}\right] \left\{\begin{array}{c} \ddot{x}_{B1} \\ \hline \ddot{x}_N^{P1} \end{array}\right\} + \left[\begin{array}{c|c} K_B+T_P^T K_P T_P+k_{BB} & 0 \\ \hline 0 & I_P^T K_P I_P+k_{PP} \end{array}\right] \left\{\begin{array}{c} x_{B1} \\ \hline x_N^{P1} \end{array}\right\} \tag{279}$$

where

$$= \left\{\begin{array}{c} F_N^{B1} \\ 0 \\ \hline 0 \end{array}\right\} \tag{280}$$

$$\left[m_{BB}\right] = \left[T_{P1}^T M_{P1} T_{P1}\right] - \left[T_P^T M_P T_P\right] \tag{281}$$

$$\left[m_{BP}\right] = \left[T_{P1}^T M_{P1} I_{P1}\right] - \left[T_P^T M_P I_P\right] = \left[(T_{P1}^T M_{P1} - T_P^T M_P)\, I_P\right]$$

$$\left[m_{PP}\right] = \left[I_{P1}^T M_{P1} I_{P1}\right] - \left[I_P^T M_P I_P\right] = \left[I_P^T (M_{P1} - M_P) I_P\right] \tag{282}$$

$$\left[k_{BB}\right] = \left[T_{P1}^T K_{P1} T_{P1}\right] - \left[T_P^T K_P T_P\right] \tag{283}$$

$$\left[k_{PP}\right] = \left[I_{P1}^T K_{P1} I_{P1}\right] - \left[I_P^T K_P I_P\right] = \left[I_P (K_{P1} - K_P) I_P\right] \tag{284}$$

Note that in case the interface is statically determinate $[k_{BB}] = [0]$ and if in addition the geometry of the payload is not changed then $[T_{P1}] = [T_P]$ and

$$\left[m_{BB}\right] = \left[T_P^T (M_{P1} - M_P) T_P\right] \tag{285}$$

$$\left[m_{BP}\right] = \left[T_P^T (M_{P1} - M_P) I_P\right] \tag{286}$$

$$\left[m_{PP}\right] = \left[I_P^T (M_{P1} - M_P) I_P\right] \tag{287}$$

$$\left[k_{BB}\right] = \left[0\right] \tag{288}$$

$$\left[k_{PP}\right] = \left[I_P (K_{P1} - K_P) I_P\right] \tag{289}$$

Also, note that if no changes are made in the mass the right hand sides of Equations (282) and (285-288) become [0] and similarly, if no stiffness changes are made we have from Equation (277) that $[T_P] = [T_{P1}]$ and consequently Equations (285-288) are valid while Equation (289) becomes $[k_{PP}] = [0]$ although the interface can still be statically indeterminate.

Next, let us define the following transformation

$$\left\{\begin{array}{c} x_{B1} \\ \hline x_N^{P1} \end{array}\right\} = \left[\begin{array}{c|c} \phi_B & 0 \\ \hline 0 & \phi_N^P \end{array}\right] \left\{\begin{array}{c} q_{B1} \\ \hline q_N^{P1} \end{array}\right\} = \left[A\right] \left\{\begin{array}{c} q_{B1} \\ \hline q_N^{P1} \end{array}\right\} \tag{290}$$

After substituting Equation (290) into Equation (279) and premultiplying by $[A]^T$ we obtain the set of equations that now replaces the set Equation (269)

$$\left[\begin{array}{c|c} I+\phi_B^T T_P^T M_P T_P \phi_B + \phi_B^T m_{BB} \phi_B & \phi_B^T T_P^T M_P I_P \bar{\phi}_N + \phi_B^T m_{BP} \bar{\phi}_N \\ \hline \phi_N^T I_P M_P T_P \phi_B + \bar{\phi}_N^T m_{BP}^T \phi_B & I + \bar{\phi}_N^T m_{PP} \bar{\phi}_N \end{array}\right] \left\{\begin{array}{c} \ddot{q}_{B1} \\ \hline \ddot{\bar{q}}_{P1} \\ \ddot{q}_N \end{array}\right\}$$

$$+ \left[\begin{array}{c|c} \left[\omega_B^2\right] + \phi_B^T T_P^T K_P T_P \phi_B + \phi_B^T k_{BB} \phi_B & 0 \\ \hline 0 & \left[\omega_P^2\right] + \bar{\phi}_N^T k_{PP} \bar{\phi}_N \end{array}\right] \left\{\begin{array}{c} q_{B1} \\ \hline \bar{q}_{P1} \\ q_N \end{array}\right\} = \left\{\begin{array}{c} \phi_B^T \left\{\begin{array}{c} F_N^{B1} \\ 0 \end{array}\right\} \\ \hline 0 \end{array}\right\} \tag{291}$$

The next step is to define the transformation

$$\left\{\begin{array}{c} q_{B1} \\ \hline \bar{q}_{P1} \\ q_N \end{array}\right\} = \left[\Psi\right] \left\{u_1\right\} \tag{292}$$

The transformation (292) is now substituted into Equation (291) after which we premultiply by $[\Psi]^T$ and invoke properties (273-274), yielding

$$\left(\left[I\right] + \left[\Psi\right]^T \left[\begin{array}{c|c} \phi_B^T m_{BB} \phi_B & \phi_B^T m_{BP} \bar{\phi}_N \\ \hline \bar{\phi}_N^T m_{BP}^T \phi_B & \bar{\phi}_N^T m_{PP} \bar{\phi}_N \end{array}\right] \left[\Psi\right]\right) \left\{\ddot{u}_1\right\}$$

$$+ \left(\left[\Omega^2\right] + \left[\Psi\right]^T \left[\begin{array}{c|c} \phi_B^T k_{BB} \phi_B & 0 \\ \hline 0 & \bar{\phi}_N^T k_{PP} \bar{\phi}_N \end{array}\right] \left[\Psi\right]\right) \left\{u_1\right\} = \left[\Psi\right]^T \left\{\begin{array}{c} \phi_B^T \left\{\begin{array}{c} F_N^{B1} \\ 0 \end{array}\right\} \\ \hline 0 \end{array}\right\} \tag{293}$$

This Equation (293) replaces Equation (275). For convenience, let us denote

$$\left[m\right] = \left[\Psi\right]^T \left[\begin{array}{c|c} \phi_B^T m_{BB} \phi_B & \phi_B^T m_{BP} \bar{\phi}_N \\ \hline \bar{\phi}_N^T m_{BP}^T \phi_B & \bar{\phi}_N^T m_{PP} \bar{\phi}_N \end{array}\right] \left[\Psi\right] \tag{294}$$

$$\left[k\right] = \left[\Psi\right]^T \left[\begin{array}{c|c} \phi_B^T k_{BB} \phi_B & 0 \\ \hline 0 & \bar{\phi}_N^T k_{PP} \bar{\phi}_N \end{array}\right] \left[\Psi\right] \tag{295}$$

Matrices [M] and [k] represent the perturbations in the mass and stiffness matrices $[I]$ and $[\Omega^2]$ of system (275). At this point, several observations can be made. First it should be noted that it is very possible that certain changes in the payload will only affect a limited number of modes and frequencies. This means that several columns in $[\Psi]$ and corresponding elements in $[\Omega^2]$ will not change after the changes in the payload are made. This reduces the size of Equation (293). Secondly, in solving the eigenvalue problem associated with Equation (293) it is possible to use a Rayleigh-Ritz approach with $[I]$ as the estimated start modes. The smaller the changes in the payload the better estimate $[I]$ will be and the less iterations will be necessary to produce the new modes and frequencies of the perturbed booster B/Payload P1 system. An even better starting set of modes could be the solution to the perturbed eigenvalue problem with all off-diagonal terms equal to zero (this is equivalent to the first term in a Taylor series expansion of the perturbed system modes and frequency). Thirdly, we wish to investigate the possibility of truncating modes in $[\Psi]$ according to the initially defined cut-off frequency. If this was possible Equation (293) could be reduced in size by approximately 50% compared to the already reduced system Equation (269). This reduction would be in addition to the one due to unaffected modes as mentioned above. However, this question must still be carefully investigated. Finally, it is also possible that the modes are grouped in subsets which show very little or no coupling between each other. This means that the eigenvalue problem associated with Equation (293) can be replaced by two or more smaller eigenvalue problems, which of course reduces the computation time.

There are additional advantages to this method: simplicity of use; accuracy of results (e.g., this method could even be used as a full-scale method); possibility of using engineering judgement and experience; the possibility to identify changes required to meet certain frequency requirements; the possibility to change branch frequencies to decouple the load problem leading to smaller eigenvalue problems, the potential for significant computational time savings.

REFERENCES

INTRODUCTION

1. "Structural Dynamics Payload Loads Estimates", Technical Proposal, MMC, P79-48144-1, Feb. 1979.

2. "Design of Space Payloads for Transient Environments", B. K. Wada, Manager, Survival of Mechanical Systems in Transient Environments, AMD-Vol. 36, ASME.

CHAPTER I

A. FULL SCALE TECHNIQUES

3. "Dynamic Analysis of Structural Systems Using Component Modes," Hurty, W.C. AIAA Journal, 3(4). April 1965, pp. 678-85 (Based upon PL Tech. Memo 32-530, Jan 1964)

4. "Dynamic Analysis of Large Structures by Modal Synthesis Techniques," Hurty, W.C., J.D. Collins, and G.C. Hart, Computers & Structures, 1. 1971, pp. 535-63.

5. "Analytical Methods in Vibrations", L. Meiroritch, The MacMillan Company, New York, 1967.

6. "Coupling of Substructures for Dynamic Analysis," Craig, R. R. and Bampton M.C.C. AIAA Journal, Vol. 6k No. 7, July 1968, pp. 1313-1319.

7. "Vibration Analysis by Dynamic Partitioning," Goldman, R. L. AIAA Journal, Vol. 7, No. 6, June 1969, pp. 1152-1154.

8. "An Improved Component - Mode Representation", S. Rubin, AIAA/ASME/SAE 15th Structures Conference, Las Vegas, Nevada (April 17-19, 1974 AIAA Paper No. 74. 386), also "Improved Component Mode Representation for Structural Dynamic Analysis", AIAA Journal Vol. 13(8), 1975, pp 996-1006.

9. Personal Conversation, C.W. White, MMC, Denver, CO April 1980.

10. Personal Conversation, R.F. Hruda and W.A Benfield, MMC, Denver, CO., April 1980.

11-50. "Government/Industry Workshop on Payload Loads Technology", NASA-George C. Marshall Space FLight Center, NASA CP-2075.

51. "A Hybrid Method of Component Mode Synthesis," MacNeal, R. H. Computers & Structures, 1, 1971, pp. 581-601.

52. "Vibration Analysis of Structures by Component Mode Substitution", Benfield, W. A. and R. F Hruda, Presented at AIAA/ASME 11th Struc., Struc. Dyn. and Matl, Conf., Denver, Colorado, April (22 -24) 1970.

53. "Load Transformation Development Consistent with Modal Synthesis Techniques", R. F. Hruda and P. J. Jones, Shock and Vibration Bulletin, No. 48, Sept. 1978.

54. "Skylab Payload Base Motion Analysis Report," H. Harcrow, T. Jester, B. Payton and D. Leston, MMC, 21 October 1971, ED-2002-1388.

55. "Response Equations for Base Motion Excitation," W. Holland, March 1, 1971, MSFC.

56. "Methodology for Base Motion Response Analysis Using Incompatible Base Motion Excitation," W. Holland, February 1975, MSFC.

57. "Coupled Base Motion Response Analysis of Payload Structural Systems," A. D. Devers, H. Harcrow, A. R. Kukreti, UCCE 75-2, April 1976, MSFC.

58. B. A. Hunn: "A Method of Calculating Normal Modes of an Aircraft." *Quart J Mech*, Vol 8, Part 1, 1955.

59. G. M. L. Gladwell: "Branch Mode Analysis of Vibrating Systems." *J Sound Vib*, Vol 1, 1964.

60. W. C. Hurty: "Vibrations of Structural Systems by Component Mode Synthesis." *Proc Amer Soc Civ Engrs*, Vol 85, No. EM4, August 1960.

61. W. C. Hurty: *Dynamic Analysis of Structural Systems by Component Mode Synthesis*. Technical Report 32-530. Jet Propulsion Laboratory, Pasadena, California, January 1964.

62. W. C. Hurty: "Dynamic Analysis of Structural Systems Using Component Modes." *AIAA J*, Vol 3, No. 4, April 1965.

63. R. L. Bajan and C. C. Feng: "Free Vibration Analysis by the Modal Substitution Method." AAS Paper 68-8-1, July 1968.

64. R. L. Bajan, C. C. Feng, and I. J. Jaszlics: "Vibration Analysis of Complex Structural Systems by Modal Substitution." *Proc 39th Shock and Vibration Symposium*, Monterey, California, October 1968.

65. R. R. Craig and M. C. C. Bampton: "Coupling of Substructures for Dynamic Analysis." *AIAA J*, Vol 6, No. 7, July 1968.

66. R. L. Goldman: "Vibration Analysis by Dynamic Partitioning." *AIAA J*, Vol 7, No. 6, June 1969.

67. S. N. Hou: "Review of Modal Synthesis Techniques and a New Approach." *The Shock and Vibration Bulletin*, No. 40, Naval Research Laboratory, Washington, D. C., December 1969.

68. W. A. Benfield and R. F. Hruda: "Vibration Analysis of Structures by Component Mode Substitution." *AIAA J*, Vol 9, No. 7, July 1971.

69. G. C. Hart, W. C. Hurty, and J. D. Collins: "A Survey of Modal Synthesis Methods." *Proc National Aeronautic and Space Engineering and Manufacturing Meeting*, Los Angeles, California, September 28-30, 1971.

70. W. C. Hurty: "Introduction To Modal Synthesis Techniques." *Synthesis of Vibrating Systems Proceedings*, American Society of Mechanical Engineers, Washington, D. C., November 30 1971.

71. R.R. Craig, Jr. and C.J. Chang : " A Review of Substructure Coupling Methods For Dynamic Analysis " Advances in Engineering Science, NASA CP-2001, November 1976.

72. R.R. Craig,Jr : " Methods of Component Mode Synthesis " The Shock and Vibration Digest, Volume 9, No. 11 November 1977.

73. R.R. Craig,Jr. and C.J. Chang : " On the Use of Attachment Modes in Substructure Coupling for Dynamic Analysis " AIAA/ASME 19th Structures, Structural Dynamics and Materials Conference, San Diego, CA, March 1977.

74. W.A. Benfield, C.S. Bodley and G. Morosow : " Modal Synthesis Methods " Presented at the Space Shuttle Dynamics and Aeroelasticity Working Group, Symposium on Substructuring, August 30-31, 1972, MSFC, Alabama .

75. W.A. Benfield : " A Modified Method of Stiffness Modal Coupling " February, 1969 , D.M. 133, MMC, Denver, Colorado.

B. SHORT CUT TECHNIQUES.

76. "Evaluation of a Cost-Effective Loads Approach," J. A. Garba, B. K. Wada, R. Bamford, M. R. Trubert. Journal of Spacecraft and Rockets, Vol. 13 No. 11, November 1976 pp 675-683.

77. "Development and Correlation: Viking Orbiter Analytical Dynamic Model with Modal Test", B. K. Wada, et al. The Shock and Vibration Bulletin, No. 44, August 1974.

78. "Modal Test Results of the Viking Orbiter" E. L. Leppert, B. K. Wada, R. Miyakawa, The Shock and Vibration Builetin, No. 44, August 1974.

79. "Matrix Perturbation Techniques in Structural Dynamics," Chen, J. C. and Wada, B. K., AIAA Journal, Vol. 15, Aug. 1977, pp. 1095-1100.

80. "Inversion of First-Order Perturbation Theory and Its Application to Structural Design," AIAA Journal, Vol. 14, April 1976, pp. 454-460.

81. "Matrix Perturbation Techniques in Structural Dynamics," Caughey, T. X., Tech. Memo. 33-652, Jet Propulsion Laboratory, Pasadena, Calif., Sept. 1, 1973.

82. "Influence of Structural Dynamics on Space Shuttle Design," Wade, D. C., AIAA Paper 77-436, AIAA/ASME/18th Structures, Structural-Dynamics and Materials Conference, San Diego, Calif., March 21-23, 1977.

83. "On the Launch Vehicle Payload Interface Responses," Chen, J. C., Wada, B. K. and Garba, J. A., Journal of Spacecraft and Rockets, Vol. 15, Jan. 1978, pp.7-11.

84. "Dynamic Analysis of Large Structural Systems," Bamford, R., Wada, B. K., Garba, J. A., and Chisholm, J., Synthesis of Vibrating Systems, The American Society of Mechanical Engineers, New York, N.Y., Nov. 1971.

85. "Equivalent Spring-Mass System: A Physical Interpretation," Wada, B. K., Bamford, R., Garba, J. A., The Shock and Vibration Bulletin, No. 45, Pt. 3, Naval Research Lab., Washington, D. C., June 1975, pp.37-57

86. "Analytical Prediction and Correlation for t[illegible] during the Viking Spacecraft Sinusoidal Vibration Test," Brownlee, G. R. Bay, F D., and Garba, J. A., The Shock and Vibration Bulletin, No. 45, Pt. 3, Naval Research Lab., Washington, D.C., June 1975, pp. 37-57.

87. "Criteria for Analysis-Test Correlation of Structural Dynamic Systems", J. C. Chen, B. K. Wada, Journal of Applied Mechanics, June 1975.

88. "Estimation of Payload Loads Using Rigid-Body Interface Accelerations", J. C. Chen, J. A. Carba, B. K. Wada, Journal of Spacecraft & Rockets, Vol. 16, No. 2, March-April 1979, pp. 74-80.

89. "An Impedance Technique for Determining Low Frequency Payload Environments," K. R. Payne, Shock and Vibration Bulletin. No. 49, Sept. 1979.

90. "A Snock Spectra and Impedance Method to Determine a Bound for the Spacecraft Structural Loads," Bamford, R. and Trubert, M., AIAA Paper 75-811 Denver, Colorado 1975. Also, Tech & Memo, 33-694, JPL, Pasadena, Calif. Sept. 1974.

91. "A Generalized Modal Shock Spectra Method for Spacecraft Loads Analysis,: Publication 79-2, JPL, Pasadena, Calif., March 15, 1979.

CHAPTERS II, III AND IV

92. Chan S. O., Cox, H. L. and Benfield, W. A., "Transient Analysis of Forced Vibrations of Complex Structural-Mechanical Systems," Journal of the Royal Aeronautical Society, Vol. 66, July 1962, pp. 457-460.

93. Hruda, R. F. and Jones, P. J., "Load Transformation Development Consistent with Modal Synthesis," Shock and Vibration Bulletin, No. 48, September 1978.

94. Devers, D., Harcrow, H. and Kudreti, A., "Coupled Base Motion Response Analysis of Payload Structural Systems; UCCE 75-2, April 1976, MFSC.

95. Engels, R. C., and Harcrow. H. W., "A New Payload Integration Method," SDM Conference, April 6-8, 1981, Atlanta, Georgia. Paper No. 81-0501.

CHAPTER V

96. "Eigensolution Sensitivity to Parametic Model Perturbations", C. W. White and B. D. Maytum, Shock and Vibration Bulletin, No. 46, part 5, August 1976.

FURTHER BIBLIOGRAPHIC MATERIAL

97. "Prediction of Payload Vibration Environments by Mechanical Admittance Test Techniques." D. D. Kana and L. M. Vargas, AIAA/ASMA/SAE 16th Structures, Structural Dynamics, and Materials Conf., Denver, CO, May 27-29, 1975.

98. "Free Vibration Analysis by the Modal Substitution Method," Bajan, R. L. and Feng, C. C. AAS Paper 68.8-1, July 1968.

99. "Review of Modal Synthesis Techniques and A New Approach," Hou, S. N. Shock and Vibration Bulletin, Bulletin 40, Pt. 4, Dec 1969.

100. "Evaluation of Techniques for Estimating Titan III-C Flight Loads," Michael H. Marx, Archibald W. Adkins, Louis L. Bicciortelli, Davis C. Hyland, AIAA Paper No. 70-485, Los Angeles, Calif., April 6-8, 1970.

101. "Payload Dynamic Behavior Study on the Ariane Launcher", A. A. Girard, B. J. F. Imbert and C. M. Vedreane, International Astronautical Congress, 28th, Praque, Czechoslovakia, Sept. 25-Oct. 1977, 24p.

102. "Introduction to Load Problems in Spacecraft Structures", Boeing Aerospace Co., Seattle, Wash., 78N78237, March 1974, 59p.

103. "Methods for Combining Payload Parameter Variations with Input Environment", A. D. M. Merchant, Boeing Aerospace Co., Seattle, Wash., 76N28583, June 1976, 124p.

104. "Dynamic Contact Problems", V. M. Seymor, Foreign Technology Division Wright-Patterson AFB, Ohio, AD-B025 668L, Dec. 77.

105. "A New Effective Method of Dynamic Contact Problem Solution", V. A. Baheshko, AD-B008 803L. Army Foreign Science and Technology Center Charlottesville, VA, May, 77.

106. "Redesign of Structural Vibration Modes by Finite Element Inverse Perturbation", K. A. Stetson, I. R. Morrison, B. N. Cassenti, U. T. R. C., East Martford, Conn., May 78, AD-1057662.

107. "Engine/Airframe/Drive Train Dynam[illegible] Interface Documentation", D, A, Richardson, J. R. Alwang, Boeing Vertol Co. Philadelphia, PA, April 1978. AS-A055 766.

108. "Some Qualitative Considerations on the Numerical Determination of Minimum Mass Structures with Specified Natural Frequencies", A. Mangiavacchi, A. Misle, Rice University, Houston, Texas, AS-A053726, Sep. 77.

109. "Approximation of Complex Aerospace Systems by Simpler Ones", Drenick, R. F., AD.A003 754 Polytech. Inst. of New York, July 74.

110. "Factor Analysis on an Exploratory Tool in the Modal Analysis of Randomly - Loaded Vibrating Structures", R. G. Christiansen, D. R. Cruise, N. W. C., China Lake Calif., AD-906 463, Dec. 72.

111. "The Normal Modes of Interconnected Structures", L. T. Niblett, Royal Aircraft Structures, L. T. Niblett, Royal Aircraft Establishment Farnborough, England, AD-881 433L, Aug. 1969.

112. "A Report of Advancements in Structural Dynamic Technology Resulting from Saturn 5 Programs," 70B10710 Langley Research Center, Dec, 1970.

113. "Vibrational Transfer Functions for Base Excited Systems", A. C. Ernst and B. P. J. Jones, 71B10441, Nov. 1971.

114. "Active Vibration Isolation for Flexible Payloads", A. J. D. Leatherwood, 68 X 12812, Jan. 1968.

115. "Space Vehicle Dynamics", R. R. McDonald, 77W70290, JPL.

116. "The Use of Coherence Functions to Determine Dynamic Excitation Sources on Launch Vehicle Payloads," Stanley Barrett and Robert M. Halverson. NAS1-14370, June 1979.

117. "Earthquake Response Analysis of Existing Buildings" T. E. Blejwas and B. Bresler, Journal of the Structural Division ASCE, Jan. 1980.

118. "The Simulation of Elastic Mechanisms using Kinematic Constraints and Lagrange Multipliers," Proceedings, 6th Applied Mechanisms Conference, Denver, CO., October 1979.

119. "A Study of Modal Coupling Procedures for the Space Shuttle," Goldenberg, S., and M. Shapiro, NASA CR-112252, Grumman Aerospace Corp.

120. "A modal Combination Program for Dynamic Analysis of Structures," Bamford, R. M. Tech. Memo. 33-290, Jet Propulsion Lab., August 1966.

121. "A Dynamic Transformation Method for Modal Synthesis," Kuhar, E. J. and C. V. Stahle, AIAA Paper 73-396, presented at AIAA/ASME/SAE 14th Struc., Struc. Syn., and Matl, Conf., Williamsburg, Virginia, March 1973.

122. "On the Experimental Determination and Use of Modal Representations of Dynamic Characteristics", Klosterman, A. L., PhD Dissertation, Dept. and Mech. Eng., Univ. of Cincinnati, 1971.

123. "Review and Development of Modal Synthesis Techniques," Tech. Rept, 1073-1, J. H. Wiggins Co., May 1972.

124. "Vibrations of Composite Systems," MacNeal, R. H., Dept. OSR TN-55-120, Air Force Office of Scientific Research, October 1954.

125. "Vibration Analysis of Dynamic Partitioning," Goldman, R. I., AIAA Journal, &(8), June 1969, pp. 1152-54.

126. "Branch Mode Analysis of Vibrating Systems," Gladwell, G. M.L., Journal of Sound and Vibration, 1, January 1964, pp. 41-59.

127. "Vibration Analysis of Structures using Fixed-Interface Component Modes", C. Szu, Shock and Vibration Bulletin, No. 46 August, 1976.

128. "Selected System Modes using the Dynamic Transformation with Modal Synthesis" E. J. Kuhar, The Shock and Vibration Bulletin, No. 44, August 1974.

129. "Design and Subsystems in Large Structures," Caughey, R. K. Tech. Memo, 33-484, Jet Propulsion Laboratory, Pasadena, Calif., 1971.

130. "A Practical Approach to Spacecraft Structural Dynamics Problems," M. R. Trubert, Journal of Spacecraft and Rockets, Vol. 9, No. 11, November 1972, pp 818-824.

131. "Structural Dynamics Computations Using an Approximate Transformation," C. S. O'Hearne and J. W. Shipley, Shock and Vibration Bulletin, No. 44 Part 2, August 1974.

132. "Predicting the Dynamic Behavior of Complex Structures Using Part Experiment, Part Theory," J. C. Cromer, M. LaLanne, Shock and Vibration Bulletin, No. 46 August 1976.

133. "Viking Orbiter - Dynamics Overview", Wada, B. K. The Shock and Vibration Bulletin, Bulletin 44, Part 2, Naval Research Laboratory, Washington, D. C. Feb 12, 1962.

134. "Stiffness Matrix Structural Analysis," Technical Memorandum 33-75, Jet Propulsion Laboratory, Pasadena, Calif., Feb 12, 1962.

135. "A Modal Combination Program for Dynamic Analyses of Structures," Bamford, R. M., Technical Memorandum 33-290, Jet Propulsion Laboratory, Pasadena, Calif., Jan. 1964.

136. "Viking Dynamic Simulator - Vibration Testing and Analysis Modeling," Leondis, A., The Shock and Vibration Bulletin, Bulletin 45, Naval Research Laboratory, Washington, D.C., 1975.

137. "Mariner 6 and 7 Low Frequency Flight Acceleration Measurements," Trubert, M., Project Document 605-236, Rev. A, Jet Propulsion Laboratory, Pasadena, Calif., June 10, 1971 (an internal document).

138. "Experiences in Using Modal Synthesis Within Project Requirements," Garba, J. A., Wada, B. K., and Chen, J. C., The Shock and Vibration Bulletin, Bulletin 46, Part 5, Aug. 1976. Also Technical Memorandum 33-729, Jet Propulsion Laboratory, Pasadena, Calif., July 1, 1975.

139. "Synthesis of Stiffness and Mass Matrices from Experimental Vibration Modes," Ross, R. G., SAE Paper 710787, Los Angeles, Calif., Sept., 1971.

140. "Determination of Propellant Effective Mass Properties Using Modal Test Data," Chen, J. C. and Garba, J. A., The Shock and Vibration Bulletin, Bulletin 45, Naval Research Laboratory, Washington, D.C., 1975.

141. "Comparison of Modal Test Results: Multipoint Sine Versus Single-Point Random," Leppert, E. L., Lee S. H. Day, F. D., Chapman, C. P., and Wada, B. K., SAE Paper No. 760879, San Diego, Calif., Nov 29 - Dec. 2, 1976.

142. "A Method for the Direct Identification of Vibration Parameters from the Free Response," Ibrahim, S. R., Mikulcik, E. C., The Shock and Vibration Bulletin, Bulletin 47, Part 4, Sept. 1977.

143. "Comparison of Modal Test Methods on the Voyager Payload," Hanks, B., Ibrahim, S. R., Miserentino, R., Lee, S., and Wada, B. K., SAE Paper No. 781044, San Diego, Calif., Nov. 1978.

144. "Space Vehicle Experimental Modal Definition Using Transfer Function Techniques," Knauer, C. D., Peterson, A. J., and Rencahl, W. B., National Aerospace Engineering and Manufacturing Meeting, Los Angeles, Calif., Nov. 17-20, 1975.

145. "Modal Test: Measurement and Analysis Requirements," Wada, B. K., SAE Paper No. 751066, Los Angeles, Calif., Nov. 17-20, 1975.

146. "Use of Ranger Flight Data in the Synthesis of a Torsional Acceleration Transient for Surveyor Vibration Qualification Testing," Trubert, M. R., Technical Memorandum 33-237, Jet Propulsion Laboratory, Pasadena, Calif., Apr. 19, 1966.

147. "Helios TC-2 Stage Zero Ignition Pulse Reconstruction for MJS'77 Load Analysis," Trubert, M. and Egwuatu, A., Project Document 618-426, Jet Propulsion Laboratory, Pasadena, Calif., Aug. 1976.

148. "A Fourier Transform Technique for the Prediction of Torsional Transients for a Spacecraft From Flight Data of Another Spacecraft Using the Same Booster," Trubert, M. R. Technical Memorandum 33-350, Jet Propulsion Laboratory, Pasadena, Calif., Oct. 15, 1976.

149. "A Note on Boundary-Condition Simulation in the Dynamic Testing of Spacecraft Structures," Gayman, W. H., Technical Report 32-938, Jet Propulsion Laboratory, Pasadena, Calif., Apr. 15, 1966.

150. "Viking Orbiter 75 Test Report, Static Ultimate Type Approval Test," Ugale, M., Volkert, K., and Fortenberry, J., Project Document 611-117, Jet Propulsion Laboratory, Pasadena, Calif., Oct. 11, 1974 (an internal document).

151. "Viking Mars Lander 1975 Dynamic Test Model/Orbiter Development Test Model Forced Vibration Test: Summary Report," Fortenberry, J. and Brownlee, G., Technical Memorandum 33-689, Jet Propulsion Laboratory, Pasadena, Calif., Nov. 15, 1974.

152. "Unique Flight Instrumentation/Data Reduction Techniques Employed on the Viking Dynamic Simulator," Day, F. D., and Wada, B. K., The Shock and Vibration Bulletin, Bulletin 45, Naval Research Laboratory, Washington, D.C., 1975.

153. "Strain Gaged Struts and Data Reduction Techniques to Maximize Quality Data From Spacecraft Flight Measurements," Day, F. D., and Wada, B. K., 21st International Instrumentation Proceedings, Philadelphia, PA., 1975.

154. "Mode Selection," Morosow, G. and Abbott, P., Synthesis of Vibrating Systems, The American Society of Mechanical Engineers, New York, N.Y., Nov. 1971.

155. "A Criterion for Selecting Realistic Natural Modes of a Structure," Hurty, W. C., Technical Memorandum 33-364, Jet Propulsion Laboratory, Pasadena, Calif., 1967.

156. "A General Dynamic Synthesis for Structures with Discrete Substructures," L. Meirovitch and A. L. Hale, AIAA/ASME/ASCE/AMS-21st. Structures, Structural Dynamics, and Materials Conference, Seattle, Wash. May 12-14, 1980.

157. "New Methods in Substructuring," H. P. Geering, AIAA/ASME/ASCE/ASME/ASCE/AMS - 21st Structures, Structural Dynamics and Materials Conference, Seattle, Wash. May 12-14, 1980.

158. "A Method of Order Reduction for Structural Dynamics," L. R. Anderson and W. L. Hallauer, Jr., AIAA/ASME/ASCE/AMS- 21st Structures, Structural Dynamics and Materials Conference, Seattle, Wash. May 12-14, 1980.

159. "Recovered Transient Load Analysis for Payload Structural Systems," J. C. Chen, K. P. Zayzebski, J. A. Garba, AIAA/ASME/ASCE/AMS - 21st Structures, Structural Dynamics and Materials Conference, Seattle, Wash. May 12-14, 1980.

00000
000
0